

# Temple University

## Annual Progress Report: 2008 Formula Grant

### Reporting Period

July 1, 2009 – June 30, 2010

### Formula Grant Overview

Temple University received \$2,005,437 in formula funds for the grant award period January 1, 2009 through December 31, 2012. Accomplishments for the reporting period are described below.

### Research Project 1: Project Title and Purpose

*Resolving Inflammation in Arthritis* - Conventionally, inflammation has been perceived as a progressive reaction that gradually dissipates, so the therapeutic approach has been to block activation of inflammation. COX-2 inhibitors, which inhibit production of the pro-inflammatory prostaglandin E<sub>2</sub> (PGE<sub>2</sub>) and reduce pain, have been widely prescribed. However, a new concept that views inflammation as an active, orderly process with phases, induction-progression-resolution, and considers chronic inflammation as “failure to resolve” has emerged. In an animal model of arthritis, collagen-induced arthritis, we found that inhibiting COX-2 during resolution exacerbated inflammation. Thus, the purpose of this project is to investigate how the resolution works, and what molecules control the machinery. This is imperative for safety as well as for designing better therapy.

### Duration of Project

7/1/2009 – 6/30/2010

### Project Overview

Based on the fact that inflammation is resolved by an active process, and considering the fact that patients seek care after symptoms become apparent, a strategy to promote resolution is more effective than ones that prevent initiation of inflammation disorder. To develop such a therapy, there is a definite need to understand the “resolution” mechanism. The objectives of this project are to compare and contrast the events that operate in the resolution phase, and identify molecules that are essential for resolving inflammation in arthritis. Since we found that COX-2 was up-regulated during resolution and blocking its activity impeded resolution, our strategy is to set forth from the COX pathway, with the prostaglandins PGE<sub>2</sub> and 15d-PGJ<sub>2</sub> as our foci. The specific aims are as follow:

1. Determine if loss of these prostaglandins is associated with “failure to resolve.”
2. Determine if replenishing the identified prostaglandin(s) would restore resolution of inflammation.

Experimentally, Specific Aim 1 will be considered as an inhibition study, whereas Specific Aim 2 will be regarded as a reconstitution study. Mice induced for arthritis will be divided into 3 groups. In the inhibition study, the experimental groups will receive the COX-2 inhibitor, NS398, the positive control will receive vehicle only (PBS, phosphate buffered saline), and age-matched normal mice will serve as the negative control. Then, the degree of inflammation and amount of prostaglandins in their arthritic feet will be determined. If “failure to resolve” is correlated to the loss of a certain prostaglandin, we will consider the molecule as, potentially, a pro-resolver. Then, we will verify this assumption by conducting a reconstitution experiment. The mice with swollen feet in the NS398 group will be divided into two groups. One will be given the prostaglandin (NS398 + prostaglandin) the other will be given PBS (NS398 + PBS) as the control. The prostaglandins will be administered after the footpads have swelled, between days 35-45. If replenishing the prostaglandin allows the inflammation to subside we will conclude that the molecule is causal for resolution.

### **Principal Investigator**

Marion M. Chan, PhD  
Associate Professor  
Temple University School of Medicine  
Room 534, Bldg. OMS  
Department of Microbiology and Immunology  
3400 North Broad Street  
Philadelphia, PA 19122

### **Other Participating Researchers**

Kyle Evans, BS - employed by Temple University

### **Expected Research Outcomes and Benefits**

Upon completion of this project, we expect to have an understanding on how prostaglandins play roles in the inflammation resolving mechanisms. In the inhibition study, we expect to learn whether PGE<sub>2</sub> and 15d-PGJ<sub>2</sub> are produced in the resolution phase and lost upon NS398 treatment. Then, by the reconstitution study, we will deduce whether they are part of the resolving machinery or an irrelevant molecule that happens to be lost with the inhibition of COX2. For example, we may find that the NS398-induced exacerbation of inflammation is associated with a reduction in the level of PGE<sub>2</sub> and 15d-PGJ<sub>2</sub>. When 15d-PGJ<sub>2</sub> is replaced, the swelling would subside, resembling the joints of the mice that have been able to resolve naturally. However, those mice that are given PGE<sub>2</sub> will remain swollen, suggesting that the prostaglandin is a by-stander that does not mediate resolution of inflammation.

Chronic inflammation, such as arthritis, reduces the quality of life for many individuals. To date, the knowledge on the resolution mechanisms is still at its infancy. By studying the newly discovered machinery of inflammation resolution in a murine collagen-induced model, which closely resembles human arthritis in etiology, we hope to deduce a therapeutic strategy for

treating arthritis by enhancing resolution. Ultimately, we anticipate the findings may precipitate a paradigm shift in the therapeutic approaches to inflammation disorders, from stopping induction to promoting resolution.

### **Summary of Research Completed**

The objectives of this project are to compare and contrast the events that operate in the resolution phase, and identify molecules that are essential for resolving inflammation in arthritis. Since COX2 inhibitors block resolution, we hypothesize that one or more of the prostaglandins synthesized by the enzyme play essential roles in subsiding inflammation. Our strategy is to set forth from the COX pathway. During the past year, we have fulfilled two out of the three specific aims: We have identified that PGE<sub>2</sub> is produced during the phase of resolution, lost upon NS398 administration and needed for resolution of inflammation. Furthermore, we have shown that replenishing PGE<sub>2</sub> would restore resolution of inflammation

In this study, we defined three distinct phases at work in the progression of collagen-induced arthritis in mice. These phases are defined as 1) induction, 2) inflammation, and 3) resolution (See Figure 1). Additionally, we have shown that the prostaglandins PGE<sub>2</sub> and 15d-PGJ<sub>2</sub>, both products of the COX-2 pathway, are expressed during the resolution phase of the disease (See Figure 2 and Figure 3). As proposed, the prostaglandin components of the COX-2 pathway play a role in the resolution, and therefore, blocking COX-2 activity during the resolution phase perpetuates inflammation (Figure. 4). Measured as reduction in footpad thickness, 97.3% of the footpads in the vehicle control group had experienced resolution (negative slope) and only 2.7% of them remained unchanged or continued to swell. In contrast, inflammation persisted or progressed ("0" or positive slope) in 97% of the footpads in the group that was fed NS398 preventively and 58% of those that were fed NS398 therapeutically. Thus it was shown that the products of the COX-2 pathway have a role not only in induction of inflammation but also the resolution of inflammation.

In effort to explore the role of PGE<sub>2</sub> in the resolution of inflammation, a reconstitution study was performed. Mice were divided into groups: 1) vehicle control which would resolve naturally, 2) NS398 & PBS treated which would fail to resolve, and 3) NS398 treated ones reconstituted with PGE analogs, dmPGE<sub>2</sub> and misoprostol. Subcutaneous injections were given in 50 µl volume along the thigh three times a week. In the vehicle control over 90% of the swollen footpads resolved naturally. In the NS398 fed group where only PBS was administered, 50% of the footpads remained swollen and their thickness increased beyond the inflamed phase. Resolution was restored by PGE reconstitution (Figure 5).

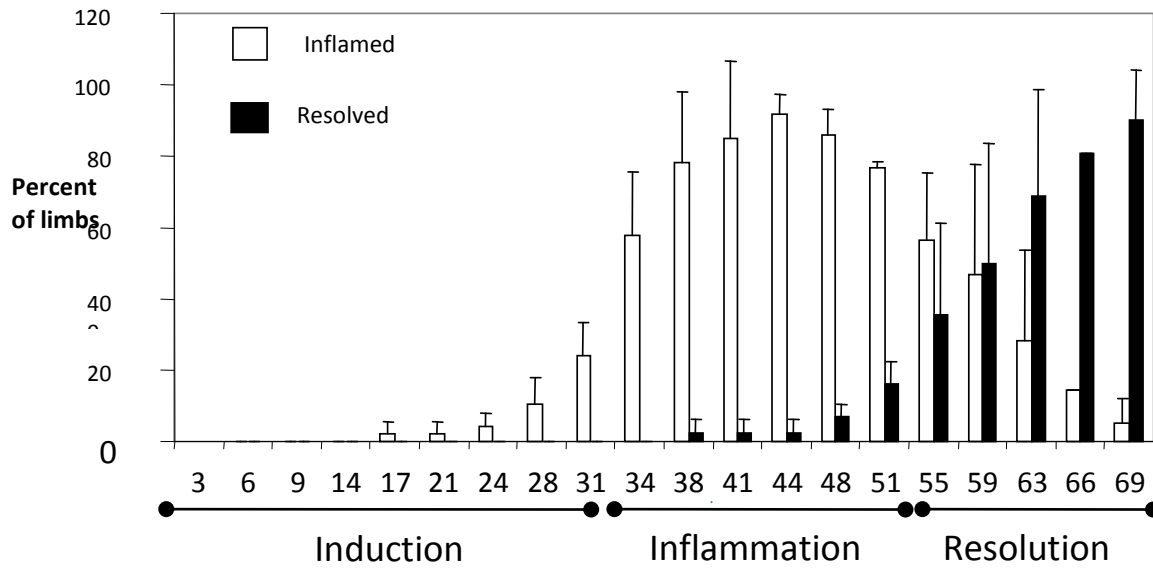
Publication. Chan MM, Moore AR, Resolution of inflammation in murine autoimmune arthritis is disrupted by cyclooxygenase-2 inhibition and restored by Prostaglandin E(2)-mediated lipoxin A(4) production. J Immunol 184:11(6418-26)2010 Jun 1

#### Impact of the study -

Rheumatoid arthritis is a debilitating disease suffered by populations in America and worldwide. In this chronic disease, inflammation goes through phases of progression and resolution. Eventually, "failure to resolve" leads to irreparable joint damage. COX2 inhibitors, which are

very effective in relieving pain, have been regarded as “the drugs” for treatment of many inflammatory diseases, including arthritis. Our findings may explain the enigma regarding why COX-2 inhibitors are palliative rather than curative in humans, because blocking resolution may mitigate the benefit of preventing induction. The findings may explain an enigma that has perplexed the medical community and provide in-sight on how to treat arthritis more efficiently.

Figure 1



Figure

2

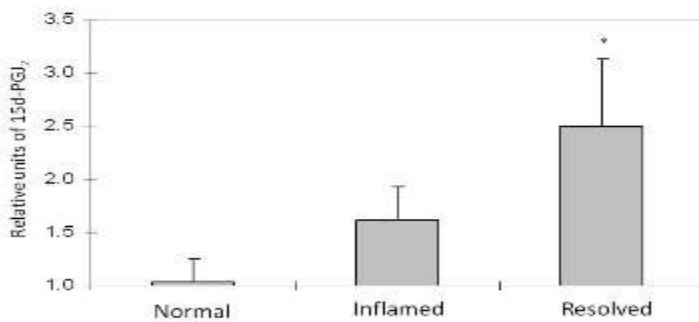


Figure 3

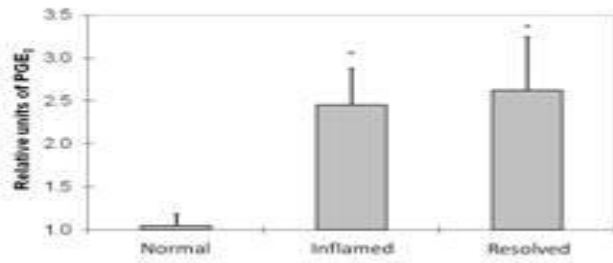


Figure 4

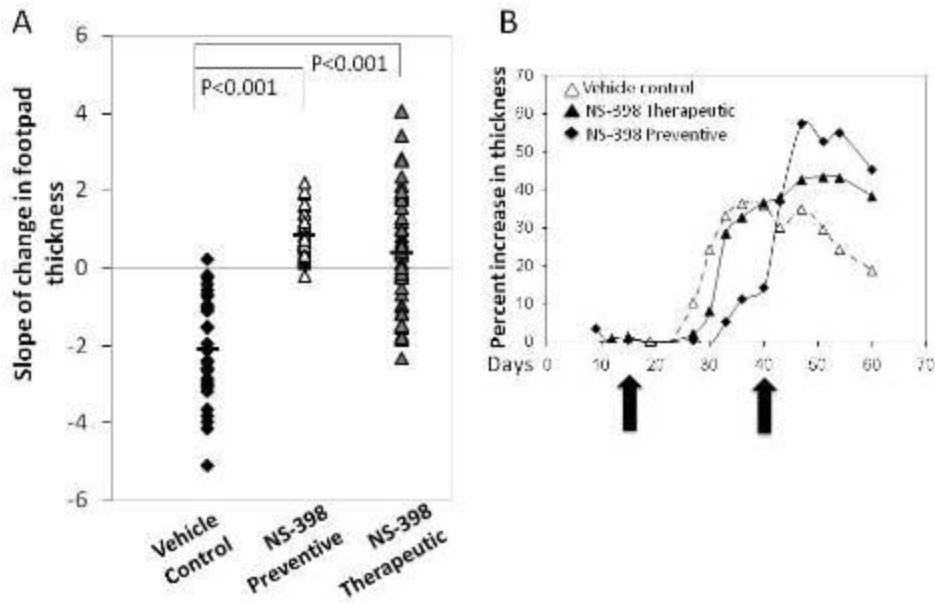
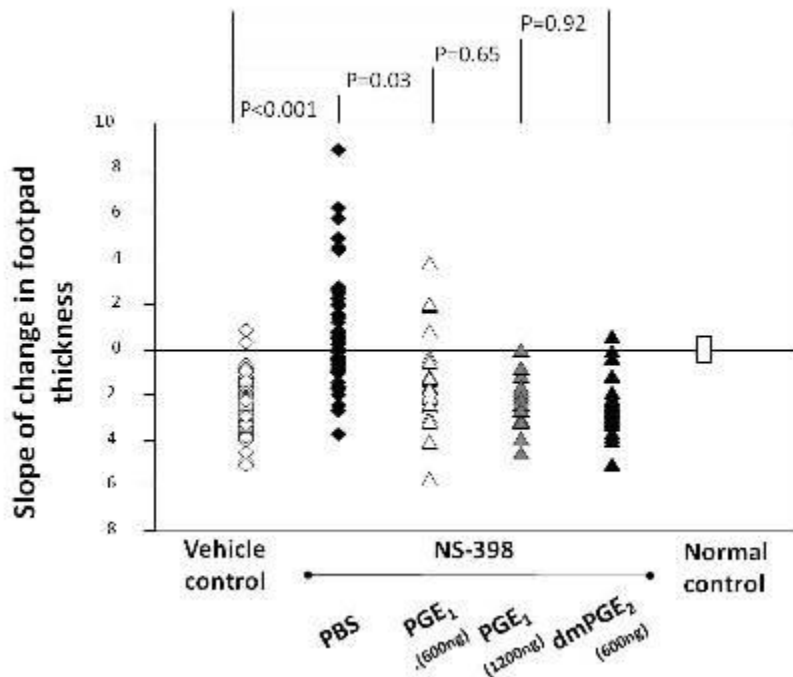


Figure 5



**Research Project 2: Project Title and Purpose**

*Identification of the Role of TULA-2 a Novel Phosphatase in Osteoclast Differentiation and Function* - Osteoporosis and other bone-related maladies afflict 150 million Americans and constitute a significant burden to ever-rising health care cost. This project will evaluate the role of TULA-2, a novel phosphatase in bone remodeling in mouse skeleton. In addition, ex vivo experiments will be performed to investigate the role of TULA-2 in differentiation and function of osteoclasts. The research proposed here will help in understanding the basic biology behind bone resorption and will help identify targets for therapeutic interventions to control bone loss.

**Duration of Project**

7/1/2009 - 6/30/2010

**Project Overview**

Bone is a dynamic tissue that depends on the intricate relationship between protein tyrosine kinases (PTK) and protein tyrosine phosphatases (PTP). PTKs and PTPs act like molecular on and off switches and help modulate differentiation and the attachment of osteoclasts to bone matrix regulating bone resorption. The novel protein T-cell Ubiquitin Ligand-2 (TULA-2), which is abundantly expressed in osteoclast, has been shown to possess phosphatase activity. We hypothesize that TULA-2 protein plays a regulatory role in osteoclastogenesis and function. Our preliminary data shows that of the two family members only TULA-2 is expressed in osteoclasts and the protein expression is sustained throughout the course of osteoclast

differentiation suggesting that TULA-2 may play a role during early as well late stages of osteoclast differentiation. Additionally, preliminary skeletal analysis of TULA double knock out mice (DKO) using x-rays of the long bone indicated that as compared to the wild type samples the DKO bones are less dense at the femur-tibia junction. Furthermore, in vitro experiments indicated that bone marrow precursor cells from DKO have a decreased potential to form osteoclasts. Taken together, these preliminary data suggest that TULA-2 is required for osteoclast differentiation and function. For this proposal we plan to further characterize the effect of absence of TULA-2 in bone remodeling. This project will undertake a comprehensive analysis to evaluate the role of TULA-2 during normal course of bone resorption by osteoclast using the DKO mice. The DKO mice will be compared with the control mice to characterize the skeletal remodeling from tissue to molecular level by using radiography, micro CT histology, RT PCR and other molecular techniques.

### **Principal Investigator**

Archana Sanjay, PhD  
Assistant Professor  
Temple University  
3500 North Broad Street, MERB 448  
Philadelphia, PA 19140

### **Other Participating Researchers**

Steven H. Back, BS - employed by Temple University

### **Expected Research Outcomes and Benefits**

Osteoporosis is a disease currently affecting 8 million women and 2 million men in the United States. The disease consists of low bone mass and structural erosion of bone tissue, which results in a greater chance of fractures. In 2005, osteoporosis-related fractures resulted in 19 billion dollars of hospital costs; however as the population gets older, these costs are expected to significantly escalate. Other diseases caused by a change in bone mass and structural composition are osteopetrosis and Paget's disease. Osteopetrosis is considered a rare disease, which affects less than 200,000 people in the United States. In osteopetrosis, bones become extremely dense, and contract the marrow cavity. Paget's disease is a chronic, progressive disease resulting in abnormal bone remodeling through osteoclasts and osteoblasts. It occurs in 3-4% of people above the age 55, and in 10% of those over 80 in the United States. The bone marrow is replaced by a disorganized trabecular bone material and fibrous tissue. Although significant advances have been made in the last decade, the understanding of the signaling pathways that regulate bone resorption is far from clear. One approach to understand the mechanisms involved is to understand the role of the critical players in the pathway. We plan to investigate the role of TULA-2 a novel phosphatase found in osteoclasts. This protein is recently identified and very little information is available regarding its role in bone biology. Therefore, this project will not only increase our understanding of the regulation of osteoclast function and bone resorption, but might also help in the development of new targets for effective therapeutics.

## Summary of Research Completed

### Summary

Our work focuses on characterizing the role of TULA proteins belonging to a novel phosphatase family whose function remains poorly understood and which has never been studied in skeletal remodeling. TULA proteins differ from classical PTPs, being members of the histidine phosphatase that have a conserved catalytic core centered on a histidine residue, which becomes phosphorylated in the course of a reaction. There are considerable differences between the TULA family members. Thus while TULA-2 is ubiquitously expressed in mammalian tissues, TULA shows expression in lymphocytes only. Most importantly, TULA-2 is the only family member with significant phosphatase activity able to dephosphorylate the tyrosine kinase Syk and Src. PCR and Western Blot studies indicated that TULA-2 is expressed throughout osteoclast differentiation. X-ray radiography and Histomorphometric analysis indicated that mice in which both TULA and TULA-2 genes are deleted (DKO mice) have a decreased trabecular bone volume and very thin cortices. In Vitro osteoclast differentiation assays indicated that bone marrow isolated from DKO mice can generate more osteoclasts compared to WT bone marrow. Serum analysis indicated that levels of collagen degradation product, a marker for osteoclast activity are elevated in the DKO mice as compared to the control mice. Additionally, ex vivo pit formation capacity of the DKO osteoclasts was also augmented suggesting that absence of TULA proteins, particularly TULA-2, results in hyperactivity of osteoclasts contributing to decreased bone mass in mice. Our data also showed that phosphorylation of Syk and Src kinases was upregulated in the DKO osteoclasts. Cumulatively, our results indicate that the novel phosphatase TULA-2 negatively regulates bone resorption by regulating the tyrosine kinases that are known to be involved in osteoclastic bone resorption.

### Materials and Methods

*MicroCt, Histology and Histomorphometry*- MicroComputed tomography of the long bones was performed using 59 kV source voltage and 167 uA as a source of current and associated software version 1.5 (Skyscan, Aatselaar, Belgium) following the Journal of Bone Mineral research guidelines. For histological and histomorphometric analysis, 6 or 12-week old littermates were sacrificed by CO<sub>2</sub> inhalation. To measure dynamic bone formation parameters, mice were injected with calcein (30mg/kg body weight) 10 and 3 days before sacrifice. Tibiae and femora were dissected and fixed in 3.7% formaldehyde in phosphate buffered saline, preserved in 70% ethanol and embedded in methlymethacrylate resin. Sections (5µm) were deplasticized and stained with Von Kossa procedure. Some sections were processed for TRAP staining as per manufacturer's instruction (Sigma). For histomorphometric analysis, to assess changes in bone structure and remodeling, tibial sections were measured in the proximal metaphysis beginning 340mm below the chondro-osseous junction of the secondary spongiosa using image analysis software (BIOQUANT Image Analysis Corp., Nashville, TN). The number of TRAP+ cells was determined in secondary spongiosa, in contact with the trabecular bone.

*Determination of Serum Collagen Telopeptide*- Serum was prepared from blood collected by cardiac puncture. Concentrations of C-telopeptide, degradation products of type-I collagen in serum of 12 week-old mice were determined using the Rat Laps ELISA (Osteometer BioTech A/S, Herlev, Denmark).

*Generation of osteoclast like cells in vitro culture-* For generation of osteoclast-like cells (OCLs), bone marrow was isolated from tibia and femur of 4-6week old mice. Following overnight incubation, the non-adherent cells were plated at  $2.5 \times 10^5/\text{cm}^2$  in a-MEM, 10% FBS, penicillin/streptomycin containing 20ng/mL M-CSF. Subsequently cells were treated with M-CSF (20ng/ml) and RANKL (50ng/ml) for additional 5-6 days.

*RT-PCR analysis-* The expression levels of osteoclast differentiation markers were analyzed by semi-quantitative polymerase chain reaction (PCR). RNA isolation was performed using TRIzol reagent (Invitrogen, Carlsbad, CA) according to the manufacturer's protocol. RNA was quantified using spectrophotometer at 260/280 nm; 1mg was used in RT reaction performed using Super Script II reverse transcriptase (Invitrogen, Carlsbad, A) following manufacturer's protocol. Oligo dT and dNTPs were purchased from Promega.

*Western Blot Analysis-* Typically, 30-40  $\mu\text{g}$  of total cell lysate protein was electrophoresed on 8 or 10% SDS-PAGE gels. Proteins were then transferred to nitrocellulose membranes (Schleicher & Schuell, Waltham, MA). Transferred proteins were visualized by staining the membrane with 0.2% Ponceau S in 3% trichloroacetic acid (Sigma). To block nonspecific binding, the membranes were incubated for 2 h at room temperature in LICOR buffer (LICOR, Lincoln, NE). Antigens were visualized by immunoblotting with an appropriate primary antibody (1:1000 dilution) followed by an appropriate LICOR secondary antibody. To quantify changes, densitometry of the phosphorylated and total protein bands was performed using the LICOR analysis program. The values for the phosphorylated band were normalized to the density of the respective total protein band in the re-probed blot.

## Results and Conclusions

### *Selective expression of TULA-2 in osteoclasts:*

We first determined whether TULA and/or TULA-2 are expressed in osteoclasts. PCR analysis of two independent osteoclast samples showed the presence of TULA-2, but not TULA mRNA (Fig. 1A). This data is consistent with the previous findings by us and other researchers that TULA-2 is ubiquitously expressed, while TULA is expressed in lymphoid cells only. Next we examined the expression pattern of TULA-2 mRNA during osteoclast differentiation and compared it to PU.1, RANK and Calcitonin receptor (CalcR), which are differentially expressed in the course of osteoclast differentiation. As shown in Fig. 1B, TULA-2 is expressed already in the osteoclast precursors and, based on an increase in the intensity of the corresponding amplified band, its expression appears to increase after addition of M-CSF or M-CSF+RANKL. These results were confirmed using Western blot analysis, which clearly revealed the presence of TULA-2 in the precursors and its increase in the course of differentiation (Fig. 1C) and the lack of detectable TULA (not shown).

### *Enhanced phosphorylation of Src, Syk and Erk proteins in the absence of TULA-2 in osteoclasts:*

Considering that TULA-2 dephosphorylates Syk, a PTK essential for RANKL-induced signaling in osteoclasts, we examined the regulatory effect of TULA-2 on this pathway by assessing phosphorylation of its key protein components. In WT OCLs Src, Syk and Erk were phosphorylated in response to RANKL in a clear time-dependent manner; their phosphorylation at  $t=0$  was low and gradually increased until  $t=30$  min (Fig.2). In the absence of TULA-2, these proteins were phosphorylated significantly higher than in WT cells by a factor of  $\geq 2$ . Notably, they were phosphorylated even in the absence of RANKL stimulation. These results indicate that

TULA-2 negatively regulates RANKL-induced signaling, which is mediated by tyrosine phosphorylation.

*Absence of TULA-2 results in increased numbers of hyperactive osteoclasts:*

Since TULA-2 downregulated RANKL-induced signaling, which is critical for OC development, we hypothesized that TULA-2 plays a role in the regulation of the OC function. To test this hypothesis, we compared differentiation and function of WT and TULA-2-deficient OCLs. The number of TRAP<sup>+</sup> multinucleated cells derived from the bone marrow macrophages (BMM) in response to MCSF+RANKL was 2 fold higher in cells lacking TULA-2 than in their WT counterparts (Fig. 3A and B). For the resorption assay OCLs were purified and cultured on dentine slices for 48 h, and the resorbed area was measured and normalized to the number of OCLs present; this pit-forming assay was described in detail in our previous publications. OCLs lacking TULA-2 formed 2-fold more pits than WT OCLs (Fig. 3C). These experiments indicate that the absence of TULA-2 facilitates both differentiation of BMM precursors into OCLs and intrinsic (i.e. in the absence of osteoblasts or T cells) bone-resorbing activity of OCLs.

*Absence of TULA-2 results in decreased bone volume:*

Our preliminary data indicates that only TULA-2 is expressed in early and mature OCs and its absence results in increased osteoclastogenesis and function (Fig. 1). To further examine the role of TULA proteins in skeletal remodeling we initiated the characterization of single and double knockouts of TULA mice that were obtained from Dr. Nick Carpino. Comparative histomorphometric analysis of 12 week-old WT, SKO1, SKO2 and DKO male mice indicated that there was a ~2-fold decrease in bone volume in DKO mice (Table1). Further analysis revealed that in DKO mice although the osteoblast numbers and bone formation rate were not altered there was a dramatic increase in the OC numbers and bone resorption parameters (Fig. 4 and Table1). Given the restricted expression of TULA protein not surprisingly, the skeletal phenotype of TULA<sup>-/-</sup> was comparable to the WT mice. In contrast, although the BV/TV in 12 wk male TULA-2<sup>-/-</sup> mice was similar to the WT, parameters of OC function were significantly different than the WT counterparts (Table1) and this data was in agreement to increased function of OC cultures in ex vivo systems (Fig.3). These data suggest that while absence of both TULA proteins results in decreased bone volume, the absence of TULA-2 has milder effect at 12 weeks of age.

*Conclusion*

Our data indicates that in osteoclasts, TULA-2, but not TULA, is an active protein tyrosine phosphatase since TULA-2, but not TULA, is expressed in the cells of the OC lineage. In osteoclasts, TULA-2 down regulates Syk-dependent RANKL-induced signaling. TULA-2 downregulates functional activity of OCs in vitro. TULA-family knockout mice exhibit a bone phenotype consistent with the enhanced OC function. All in all the above results indicate that TULA-2 is a negative regulator of OC signaling and function *in vitro* and *in vivo*

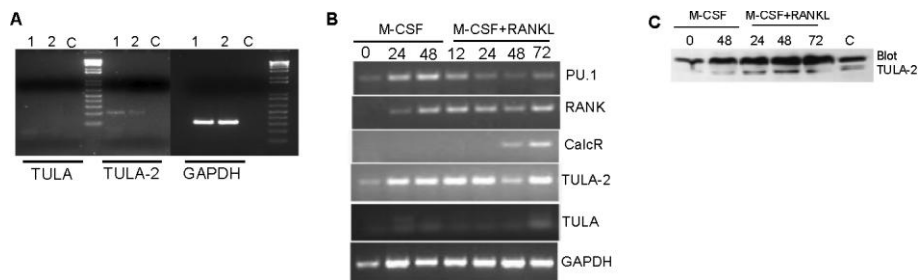


**Figure. 1 Expression profile of TULA-2 in OC differentiation.** **A)** Two different preparations of OCs labeled as 1 or 2 were used. Expression levels of TULA, TULA-2 and GAPDH were determined by using specific primers. PCR reaction with primers alone was used as control (C). TULA and TULA-2 were amplified for 30 cycles. GAPDH was amplified for 19 cycles. 5 ml of the sample was loaded on gel to visualize the bands. **B)** Bone marrow precursors were cultured in the presence of M-CSF alone or with M-CSF and RANKL for the times indicated. Expression levels of PU.1, RANK, Calcitonin Receptor, TULA-2, TULA and GAPDH were determined by using specific primers. 5 ml of the sample was loaded on gel to visualize the bands. **C)** TULA-2 was detected in precursor and mature OCLs. Cells were treated with cytokines for indicated time points. Equal amount of protein from total cell lysates were electrophoresed and blotted with anti-TULA-2 antibodies. T cell lysate from sample 2 was used as control (C).

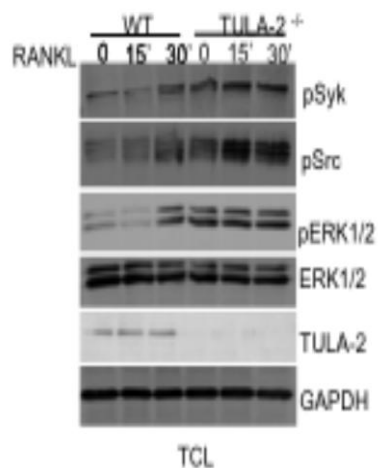


**Figure.2. Enhanced phosphorylation of Src, Syk and Erk proteins in the DKO OCLs-** WT or DKO OCLs were serum-starved for 30 min and treated with RANKL (50 ng/ml) for 0, 15 or 30 min. Cell lysates were processed for Western blot analysis. Blots were probed with indicated phospho-specific antibodies Anti pSykY519/520; Ant-Src Y416, Anti pErk p42/44. Membranes were stripped and reprobred with antibodies to ERK1/2 and GAPDH to determine equal loading. Expression of TULA-2 was also determined by probing with anti-TULA-2 antibodies.

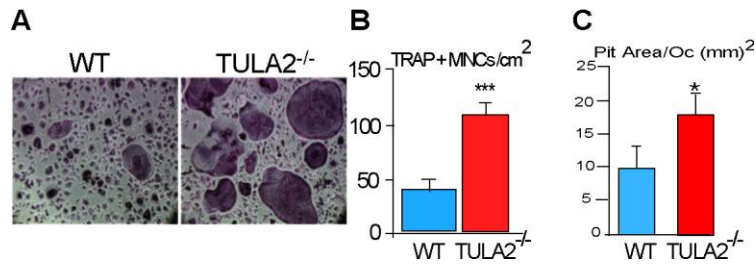


**Figure .3. Enhanced bone resorption by TULA-2<sup>-/-</sup> OCs.** **A)** Non-adherent bone marrow precursors were cultured with M-CSF for 2 days and with M-CSF and RANKL for 5 more days. **A)** TRAP staining shows increased numbers and larger TULA-2<sup>-/-</sup> OCLs **B)** The numbers of TRAP+ multinucleated OCs in TULA-2<sup>-/-</sup> cultures were significantly higher than WT cultures at day 7. \*\*\*p<0.001 vs. WT. **C)** WT and TULA-2<sup>-/-</sup> OCLs were seeded on dentin discs. Pits were stained with toulidene blue, and their area after 48h was normalized for the OCLs number and shown as mean ± SD (n=9). \*p<0.05 vs WT OCLs.

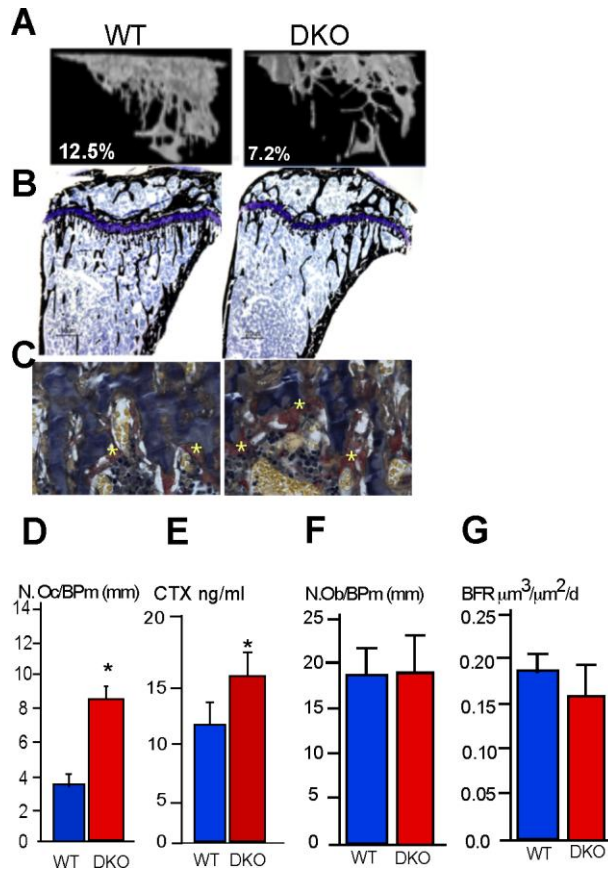


**Figure.4. Bone phenotype of the DKO mice - A.** MicroCT analysis of trabecular bone volume tibiae from WT or DKO mice indicated decreased in bone volumes in DKO samples. % BV/TV (Bone volume/tissue volume) is indicated for each sample. **B.** Photomicrographs of the undecalcified section of tibiae from 12 wk old male WT and DKO mice visualized at 4x

magnification. Sections were stained with Von kossa to visualize mineralized bone and counter stained with toulidene blue. **C&D.** DKO mice have more OCs. Sections were stained with Non esterase stain (Sigma). OCs were identified by TRAP activity reaction product (red) and are indicated by yellow asteriks. Sections are at 40x magnification. Histomorphometric analysis showed that there were ~ 2-fold more OCs in DKO samples as compared to WT. **E.** Measurement of serum collagenase telopeptide (CTX) demonstrated increased OC activity in the DKO mice. **F&G.** Histomorphometric analysis of osteoblast numbers and bone formation rate (BFR) measured by double calcein labeling indicated that osteoblast numbers and activity were intact in the DKO mice. Data are presented as mean  $\pm$  SD activity from 3 mice; \* p<.05 compared to the WT samples.

**Table1. Comparative histomorphometric analysis of the cancellous region of the tibial metaphysis of TULA deficient mice**

	<b>WT</b>	<b>SKO1</b>	<b>SKO2</b>	<b>DKO</b>
Bone volume/Tissue Volume (%)	18.71 $\pm$ 0.95	18.13 $\pm$ 0.71	16.46 $\pm$ 1.9	10.0 $\pm$ 0.70*
Trabecular Number (no./mm)	6.87 $\pm$ 0.58	7.10 $\pm$ 0.45	5.89 $\pm$ 0.71	3.70 $\pm$ 0.27*
Trabecular Separation (mm)	114 $\pm$ 18.63	90.0 $\pm$ 16.98	97.4 $\pm$ 22.69	215.4 $\pm$ 38.27*
OC surface/Bone Surface (%)	10.84 $\pm$ 1.4	13.14 $\pm$ 2.9	17.71 $\pm$ 3.8*	27.54 $\pm$ 3.5**
Erosion Surface/Bone Surface (%)	10.58 $\pm$ 1.65	12.97 $\pm$ 3.08	18.36 $\pm$ 3.7*	30.03 $\pm$ 3.4**

Data are presented as mean SD \*p < 0.05 \*\*p < 0.001 compared with the wild type (WT) mice; (n= 4 mice/group).

### **Research Project 3: Project Title and Purpose**

*C/EBP(s) and the Transcription of Dihydrodiol Dehydrogenase 1 in Human Ovarian Cancer Cells* - Transcription factors (TFs) induce the expression of the target gene by binding regulatory sequences on the target gene's promoter region. CCAAT/enhancer binding proteins (C/EBPs) are a family of TFs that are important for cellular differentiation and proliferation. The expression levels of C/EBPs transcription factors have been found to change during pathophysiological conditions of the cell. Preliminary studies have identified potential C/EBP binding sites on the dihydrodiol dehydrogenase gene 1 (DDH1) promoter in ovarian cancer cells. DDH are a family of aldo-keto reductases involved in the de novo detoxification of xenobiotics. This study aims to clarify the role of C/EBP TFs in regulating the transcription of DDH1 in ovarian cancer cells.

### **Duration of Project**

7/1/2009 - 5/10/2010

## **Project Overview**

Ovarian cancer is one of the leading causes of female mortality in the United States. Chemotherapy with platinum-containing compounds is often effective in the treatment of this disease. However, ovarian cancers can develop resistance to these drugs via diverse mechanisms. Preliminary studies from our lab have demonstrated that overexpression of dihydrodiol dehydrogenase (DDH) is intimately involved in the development of the cisplatin resistance phenotype. Dihydrodiol dehydrogenases (DDH) are a family of aldo-keto reductase enzymes involved in the *de novo* detoxification of xenobiotics, steroids and polycyclic aromatic hydrocarbons (PAH). Increased expression of Dihydrodiol dehydrogenase 1 (DDH1) protein has been demonstrated to induce cisplatin/carboplatin resistance in human ovarian carcinoma cells. The observed increase in protein expression was associated with the changes in the transcription of the DDH gene. In order to identify the factors that control the expression of DDH1 gene in human ovarian cancer cells, we cloned approximately 3000 bps of the 5'-end of the human DDH1 gene. Promoter deletion analysis indicated a complex control mechanism with the proximal -181 bp positively associated with basal transcription of the DDH1 gene in human ovarian carcinoma cells. This proximal promoter region contains overlapping binding sites for the following transcription factors; Sp1, CP1, C/EBP as well as USF. Further results from site-directed mutagenesis indicated that C/EBP may be involved in the basal transcription levels of DDH1 gene in ovarian cancer cells (2008).

CCAAT/enhancer binding proteins (C/EBPs) are a family of transcription factors involved in regulation of cellular differentiation and proliferation, control of apoptosis and inflammatory process. The six different members of the C/EBP family are C/EBP $\alpha$ , C/EBP $\beta$ , C/EBP $\gamma$ , C/EBP $\delta$ , C/EBP $\epsilon$  and C/EBP $\zeta$ . All six proteins share the conserved dimerization bZIP region at the C-terminus responsible for DNA binding. *In vitro* experiments and mouse knockout models have identified the importance of each of these specific TFs in various cellular processes. *This project aims to identify and decipher the role of specific C/EBP member(s) involved in regulating the transcription of DDH1 gene in ovarian cancer cells.* The results obtained herein will aid in our understanding of the role of C/EBPs involved in control of DDH1 gene expression.

## **Principal Investigator**

Hemant Parekh, PhD  
Associate Professor  
Temple University School of Medicine  
Dept. Pathology and Lab. Medicine  
3400 N. Broad Street  
Philadelphia PA 19140

## **Other Participating Researchers**

Rajash Pallai, MS - employed by Temple University School of Medicine

## Expected Research Outcomes and Benefits

Ovarian cancer is an important cause of death in women. Unfortunately, it is generally discovered late when the cancer has spread from the ovary to other parts of the body. This means that surgery, while important to remove most of the tumor, has to be followed by treatment with anticancer drugs. The side effects of the anti-cancer drugs are controlled to a certain extent by enzymes (that metabolize the drug) synthesized in the host. These enzymes act upon the anticancer drug and control the associated toxicity. In cases of cancer cells developing resistance to anticancer drugs an increased production of enzymes metabolising the drug has been observed. We have recently demonstrated in a series of human cancer cell lines that the protein Dihydrodiol Dehydrogenase (DDH) produces resistance to platinum drug based chemotherapy. In order to identify the mechanisms that control the expression of DDH in human ovarian tumor cells we have characterized the DDH1 gene promoter region. This has led to the identification of the several potential transcriptional elements that may be involved in upregulating DDH1 expression in drug-resistant human ovarian carcinoma. This project is aimed at characterizing the C/EBP transcription factor that will influence the expression of DDH1 in ovarian cancer cells.

## Summary of Research Completed

*Analysis of constitutive and cisplatin- induced differential expression of CCAAT enhancer binding protein (C/EBP) isoforms in human ovarian carcinoma cells 2008 (cisplatin-sensitive) and 2008/C13\* (-resistant):*

In order to analyze the differential expression of C/EBP isoforms (alpha ( $\alpha$ ), beta ( $\beta$ ), delta ( $\delta$ ), gamma ( $\gamma$ ) and zeta ( $\zeta$ )), ovarian cancer cells 2008 and 2008/C13\* were seeded at a density of  $1 \times 10^6$  cells in a 100mm dish 24 h before isolation of RNA using RNazolB as described by Deng *et al.* In the case of treatment, cells were exposed to 10 $\mu$ M concentration of cisplatin for an additional 16-18h and RNA was isolated. One microgram of the RNA was to be utilized to generate cDNA using the Omniscript RT kit (Qiagen) as detailed by the manufacturer. Ten percent of the RT product was to be utilized for C/EBPs real-time PCR analysis with primers specific for C/EBP $\alpha$ , C/EBP $\beta$ , C/EBP $\delta$ , C/EBP $\gamma$  and C/EBP $\zeta$  (GADD153) (Table 1). The expression of C/EBPs were normalized relative to GAPDH gene expression.

The results clearly indicated that there was no significant changes in the basal expression levels of C/EBP isoforms in the cisplatin-sensitive (2008) and –resistant (2008/C13\*) human ovarian carcinoma cells (Table 2). In contrast there was an 8-fold increase in the expression levels of C/EBP $\zeta$  (GADD153) isoform in cisplatin treatment 2008 cells, whereas there was a two fold decrease in C/EBP $\zeta$  in the case of 2008/C13\* cells treated with cisplatin. Further it was identified that on treatment with cisplatin there was no significant change in the expression levels of other C/EBP isoforms in cisplatin-sensitive (2008) and –resistant (2008/C13\*) human ovarian carcinoma cells (Table 2).

*Invitro binding of NF-Y and C/EBP to the DDH1 proximal promoter region:*

Based on previous observations from site-directed mutagenesis, it was clearly identified that the tandem of transcription factor binding sites for NF-Y and C/EBP was critical in regulating the

transcription of DDH1 proximal promoter in human ovarian carcinoma cells (2008 & 2008/C13\*). In order to further substantiate the observations, electrophoretic shift assay (EMSA) was performed with nuclear extracts obtained from 2008 and 2008/C13\* cells. The region between -120/-91 of the DDH1 gene promoter was utilized as the wild-type probe, along with NF-Y and C/EBP transcription factor consensus sequences. Results from EMSA clearly demonstrated that NF-Y is essential in regulating the basal transcription of DDH1 by binding to the -120 to -91 region of the DDH1 gene promoter, while C/EBP did not have any functional role. These results led us to concentrate on the functional role of NF-Y in regulating the transcription of DDH1 gene promoter.

To corroborate the results from EMSA, gel super-shift was performed. For the gel super-shift assay, following the incubation of the nuclear extracts with the 30bp WT DDH1 promoter fragment for 30 min, 2 $\mu$ g of NF-YA polyclonal antibody, 2 $\mu$ g of NF-YB polyclonal antibody and/or the three polyclonal antibodies (anti-NF-YA, -NF-YB and -NF-YC) (Santa Cruz Biotechnology, Santa Cruz, CA) were added to the binding reaction and the mixture incubated at for an additional 1h. The rabbit pre-immune IgG (Santa Cruz Biotechnology, Santa Cruz, CA) was utilized as negative control in the super-shift assay. The mixture was fractionated on a 5% nondenaturing polyacrylamide gel. Transfer and detection was performed utilizing chemiluminescence with charge-coupled device.

Our results indicated that in the presence of NF-YA or NF-YB or NF-Y (A, B and C) antibodies, there was a shift in the protein-DNA complex from the nuclear extracts obtained from the cisplatin-sensitive (2008) and -resistant (2008/C13\*) human ovarian carcinoma cells (Fig 1). These results confirm the *in vitro* binding of transcription factor NF-Y to the -120/-91 region of DDH1 gene promoter.

#### *Functional analysis of NF-Y in regulating the transcription of DDH1 gene:*

To assess the effect of overexpression of NF-Y in regulating the DDH1 mRNA expression levels, 2008 (human ovarian carcinoma cells) were transiently transfected with 1 $\mu$ g of NF-YA, -YB and -YC cDNA expression vector or pCMV vector as negative control using lipofectamine 2000. After 24h, RNA was isolated from cells using Trizol (Invitrogen, CA) and used in the reverse transcription reaction and RT-PCR was performed.

Alternatively, the 2008 cells were transiently transfected with 500 picomoles of human NF-YA siRNA (siGENOME smart pool, Dharamacon, IL) or the control si-RNA (siGENOME Non-targeting siRNA pool#1, Dharamacon, IL). Transfection was performed utilizing siPORT NeoFX transfection reagent (Ambion, CA). RNA was isolated 24h after transfection using Trizol reagent (Invitrogen, CA) as instructed by the manufacturer. One microgram of the RNA was used in the reverse transcription reaction and RT-PCR was performed

Ectopic expression of NF-YA, -B and -YC also led to a 2-fold increase in DDH1 mRNA levels in 2008 human ovarian carcinoma cells (Fig 2A) compared to the pCMV control vector transfected cells. Furthermore, when 2008 cells were transfected with si-RNA directed against NF-YA, a 4-fold decrease in DDH1 mRNA expression levels was observed compared to control si-RNA (Fig 2B). Taken together these results confirm a direct role of NF-Y in regulating the basal transcription of DDH1 gene in human ovarian carcinoma cells.

**Table 1 List of primers utilized for amplification of the gene(s) of interest by quantitative real-time RT-PCR assay**

<i>Gene</i>	<i>Forward</i>	<i>Reverse</i>	<i>Annealing temperature</i>
GAPDH	5'-accactcctccaccttg-3'	5'-ctcttgctcttgctggg-3'	55°C
CEBPA	5'-gtccagaccctccaggtagt-3'	5'-gggaccaactgtattgct-3'	58°C
CEBPB	5'-tgaattgctgggttaccaaa-3'	5'-taggcatgagacccccata-3'	58°C
CEBPD	5'-cccccgccatgtacgacgacgaga-3'	5'-gccgcccgcttgattgctgtt-3'	55°C
CEBPG	5'-atggcgacaatgcaggacagtaga-3'	5'-gatcccagaaaatgcctccaatg-3'	55°C
CEBPZ	5'-ggagctggaagcctggtatg-3'	5'-gctctgggaggtgctgtg-3'	55°C

GAPDH- Glyceraldehyde-6-phosphate dehydrogenase; CEBPA- CCAAT enhancer binding protein alpha; CEBPB- CCAAT enhancer binding protein beta; CEBPD- CCAAT enhancer binding protein delta; CEBPG- CCAAT enhancer binding protein gamma; CEBPZ- CCAAT enhancer binding protein zeta. The PCR was performed with an initial denaturation at 95°C for 15 mins, followed by 45 cycles of 94°C for 15 s, annealing for 30s and extension at 72°C for 30s with a final melting curve analysis.

**Table 2 Differential expression of C/EBP isoforms in human ovarian carcinoma cells (2008, 2008/C13\*)**

<i>Genes</i>	<i>2008 Ct values</i>	<i>2008T Ct values</i>	<i>2008/C13* Ct values</i>	<i>2008/C13*T Ct values</i>	<i>Fold difference between 2008T and 2008</i>	<i>Fold different between C13 and 2008</i>	<i>Fold difference between C13T and C13</i>
<b>GAPDH</b>	16.0±0.7	16.4±0.2	17.1±0.7	16.7±0.5	-	-	-
<b>C/EBP<math>\alpha</math></b>	26.0±0.6	25.3±1.0	28.0±1.2	26.2±1.8	<b>2.1</b>	<b>0.5</b>	<b>2.8</b>
<b>C/EBP<math>\beta</math></b>	22.7±0.9	21.9±0.1	23.7±0.7	23.0±1.6	<b>2.3</b>	<b>1.1</b>	<b>1.2</b>
<b>C/EBP<math>\delta</math></b>	25.9±0.7	26.7±0.8	26.3±0.6	25.6±1.2	<b>0.7</b>	<b>1.6</b>	<b>1.2</b>
<b>C/EBP<math>\gamma</math></b>	22.8±0.5	22.6±1.5	23.4±1.7	23.3±1.9	<b>1.5</b>	<b>1.4</b>	<b>0.8</b>
<b>C/EBP<math>\zeta</math></b>	26.3±0.5	23.7±1.1	27.0±0.6	27.5±0.4	<b>8.0</b>	<b>1.3</b>	<b>0.5</b>
<b>or GADD 153</b>							

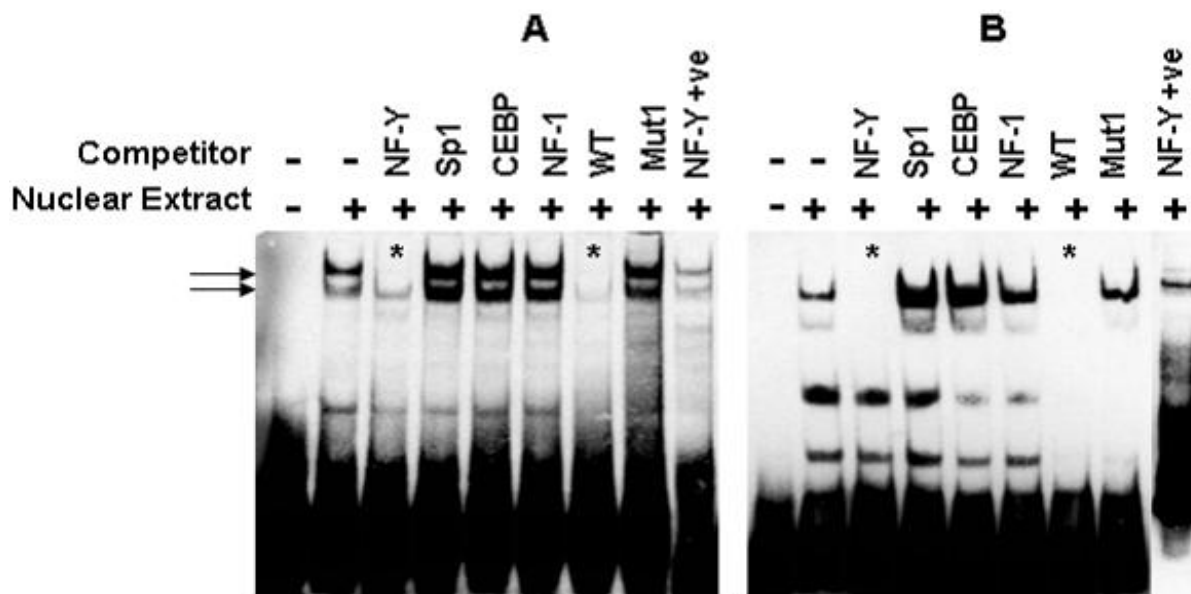


**Figure 1. Confirmation of NF-Y binding to the proximal promoter region of the AKR1C1 gene.** NF-Y is composed of three subunits NF-YA, NF-YB and NF-YC that are required for interaction with the CCAAT pentanucleotide sequence in the AKR1C1 gene promoter. Nuclear extracts (8 $\mu$ g) from (A) 2008, (B) 2008/C13\*, were incubated with WT probe (-120 to -91) from DDH1 gene along with 2 $\mu$ g of polyclonal antibody directed towards NF-YA, NF-YB or NF-Y (NF-YA+NF-YB+NF-YC). The negative control consisted of rabbit pre-immune control IgG (C-IgG). The formation of DNA-protein complexes is designated by solid arrows and the loss of protein-DNA complex's and/or gel super-shift in the presence of the antibody is denoted by an asterisk. Each of the experiments was repeated at least three times with similar results.

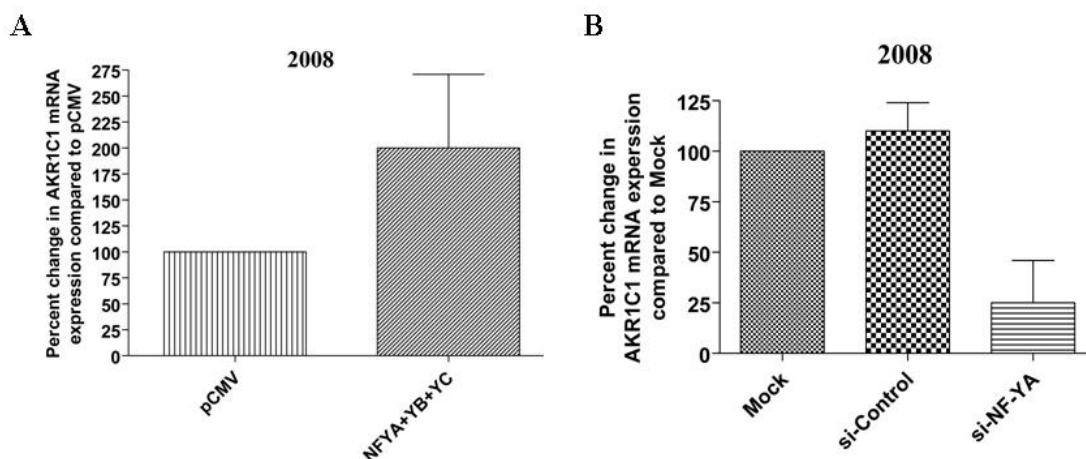


**Figure 2. Functional analysis of NF-Y in regulating the transcription of human AKR1C1 in human ovarian, lung and liver carcinoma cells. (A)** 1 $\mu$ g of NF-YA, -YB and -YC cDNA expression vector or pCMV control vector and **(B)** Five hundred picomoles of NF-YA siRNA or siRNA-scramble as the negative control. Twenty four hours after transfection RNA was isolated and the expression of AKR1C1 mRNA was assayed using real-time RT-PCR. Each experiment was performed in duplicates and repeated at least two times.

#### **Research Project 4: Project Title and Purpose**

*Development of a Microvascular Network on a Chip* - Recognition of drastically altered endothelial surfaces in various pathologies (e.g., tumors) has led to the concept of endothelial cell adhesion molecule mediated targeted delivery using nanoparticles as drug carriers. However, currently there are no realistic test beds for preclinical testing and optimization of these nanoparticles in a realistic environment. Development of more complex, realistic in vitro flow chambers will not only advance our knowledge in targeted drug delivery but may also reduce the need for animal experimentation. In this project we will design an anatomically realistic in vitro microfluidic chip for testing and optimization of drug carriers and develop protocols for successful growth of cells on the chips to study drug carrier-cell interaction.

#### **Duration of Project**

7/1/2009 - 6/30/2010

#### **Project Overview**

Drug carrier adhesion to tissue (vascular endothelium) depends critically upon particle/cell property (size, receptors), scale/geometric features of vasculature (diameter, bifurcation, etc.) and local hemodynamic factors (stress, torque etc). Currently, this is investigated using in-vitro parallel-plate flow chambers which suffer from several serious limitations including (a) idealized, macrocirculatory scaling (b) lack of critical morphological features (junctions, network), healthy vs. diseased vasculature and (c) large volumes (several ml) and (d) contamination due to non-disposability. We propose to develop a novel microfluidics-based

platform for cell/drug-particle adhesion which overcomes these limitations. The proposed microvascular environment will be used to gain new insights and make quantitative predictions on particle adhesion in the microvasculature.

Anatomically detailed microvascular network structures will be obtained from in-vivo image data and patterned onto a plastic, disposable substrate (PDMS). Perfusion and particle adhesion studies will be carried-out and the data will be analyzed using high-fidelity computational models. The presence of significant stagnant regions, non-intuitive particle and flow splits, spatially non-uniform adhesion as well as first evidence of dependence of particle adhesion on vessel branching angle will be identified and documented. In addition, endothelial cells will be cultured on the PDMS and the upregulation of adhesion molecule (P-selectin) and subsequent adhesion of anti-P-selectin coated particle to the cultured endothelial cells will be demonstrated. Net usage of reagents in these models will be quantified. By enabling the study of particle/cell-tissue interactions under controlled conditions that truly mimic the microvascular environment, the proposed study will advance drug discovery and delivery research in a variety of therapeutic areas including inflammation, allergy/infectious disease, cardiovascular disease and cancer among others. A multidisciplinary team has been assembled with expertise in microcirculation and cell adhesion research, microfabrication/microfluidics, computational modeling and intra-vital microscopy.

### **Principal Investigator**

Mohammad F. Kiani, PhD  
Professor and Chair  
Temple University  
Department of Mechanical Engineering  
1947 N. 12<sup>th</sup> St.  
Philadelphia, PA 19122

### **Other Participating Researchers**

Jenna Rosano, BS - employed by Temple University

### **Expected Research Outcomes and Benefits**

Expected research outcomes of the project are:

- a. The design of an anatomically realistic in vitro microfluidic chip for testing and optimization of nanoparticle drug carriers,
- b. Development of protocols for successful growth of cells (endothelial and/or cancer cells) on the chips to study nanoparticle-cell interaction.

Currently available flow chambers feature a common theme of mathematically idealized geometries (rectangular, circular, etc.). These simplifications have the benefit of readily characterized (indeed constant) shear stress and other fluidic parameters, which can be used directly in the interpretation of experimental results. However, in-vitro flow chambers as used currently have many limitations (e.g., over-simplified geometries). The field of targeted drug

delivery will be advanced significantly by the proposed new in vitro system which truly mimics microvascular dimensions and geometry. The proposed integrated system will be superior to currently available technologies in the following aspects:

- Realistic in-vivo structures tested in-vitro (bifurcations, networks, etc.)
- Disposable chips with innovations for growth of cells (cell matrix, supply of nutrients, etc.)
- Reduced reagent/cell use, disposable chips
- Better fundamental understanding of drug carrier-cell interaction and its corroborations with flow/geometry features.

## **Summary of Research Completed**

### Materials and Methods

#### *Antibodies and Reagents*

A mouse monoclonal anti-ICAM-1 (cat. No. NB500-318) which cross-reacts with bovine was purchased from Novus Biologicals. Human IgG1 Kappa (cat. No. PHP010) purified from myeloma serum was obtained from Serotec, MorphoSys (Raleigh, NC). Human fibronectin was obtained from BD Biosciences (San Jose, CA). Recombinant Human TNF- $\alpha$  was purchased from BioVision (Mountain View, CA). Protein A was purchased from Zymed (San Francisco, CA). Fluorescent 2- $\mu$ m microspheres (red: excitation 543 nm, emission 612 nm; blue: excitation 412 nm, emission 473 nm) were purchased from Duke Scientific (Palo Alto, CA). Bovine aortic endothelial cells (BAEC), EBM cell media, and EGM SingleQuots media supplements were purchased from Lonza (Allendale, NJ).

#### *Creating Synthetic Microvascular Networks*

The microvascular network of a hamster cremaster muscle was mapped using a modified Geographic Information Systems (GIS) approach. Polydimethylsiloxane (PDMS) microvascular networks were created using soft lithography techniques described previously. In brief, the digitized networks were printed at high resolution on Mylar film, which served as a photo mask for ultraviolet light for patterning a positive photoresist mold on top of a silicon wafer. Sylgard 184 PDMS was prepared according to manufacturer's instructions (Dow Corning, Midland, MI) and cast over the photoresist mold. A beveled 16-gauge needle was used to punch the inlets and outlets in the molded PDMS. The bonding surfaces of the PDMS and a pre-cleaned 1 $\times$ 3 inches glass slide (Fisher Scientific, Pittsburgh, PA) were treated with oxygen plasma (200 m Torr, 18 W, 30 s) produced in a plasma cleaner (Harrick Scientific, Ithaca, NY). The assembly was heated at 75°C for 10 min on a hotplate to achieve a good seal between PDMS and glass. Tygon Microbore tubing with an outside diameter of 0.06 in. and inner diameter of 0.02 in. connected to a 22 gauge stainless steel needle served as the connecting port to the synthetic microvascular network (SMN). The devices were sterilized by autoclaving following bonding. This study was performed on networks with constant depths of either 50 or 100  $\mu$ m.

#### *Seeding of Bovine Aortic Endothelial Cells in Synthetic Microvascular Networks*

Prior to cell seeding, each SMN was flushed with sterile EBM cell culture medium to prepare the device for seeding, then perfused with fibronectin (50 µg/ml) and allowed to incubate at room temperature for 30 min. The SMN was flushed again with cell culture medium supplemented with EGM SingleQuots and 20% Fetal Bovine Serum (FBS) to remove excess fibronectin. The fibronectin-coated SMN was kept in an incubator at 37°C, 5% CO<sub>2</sub>, while BAEC in flasks were prepared for injection.

Bovine aortic endothelial cells (BAEC) were cultured in treated 75 cm<sup>2</sup> polystyrene flasks. Cells were maintained using endothelial cell basal medium (EBM) supplemented with EGM SingleQuots. The cultured BAEC were lifted from the flasks with trypsin and diluted to 10<sup>7</sup> cells/ml with EBM medium supplemented with EGM SingleQuots and 20% FBS. The SMN was seeded through an inlet via syringe using approximately 0.1 ml of the 10<sup>7</sup> cells/ml suspension. A Nikon Eclipse TE200 inverted microscope was used to observe cell injection to ensure an even spread of cells throughout the network. The seeded SMN was incubated at 37°C and fresh cell medium was perfused through the SMN once per day, starting 1 day after seeding. To change the medium, room temperature EBM medium was perfused through a single inlet of the SMN at a flow rate of 10 µl/min via a syringe pump.

#### *Propidium Iodide Staining*

Propidium iodide (PI) staining of live cells was used to show the viability of confluent BAECs in the SMNs. Viable cells with intact membranes exclude PI, whereas permeabilized cells stain positive with PI. Briefly, 4 days after seeding, live endothelial cells were stained with 1.5 µg/ml of PI for 20 min. This was performed without washing to avoid loss of floating nonviable cells. For positive controls, endothelial cells were permeabilized with 80% ethanol for 5 min before being stained with PI. PI positive cells were observed under a Nikon Eclipse TE200 inverted microscope equipped with UV fluorescence. Images of PI stained cells were taken using a Q Imaging Retiga 1300 (Surrey, BC, Canada) camera and Image-Pro Plus (Bethesda, MD) imaging software.

#### *Antibody Conjugated Microspheres*

2 µm fluorescent polystyrene microspheres were washed with a sodium bicarbonate buffer and coated with protein A via passive adsorption and incubated overnight at room temperature. The microspheres were then washed and incubated in a blocking buffer (Hank's balanced saline solution supplemented with 1% bovine serum albumin) at room temperature. The microspheres were conjugated with a mAb solution of either anti-ICAM-1 (red microspheres) or IgG1 (blue microspheres) and stored at 4°C until use. IgG conjugated microspheres served as a control for nonspecific binding. Immediately before use, the microspheres were resuspended in EGM media supplemented with 20% FBS, and diluted to a concentration of 10<sup>7</sup> microspheres/ml.

#### *Microsphere Adhesion to Upregulated Endothelial Cells*

The SMN (80 to 90% confluent with BAEC) was perfused with EBM medium containing 10 U/ml TNF-α to activate the endothelial cell layer; non-activated SMNs were used as negative control. The SMN was incubated for either 4 or 24 h. Equal numbers of anti-ICAM-1 and IgG

conjugated microspheres were diluted together in EBM medium to  $10^7$  microspheres/ml and injected at a flow rate of 0.5  $\mu$ l/min using a syringe pump and allowed to settle for 30 min in an incubator at 37°C. EBM medium was perfused through the SMN to remove non-adhered microspheres.

## Results

Our GIS-based system was used to map microvascular networks of the hamster cremaster muscle from a montage of fluorescent images (Figure 1(a)) which were then digitized (Figure 1(b)) and used as a geometric blueprint for fabrication of the PDMS synthetic microvascular networks (Figure 1(c)). Endothelial cells readily attached to the walls of the synthetic microvascular network (SMN) within 2 h after seeding. Figure 2 shows the progression of BAEC growth in the SMN towards confluency, peaking at 4 days after seeding. Cells grew as monolayers and exhibited a cobblestone morphology, elongated in the direction of fluid flow, typical of endothelial cells found in vivo. No detectable cell death in BAECs cultured in the SMN was observed, as demonstrated by negative labeling of live endothelial cells with propidium iodine (PI) which labels membrane compromised cells. As shown in Figure 3(a), confluent BAECs cultured in the SMN showed efficient exclusion of PI, indicating their viability at confluency. On the other hand, BAECs permeabilized with ethanol, used as positive controls, demonstrated PI fluorescence, see Figure 3(b).

The level of adhesion of anti-ICAM-1 conjugated microspheres to the endothelial lining of the SMNs was quantified after activation of BAECs with TNF- $\alpha$  and compared to the level of adhesion to activated cells in cell culture flasks. As shown in Figure 4, a significantly larger number of anti-ICAM-1 conjugated microspheres (shown in red) adhered to activated endothelial cells as compared to IgG conjugated microspheres (green), indicating preferential adherence of anti-ICAM-1 microspheres. In agreement with our previous findings, we observed a basal level of adhesion of anti-ICAM-1 conjugated microspheres to non-activated endothelial cells (Figure 5). However, the adhesion patterns of these antibody conjugated microspheres were not uniform throughout these SMNs similar to our previous observations on protein coated SMN. Furthermore, as shown in Figure 5, a significant increase in the number of anti-ICAM-1 conjugated microspheres adhering to activated endothelial cells at 4 and 24 h after activation, compared to non-activated control cells, was observed (79% and 161% increase in microsphere adhesion to activated cells compared to non-activated cells, respectively). Endothelial cell adhesion molecules (ECAMs) of endothelial cells lining the SMN, upregulated by either 4 or 24 hr of incubation with TNF- $\alpha$ , demonstrated an adhesion molecule profile consistent with other studies both in vitro and in vivo. In addition, the increase in the number of anti-ICAM-1 microsphere adhesion 24 hr after activation of endothelial cells is in general agreement with previous finding from our group and others.

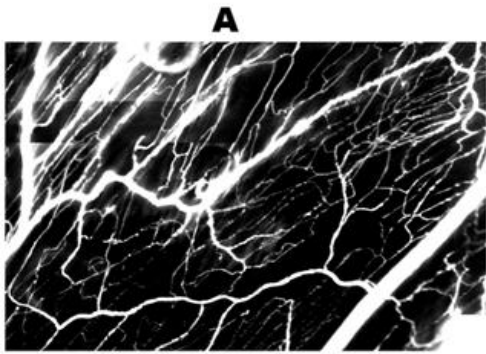
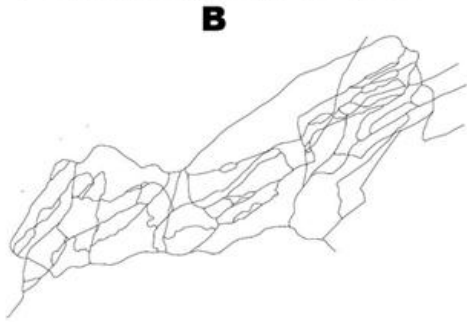
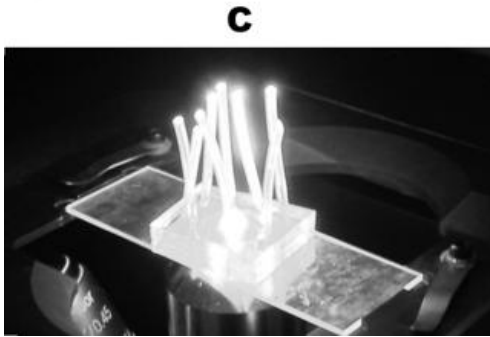


Figure 1. Panel (a) shows a montage of fluorescent images obtained in vivo from the cremaster muscle after I.V. injection of FITC-dextran.



Our GIS-based system was used to digitize this microvascular network, panel (b).



This digitized map was then used to generate the synthetic microvascular network on PDMS, shown here perfused with trypan blue, panel (c).

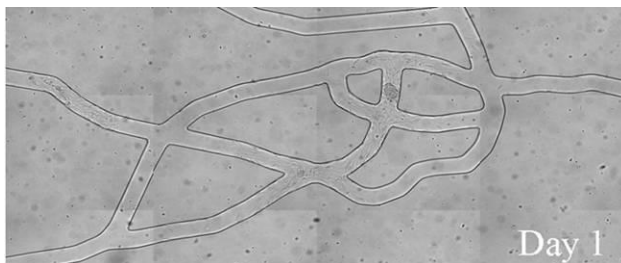
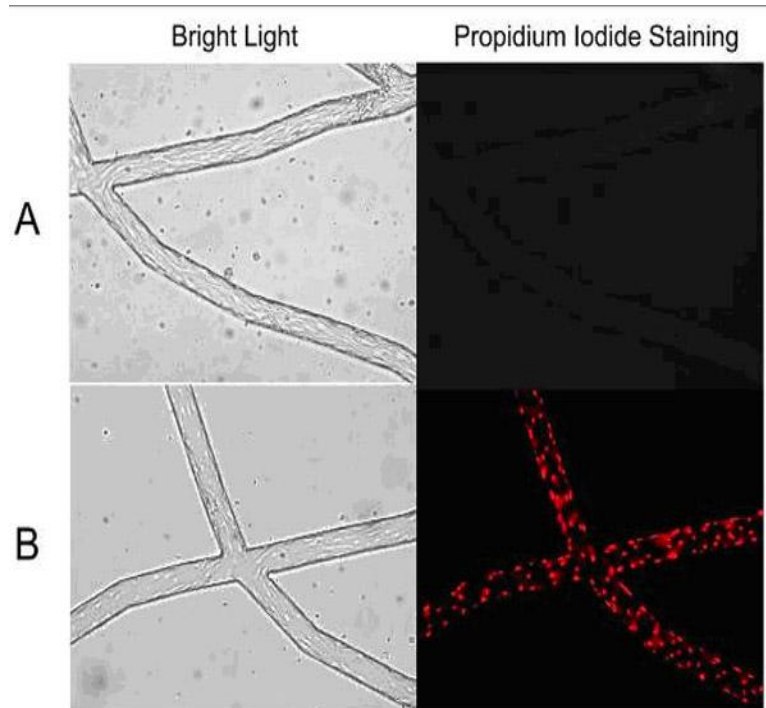


Figure 2. Bovine aortic endothelial cells seeded in the PDMS chambers became confluent throughout the network after 3 to 4 days. Cells exhibited the normal cobblestone configuration in the direction of flow.



Figure 3. Endothelial cells cultured in the synthetic microvascular network were stained with propidium iodide (PI) to examine cell viability. (a) The left panel demonstrates representative phase image of endothelial cells cultured in the SMN. Live endothelial cells cultured in the SMN were stained with PI at confluency. The right panel illustrates exclusion of PI in these cells, demonstrating their viability. (b) The left panel shows representative phase images of control endothelial cells following fixation with ethanol. The right panel represents uptake of PI in positive controls, following fixation/permeabilization of these cells with ethanol.



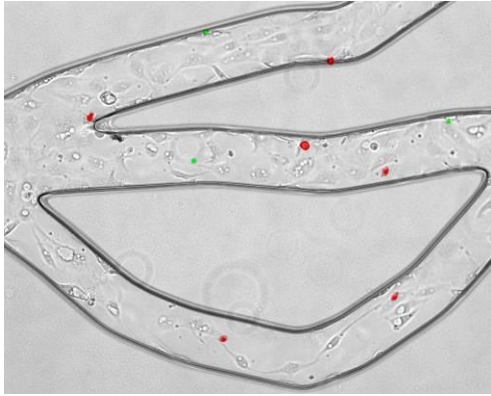
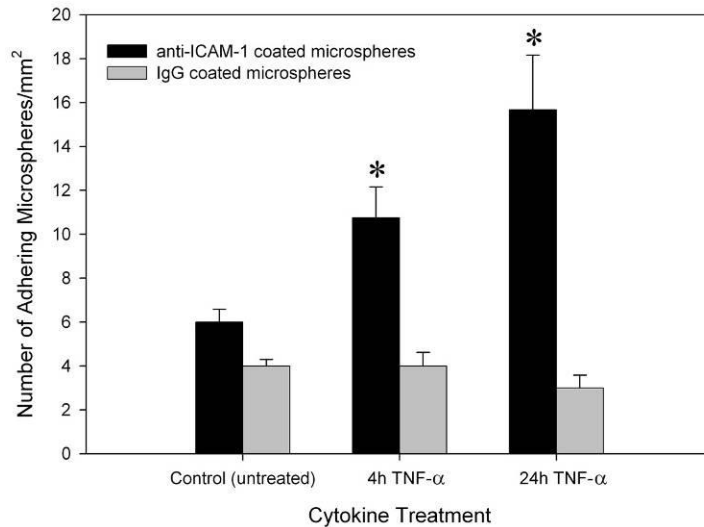


Figure 4. Anti-ICAM-1 (red) and IgG1 (green) conjugated microspheres attached to activated bovine aortic endothelial cells in one region of the network. Anti-ICAM-1 conjugated microspheres show preferential adhesion to endothelial cells as compared to IgG conjugated microspheres.

Figure 5. Anti-ICAM-1 conjugated microspheres were found to adhere preferentially to bovine aortic endothelial cells within the synthetic microvascular network (SMN) after 4 and 24 hr activation with TNF- $\alpha$ . Mean  $\pm$  SEM; n=4 SMN per TNF- $\alpha$  treated groups and n=3 SMN for untreated control group, \* P<0.05 indicates significant differences in anti-ICAM-1 adhesion in SMN compared to the non-activated control group.



## **Research Project 5: Project Title and Purpose**

*CB1 Antagonists as Neuroprotective Drugs* - The purpose of this project is to improve our understanding of how a drug that was designed to block the effect of chemicals produced by the brain called cannabinoids might be used to protect the central nervous system from injury following trauma or an interruption in blood flow.

### **Duration of Project**

7/1/2009 - 6/30/2010

### **Project Overview**

The hypothesis that will be investigated in this project is that the drug SR141716A, originally developed as a selective CB<sub>1</sub> antagonist, has activity at receptors other than the CB<sub>1</sub> receptor that contribute to its neuroprotective activity and that the mechanisms responsible for its neuroprotective effect are different from those responsible for the protective effect of CB<sub>2</sub> agonists. Preliminary results from our laboratory have provided evidence that the CB<sub>1</sub>

antagonist SR141716A provides protection for the CNS (central nervous system) during ischemia and trauma. We have also shown that the combination of a CB<sub>1</sub> antagonist and a CB<sub>2</sub> agonist has a synergistic effect in protecting the nervous system. These findings are novel in that it is speculated that activation of the CB<sub>1</sub> receptor should be neuroprotective. An explanation for the discrepancy between our findings (that a CB<sub>1</sub> antagonist is neuroprotective) and the prediction that CB<sub>1</sub> activation would be neuroprotective is that SR141716A functions as an agonist at receptors other than CB<sub>1</sub>. Elucidation of the mechanism through which SR141716A has a neuroprotective effect could lead to the development of more effective therapies for the treatment of CNS diseases such as stroke and trauma. The therapeutic measures currently available for treatment of these diseases are very limited. In specific aim 1 SR141716A will be administered to genetically altered animals that lack the CB<sub>1</sub> receptor to determine whether the drug still has a neuroprotective effect following cerebral ischemia and reperfusion. Dose response studies with both SR141716A and a CB<sub>2</sub> agonist will be conducted to provide data to evaluate receptor interactions using mathematical modeling techniques. In the second specific aim the drug will be administered to animals that have been treated with antagonists for the other receptors (vanilloid and serotonin) that may be activated by SR141716A and contribute to the neuroprotective effect following stroke.

### **Principal Investigator**

Ronald F. Tuma, PhD  
Professor  
Temple University School of Medicine  
3400 North Broad Street  
Philadelphia, PA 19140

### **Other Participating Researchers**

Zachary Reichenbach, BS, Ming Zhang, MD, PhD - employed by Temple University

### **Expected Research Outcomes and Benefits**

It is expected that the results obtained from this project will significantly enhance our understanding of how activation specific molecules (receptors) on cells within the central nervous system may provide protection from injury. Currently there are no effective treatments to attenuate the damage to the central nervous system following trauma or an interruption in blood flow. The development of more effective drugs that can provide protection to the central nervous system would significantly reduce the damage that occurs following trauma or stroke, and improve the quality of life for individuals suffering from these problems.

### **Summary of Research Completed**

The primary goal of this investigation was to determine if the drug rimonabant (SR141716A), originally developed as a selective CB<sub>1</sub> receptor antagonist, has activity at receptors other than the CB<sub>1</sub> receptor that contribute to its neuroprotective activity and that the mechanisms

responsible for its neuroprotective effect are different from those responsible for the protective effect of CB<sub>2</sub> agonists.

## Methods

To accomplish this goal, the effect of rimonabant on a number of outcome parameters following stroke were examined in the presence of selective antagonists for the vanilloid and serotonin receptors and in CB<sub>1</sub> and CB<sub>2</sub> knockout mice. Included among the outcome parameters evaluated were white cell rolling and adhesion, infarct size and neurologic score. White cell rolling and adhesion are a prerequisite for white cell invasion, a factor clearly demonstrated to exacerbate damage in ischemia/reperfusion injury. All studies were carried out using C57/Bl6 mice as the animal model.

Cranial Windows were implanted to allow for direct visualization and measurement of the pial microcirculation in the region of ischemia/reperfusion. On the day of cranial window implantation, the animals were anesthetized with an intraperitoneal injection of Ketamine (100mg/ml) - Xylazine (20mg/kg) mixture (1:1) at a dose of 1ml/kg. The head was shaved and positioned in a stereotactic head holder. A 1cm area of skin on the dorsal surface of the skull over the right cortical hemisphere was excised and the periosteum was removed. A 4mm diameter circular craniotomy was performed using a high speed drill (Champ-Air Dental Drill Benco Dental) over the right parietal cortex extending from attachment of temporal muscle to midpoint of sagittal suture in the coronal direction and aligned to middle of sagittal suture so that the window contained some terminal branches of middle cerebral artery. Normal saline (37 °C) was dripped over the cranium to avoid thermal injury of the cortex. The dura was removed and exposed brain was kept moist with 37 °C artificial cerebrospinal fluid (CSF) solution. A 5mm diameter coverglass was then placed over the exposed brain, and an airtight seal was produced using Nexaband Quick seal. The coverglass provided adequate mechanical protection from infection or contamination. A recovery period of four days was allowed between implantation of the cranial window and the induction of transient focal ischemia.

Ischemia/reperfusion injury was induced by transient occlusion of the middle cerebral artery. The animals were anesthetized with an intraperitoneal injection of Ketamine (100mg/ml) - Xylazine (20mg/kg) mixture (1:1) at a dose of 1ml/kg. Body temperature was maintained at 37±5 °C by a heating lamp and heating pad. Middle cerebral artery occlusion was achieved by the intraluminal filament methods.(Hata, Mies et al. 1998) Briefly, a midline neck incision was made under the operation microscope; the right common carotid artery (CCA), external carotid artery (ECA) and internal carotid artery (ICA) were isolated. The ECA was ligated with 6-0 silk suture distal from the ICA-ECA branch and then cut distally from the ligation point. Another 6-0 silk suture was tied loosely around the ECA at close to the origin of the CCA. A blunted 5-0 monofilament nylon suture coated with poly-L-lysine (0.1% in deionized water, Sigma) was introduced through a small incision on the ECA and then advanced into the circle of Willis, and finally to the origin of the middle cerebral artery. The silk suture around the ECA stump was tied tightly to prevent bleeding and secure the nylon suture. The nylon suture was removed after 60 minutes occlusion, and the ECA was permanently tied. Reperfusion was confirmed when pulsations were again observed in the ICA. A laserPro Blood Perfusion Monitor (TSI Inc) was used to monitor regional cerebral blood flow (rCBF) prior to ischemia, during Middle Cerebral

Artery Occlusion (MCAO) and during reperfusion. A 1mm diameter microfiber laser-Doppler probe was attached to the skull 4mm lateral and 2mm posterior of the bregma. The MCAO was considered adequate if rCBF showed a sharp drop to 25% of the baseline (pre-ischemia) level, otherwise, animals were excluded.

Leukocyte/endothelial interactions were evaluated before MCAO, 1 hour after MCAO and 24 hours after MCAO. Each vessel was exposed to the light of the microscope for 30 seconds at each viewing to minimizing phototoxicity.<sup>14</sup> Three venules (with diameter 30-50  $\mu\text{m}$ ) and three arterioles (with diameter 20-40  $\mu\text{m}$ ) in each animal were assessed. The number of rolling leukocyte was considered to be the total number of leukocytes moving along the endothelial cells at substantially slower velocity compared with the midstream blood cell velocity. They were counted when they passed an arbitrary line perpendicular to the longitudinal axis of the vessel over a period of 30 seconds. Adhering leukocytes were defined as the total number of the leukocytes firmly attached to the microvascular endothelium that did not change their location during the entire 30 seconds of observation period. Adhering leukocytes were scored as the number of cells per  $\text{mm}^2$  of the vascular surface area, calculated from the diameter and standardized length (100  $\mu\text{m}$ ) of the vessel segment under investigation.

For assessment of infarct volume, the animals were euthanized with an overdose of pentobarbital (200mg/kg i.p) 24 hours after MCAO, and then the brains were removed. The brains were chilled in ice for 10 minutes to slightly harden the tissue. Five 2mm coronal sections were cut using a mouse brain matrix (Zivic lab). The brain sections were placed in 2% triphenyltetrazolium chloride (TTC) (Sigma, Inc) dissolved in saline and stained for 20 minutes at 37°C in the dark. The brain sections were then fixed in 4% paraformaldehyde at 4°C for 24 hours, and the anterior and caudal face of each section was scanned by a flatbed color scanner (Microtek Inc). The resulting images were captured as JPEG files and analyzed with NIH image software. The infarct volumes were expressed as  $\text{mm}^3$  as well as the percentage of the ipsilateral hemisphere.

The severity of neurological deficits was evaluated twenty four hours after ischemic insult using a five-point deficit score (0=normal motor function; 1=flexion of torso and of contralateral forelimb upon lifting of the animal by tail; 2=circling to the contralateral side but normal posture at rest; 3=leaning to contralateral side at rest; and 4=no spontaneous motor activity).

#### Statistical analysis

Numbers of leukocytes rolling on and adhering to venules or arterioles were analyzed by two-way (treatments, times) analysis of variance (ANOVA) with repeated measurements followed by Bonferroni test. One-way ANOVA was used for analyzing differences in either infarct volume or neurological score. Data were presented as means  $\pm$ SEM. A statistically significant difference was assumed at  $P < 0.05$ .

#### Results

The results of our investigation demonstrated that when rimonabant and a selective CB<sub>2</sub> agonist (O-1966) were co-administered, cerebral blood flow during occlusion increased above the levels measured in untreated animals (Figure 1). Neither the selective CB<sub>1</sub> antagonist nor CB<sub>2</sub> agonist given in isolation were able to increase flow during occlusion. This increase in flow was

accompanied by an increase in the diameter of pial arterioles (Figure 2). This is an important finding since this drug combination may have potential to enhance collateral blood flow during stroke and perhaps myocardial infarction. We were also able to demonstrate that this effect was not influenced when administered in the presence of an antagonist for the vanilloid receptor (capsazepine), but was significantly attenuated when administered in the presence of an antagonist for the serotonin receptor (WAY100135). This was the first evidence that rimonabant may have activity at the serotonin receptor.

We were also able to demonstrate that the synergistic effect of the selective CB2 agonist and CB1 antagonist in reducing infarct size was not influenced by capsazepine, but was significantly attenuated when a serotonin antagonist was administered (Figure 3). In addition the synergistic effect of the combined CB1 antagonist and CB2 agonist were maintained when given to CB1, but not CB2 deficient animals. This provided evidence that the protective effect of the combined therapy did not require CB1 activation.

Although the synergistic effect of the CB1 antagonist and CB2 agonist involve the serotonin receptor, we were also able to demonstrate the rimonabant, when given alone is still neuroprotective, but this mechanism of neuroprotection is independent of the serotonin receptor (Figure 4). The results from this component of the study correct a number of misconceptions in the literature. Although CB1 receptor activation was reported to be neuroprotective through inhibition of excitotoxicity, this was later shown to be the effect of CB1 induced hypothermia. The results of our investigation showed that the CB1 receptor antagonist reduced infarct size and improved neurologic score when given alone. It also showed that blocking the serotonin receptor had no influence on this protective effect.

It is usually reported in the literature that the CB2 receptor predominantly influences inflammatory cells while the CB1 receptor only influence synaptic transmission. The results of our investigation also provided evidence that this is not the case, since administration of rimonabant significantly attenuated white blood cell rolling and adhesion (Figure 5). The results of this component of the study indicate a direct effect of the CB1 antagonist on endothelial and/or white blood cells. These studies provide evidence for a proinflammatory effect of the CB1 receptor.

### Summary

The results of our investigation provide new information about the actions of rimonabant and the CB1 receptor. These results demonstrate that the combination of a CB2 agonist and CB1 antagonists produces unique effects, including: enhanced blood flow, reduced infarct size and improved neurologic function, and that these effects involve activation of the serotonin receptor. The vanilloid receptor does not appear to be involved in these responses. In addition the results of this project demonstrate a proinflammatory effect for the CB1 receptor, and that this effect involves endothelial cells and/or white blood cells.

FIGURE 1

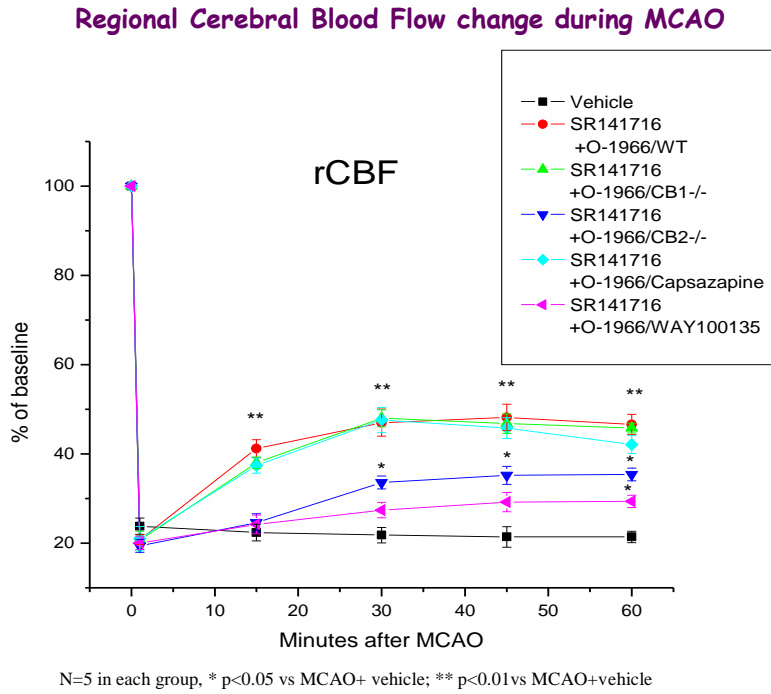


FIGURE 2

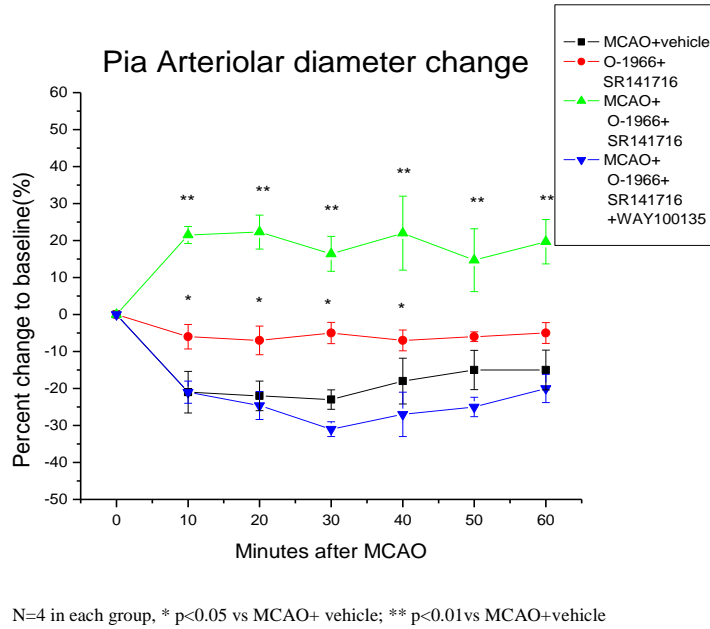


FIGURE 3

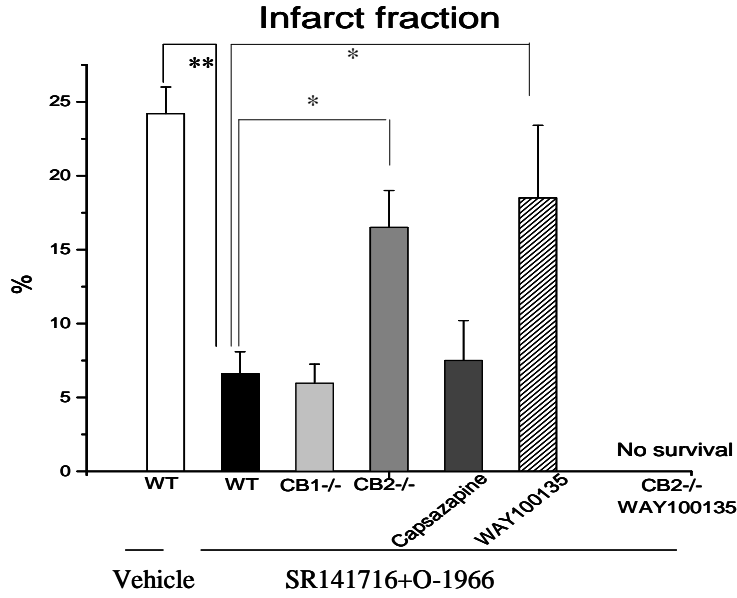
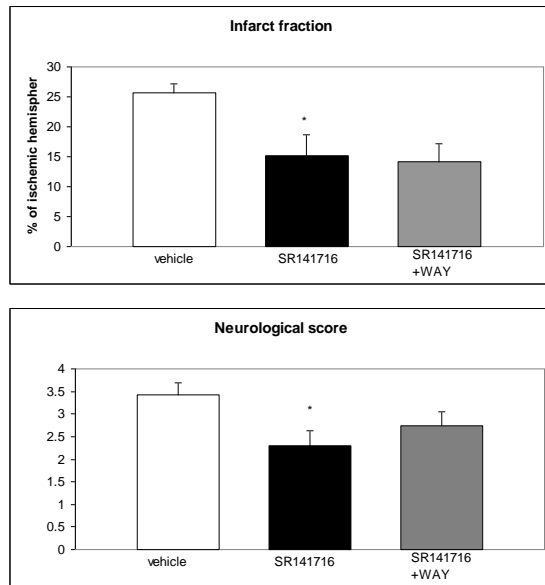
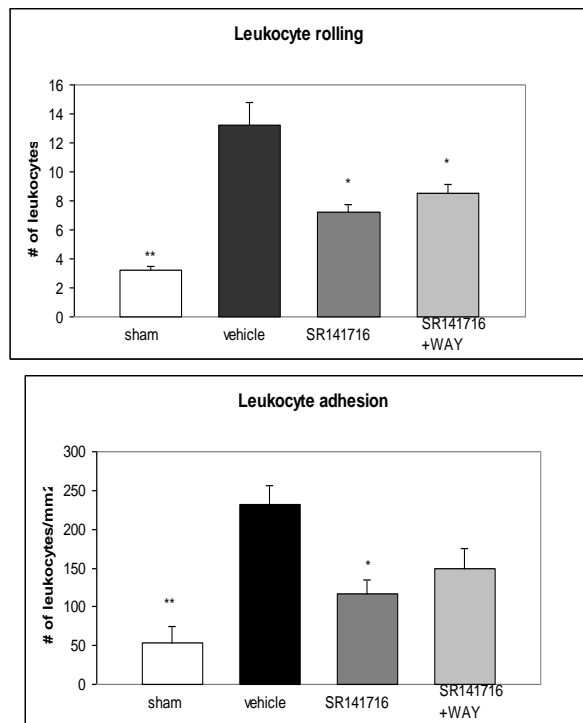


FIGURE 4



SR141716 and WAY were given at 1 hour after ischemia, at both 5mg/kg by i.p.

FIGURE 5



SR141716 and WAY were given at 1 hour after ischemia, at both 5mg/kg by i.p.

### **Research Project 6: Project Title and Purpose**

*The Role of GSK3 in Psychostimulant-Induced Behaviors* - Abuse of psychostimulants including cocaine and amphetamine continues to be a major public health problem that leads to loss of employment productivity, breakdown of families and communities, increases in crime and violence, and a variety of health issues not only for the individual but also for their children. Treatments for addiction to psychostimulants are lacking. As such, identification of potential novel targets for treatment of psychostimulant abuse is needed. This project will examine a novel cellular pathway that mediates some of the behavioral effects of cocaine and amphetamine. The role of the Akt-GSK3 pathway in psychostimulant-induced behaviors will be investigated, as will methods to regulate its function in order to reduce the addictive properties of these drugs.

### **Anticipated Duration of Project**

2/1/2009 - 7/31/2010

### **Project Overview**

Identifying the mechanisms underlying drug-induced reward and plasticity is critical for the design of therapeutics to treat psychostimulant addiction. One molecule that has received attention recently for its role in psychiatric disorders and the therapeutics used to treat them is

glycogen synthase kinase-3 (GSK3). Evidence suggests that GSK3 is uniquely situated to modulate neuronal function and plasticity. Further, our published and preliminary data demonstrate that GSK3 activity is necessary for the manifestation of cocaine-induced behaviors and that the activity of GSK3 is regulated during cocaine exposure in a brain-region specific manner. The central hypothesis that will be investigated is that GSK3 is a critical molecular mediator of psychostimulant-induced actions including drug reward and drug-seeking behaviors. Further, we hypothesize that exposure to psychostimulants results in adaptations in GSK3 signaling and that these adaptations may underlie drug-induced neural plasticity contributing to the perpetuation of addictive disease.

The first research aim will be to determine the role of GSK3 in cocaine- and amphetamine-induced reward, extinction, and reinstatement. The contribution of GSK3 to the rewarding effects of cocaine and amphetamine will be determined using the conditioned place preference procedure in adult male mice. The role of GSK3 in the different phases of drug-induced reward will be evaluated including the development and expression of conditioned reward and the retrieval and reconsolidation of drug-associated contextual memories. The goal of this aim is to establish GSK3 as a target for new therapeutics for the treatment of addictive disease.

The second research aim will be to define the regulation of the GSK3 signaling pathway during cocaine and amphetamine exposure. The activity of GSK3 is regulated by its phosphorylation state. Changes in GSK3 phosphorylation, and hence activity, will be measured following acute and repeated administration of cocaine and amphetamine. Immunohistochemistry with antibodies that are selective for the phosphorylated state of GSK3 will be used to characterize the cellular and subcellular localization of drug-induced changes in GSK3 function. Identification of the cell types showing regulation of GSK3 activity will be determined, as will drug-induced changes in the subcellular distribution of GSK3. GSK3 will be identified on tissue sections from mouse brain following administration of cocaine and amphetamine.

### **Principal Investigator**

Ellen M. Unterwald, PhD  
Professor of Pharmacology,  
Director of the Center for Substance Abuse Research  
Temple University School of Medicine  
3420 N. Broad Street  
Philadelphia, PA 19140

### **Other Participating Researchers**

Nicole M. Enman, BS – PhD student in the Department of Pharmacology at Temple University School of Medicine

### **Expected Research Outcomes and Benefits**

The goal of this project is to provide pre-clinical evidence to support the potential use of modulators of the GSK3 signaling pathway for the treatment of cocaine and/or amphetamine

addiction. These studies will determine if modulation of GSK3 can interfere with processes involved in addiction to these psychostimulants. In addition, this project will investigate how exposure to cocaine and amphetamine alters this important intracellular pathway in brain regions critically involved in mediating the rewarding and conditioned stimulus effects of drugs of abuse. Establishment of GSK3 as a novel target for the treatment of psychostimulant addiction could be a major public health advancement and significantly reduce the costs of addiction to the individual and to society.

## Summary of Research Completed

### Materials and Methods

*Study 1: The effect of valproic acid (VPA) and SB 216763 on acute amphetamine-induced hyperactivity.*

Subjects: Male CD-1 mice (8 weeks old) were obtained from Charles River Laboratories (Wilmington, MA). Mice were housed five per cage on a 12-h light/dark cycle with *ad libitum* access to food and water. Animals were allowed to acclimate to the animal facility for seven days prior to behavioral testing, and were weighed and handled daily. All animal testing was conducted in accordance with the National Institutes of Health guidelines for the Care and Use of Laboratory Animals. All experimental protocols were approved by the Institutional Animal Care and Use Committee of Temple University School of Medicine.

Drugs: Sodium valproate (Sigma Aldrich; St. Louis, MO) and *D*-amphetamine (NIDA; Bethesda MD) were dissolved in sterile saline (0.9% NaCl). SB 216763 (Tocris Bioscience; Ellisville, MO) was dissolved in 3.6% DMSO (Sigma) and brought up to volume in Tocrisolve 100 (Tocris Bioscience).

Locomotor activity: Locomotor activity was evaluated in automated monitors (AccuScan Instruments, Inc., Columbus, OH). The number of photocell beam breaks in each chamber was recorded by a computer equipped with the Digiscan DMicro system. The system differentially measures horizontal movement and repetitive beam breaks, which characterize ambulatory activity and stereotypic activity, respectively. Mice (n=11/group) were placed in the activity monitors for 30 minutes to acclimate, and then pretreated with saline or valproate (50-300 mg/kg, i.p.). Thirty minutes later mice were injected with saline or amphetamine (2 mg/kg, i.p.), and activity was measured for 60 minutes. Separate sets of mice (n=12/group) were pretreated with SB 216763 (2.5-5.0 mg/kg, i.p.) or vehicle 20 minutes prior to saline or amphetamine (2 mg/kg, i.p.), and locomotor activity was recorded for 60 minutes.

Data analysis: Ambulatory and stereotypy data were analyzed for significance using two-way ANOVA and Bonferroni post-hoc analysis.

*Study 2: The effect of VPA and SB 216763 on the development of amphetamine-induced behavioral sensitization.*

Subjects: See Study 1.

Drugs: Sodium valproate (Sigma Aldrich; St. Louis, MO) and *D*-amphetamine (NIDA; Bethesda MD) were dissolved in sterile saline (0.9% NaCl). SB 216763 (Tocris Bioscience; Ellisville, MO) was dissolved in 3.6% DMSO (Sigma) and brought up to volume in Tocrisolve 100 (Tocris Bioscience).

Behavioral Sensitization: Mice (n=10-12/group) were pretreated once daily with VPA (300 mg/kg, i.p.) or saline 30 minutes prior to amphetamine (2 mg/kg, i.p.) or saline for five days. All mice were challenged with amphetamine (1 mg/kg, i.p.) in the absence of VPA seven days later. Ambulatory and stereotypic activities were measured for 30 minutes following amphetamine challenge. Separate sets of mice (n=8-12/group) were pretreated with vehicle or SB 216763 (5 mg/kg, i.p.) 20 minutes prior to amphetamine (2 mg/kg, i.p.) or saline once daily for five days. All mice were challenged with amphetamine (1 mg/kg, i.p.) in the absence of SB 216763 seven days later. Ambulatory and stereotypic activities were measured for 30 minutes upon amphetamine challenge.

Data Analysis: Ambulatory and stereotypy data were analyzed for significance using two-way ANOVA and Bonferroni post-hoc analysis.

*Study 3: The effect of VPA and SB 216763 on the development of amphetamine-conditioned reward.*

Subjects: See Study 1.

Drugs: Sodium valproate (Sigma Aldrich; St. Louis, MO) and *D*-amphetamine (NIDA; Bethesda MD) were dissolved in sterile saline (0.9% NaCl). SB 216763 (Tocris Bioscience; Ellisville, MO) was dissolved in 3.6% DMSO (Sigma) and brought up to volume in Tocrisolve 100 (Tocris Bioscience).

Conditioned Place Preference: An unbiased CPP procedure was used. On days 1-4, mice (n=8-11/group) were pretreated with saline or valproic acid (300 mg/kg, i.p.) in their home cages. Thirty minutes post-injection, mice received saline or amphetamine (2 mg/kg, i.p.) and were confined to one side of the CPP chamber for 30 minutes. On day 5, animals had free access to both sides of the conditioning chamber in a drug-free state and time on each side of the chamber was recorded for 30 minutes. Separate sets of mice (n=8/group) were pretreated with vehicle or SB 216763 (5 mg/kg, i.p.) in their home cages. Mice received saline or amphetamine (2 mg/kg, i.p.) 20 minutes later, and were confined to one side of the chamber for 30 minutes. On day 5, time spent on each side of the conditioning chamber in a drug-free state was recorded.

Data Analysis: Time spent on each side of the conditioning chamber was analyzed for significance using two-way ANOVA and Bonferroni post-hoc analysis.

### *Summary of Results*

*Study 1: The effect of valproic acid (VPA) and SB 216763 on acute amphetamine-induced hyperactivity.*

In our first study, we investigated the effect of a non-selective inhibitor of GSK3, valproic acid, as well as a selective inhibitor of GSK3, SB 216763 on acute amphetamine-induced activity (Figure 1). Mice were pretreated with valproic acid (50-300 mg/kg, i.p.) prior to amphetamine, and activity was measured for 60 minutes. Two-way ANOVA of the ambulatory data showed significant interaction, pretreatment, treatment effects (Interaction:  $F(3,80) = 2.757, p = 0.0477$ ; Pretreatment:  $F(3,80) = 3.758, p = 0.0140$ ; Treatment:  $F(1,80) = 12.64, p = 0.0006$ ). Bonferroni post-hoc analysis showed that saline-amphetamine significantly increased ambulatory counts compared to saline-saline treated controls (\*\* $p < 0.01$ ). Also, pretreatment with valproic acid significantly attenuated amphetamine-induced ambulation (\*\* $p < 0.001$ ). Analysis of the stereotypy data revealed significant interaction, pretreatment, and treatment effects (Interaction:  $F(3,80) = 2.857, p = 0.0422$ ; Pretreatment:  $F(3,80) = 4.258, p = 0.0076$ ; Treatment:  $F(1,80) =$

14.23,  $p = 0.0003$ ). Bonferroni post-hoc analysis indicated that pretreatment with each dose of VPA significantly attenuated stereotypic activity (50 mg/kg,  $*p < 0.05$ ; 150 mg/kg,  $**p < 0.01$ ; 300 mg/kg,  $***p < 0.001$ ).

Separate sets of mice were pretreated with SB 216763 (2.5-5.0 mg/kg, i.p.) prior to amphetamine, and activity was measured for 60 minutes (Figure 2). Two-way ANOVA of the ambulatory data revealed significant pretreatment and treatment effects (Interaction:  $F(2,62) = 1.092$ ,  $p = 0.3419$ ; Pretreatment:  $F(2,62) = 3.470$ ,  $p = 0.0373$ ; Treatment:  $F(1,62) = 35.01$ ,  $p < 0.0001$ ). Bonferroni post-hoc analysis showed increased ambulatory activity in mice treated with vehicle-amphetamine compared to vehicle-saline treated controls ( $***p < 0.001$ ). Pretreatment with SB 216763 significantly attenuated ambulation compared to mice treated with vehicle-amphetamine (2.5 mg/kg,  $*p < 0.05$ ; 5 mg/kg,  $*p < 0.05$ ). Two-way ANOVA of stereotypic activity revealed significant treatment effects (Interaction:  $F(2,62) = 1.480$ ,  $p = 0.2356$ ; Pretreatment:  $F(2,62) = 1.092$ ,  $p = 0.3418$ ; Treatment:  $F(1,62) = 38.84$ ,  $p < 0.0001$ ). Bonferroni post-hoc analysis indicated a significant increase in stereotypy in mice treated with vehicle-amphetamine compared to those treated with vehicle-saline ( $***p < 0.001$ ). Pretreatment with 5 mg/kg of SB 216763 significantly attenuated amphetamine-induced stereotypy ( $*p < 0.05$ ).

*Study 2: The effect of VPA and SB 216763 on the development of amphetamine-induced behavioral sensitization.*

The second study examined the effect of daily pretreatment of valproic acid on the development of amphetamine-induced behavioral sensitization to stereotypy (Figure 3). Two-way ANOVA of the stereotypy data revealed significant interaction, pretreatment, and treatment effects (Interaction:  $F(1,42) = 8.73$ ,  $p = 0.0051$ ; Pretreatment:  $F(1,42) = 6.956$ ,  $p = 0.0117$ ; Treatment:  $F(1,42) = 11.46$ ,  $p = 0.0016$ ). Bonferroni post-hoc analysis revealed a significant increase in stereotypy counts ( $***p < 0.001$ ) in mice treated with daily saline-amphetamine compared to saline-saline controls, indicating the development of amphetamine-induced sensitization. Analysis also showed daily pretreatment with valproic acid (300 mg/kg) significantly attenuated the development of amphetamine-induced sensitization of stereotypy in mice treated with VPA-amphetamine compared to saline-amphetamine controls ( $***p < 0.001$ ).

Separate sets of mice were pretreated daily with SB 216763 prior to amphetamine to test the effect of selective inhibition of GSK3 of the development of amphetamine-induced sensitization to stereotypy (Figure 4). Two-way ANOVA of the stereotypy data indicated significant treatment effects (Interaction:  $F(1,36) = 0.5903$ ,  $p = 0.4473$ ; Pretreatment:  $F(1,36) = 0.8391$ ,  $p = 0.3658$ ; Treatment:  $F(1,36) = 25.67$ ,  $p < 0.0001$ ). Bonferroni post-hoc analysis revealed a significant increase in stereotypy upon amphetamine challenge in mice treated daily with vehicle-amphetamine compared to vehicle-saline controls ( $***p < 0.001$ ). Mice pretreated daily with SB 216763 (5 mg/kg) also exhibited significantly greater stereotypic counts than saline treated control mice ( $**p < 0.01$ ). Analysis indicated no significant difference between mice treated with daily SB 216763-amphetamine and those that received vehicle-amphetamine ( $p > 0.05$ ).

*Study 3: The effect of VPA and SB 216763 on the development of amphetamine-conditioned reward.*

Our third study investigated the effect of pretreatment valproic acid on amphetamine-induced place preference (Figure 5). Analysis of the results revealed that mice treated with saline-amphetamine (\*\* $p < 0.001$ ) and VPA-amphetamine (\*\* $p < 0.001$ ) spent significantly more time on the drug paired side of the chamber as opposed to the saline paired side of the chamber compared to the saline pretreated controls. These results indicate the development of amphetamine-induced place preference in all mice conditioned with amphetamine, and VPA did not attenuate amphetamine-induced reward.

Separate sets of mice were pretreated with SB 216763 prior to amphetamine and confined to one side of the conditioning chamber (Figure 6). Analysis of the results indicated that mice treated with vehicle-amphetamine spent more time on the drug paired side than the saline paired side of the chamber ( $p < 0.05$ ) indicating the development of amphetamine-conditioned reward. Mice treated with SB 216763-amphetamine also spent more time on the drug paired side than the saline paired side of the chamber, indicating the development of amphetamine-induced place preference (\*\* $p < 0.001$ ).

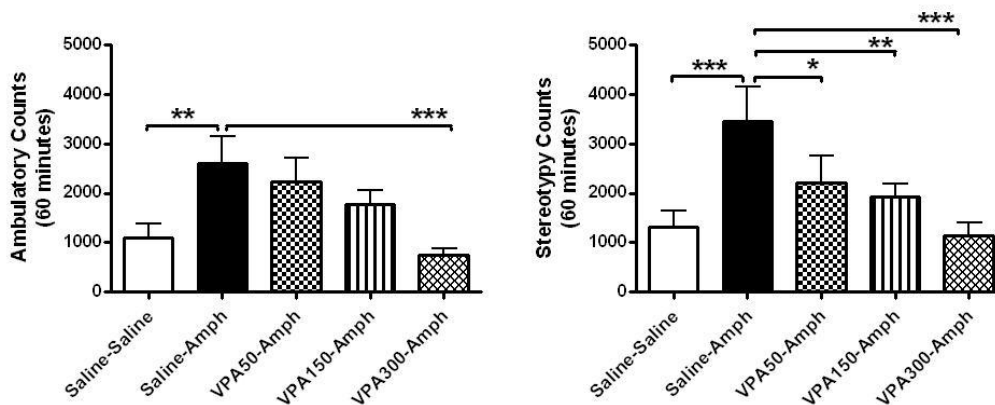


Figure 1. Amphetamine-induced ambulatory (left) and stereotypy (right) in mice pretreated with VPA (50-300 mg/kg). VPA significantly attenuated ambulatory activity (300 mg/kg, \*\*\* $p < 0.001$ ) and stereotypy (50 mg/kg,  $p < 0.05$ ; 150 mg/kg, \*\* $p < 0.01$ ; 300 mg/kg, \*\*\* $p < 0.001$ ).

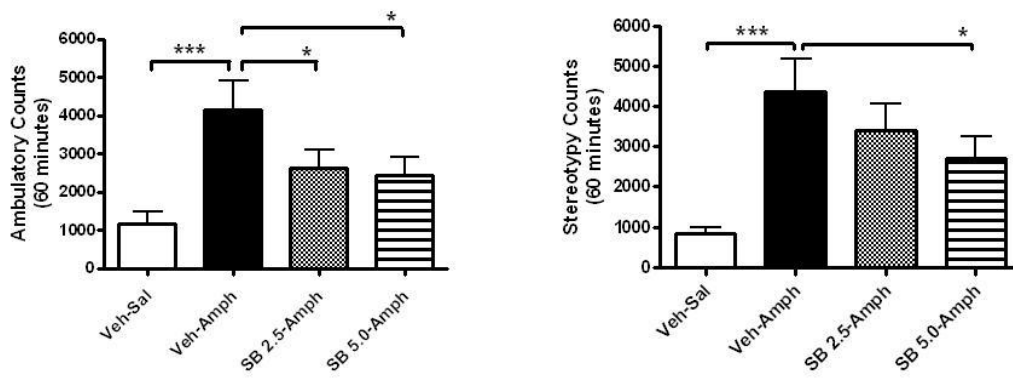


Figure 2. Amphetamine-induced ambulation (left) and stereotypy (right) in mice pretreated with the selective GSK3 inhibitor SB 216763 (2.5-5 mg/kg). SB 216763 significantly attenuated ambulation (2.5-5 mg/kg, \* $p < 0.05$ ) and stereotypy (5 mg/kg, \* $p < 0.05$ ).

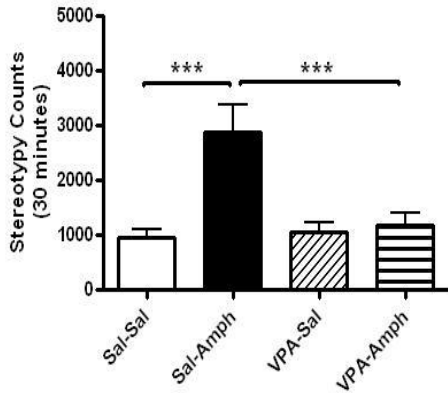


Figure 3. Pretreatment with VPA significantly attenuated the development of amphetamine-induced sensitization to stereotypy after repeated amphetamine administration ( $***p < 0.001$ ).

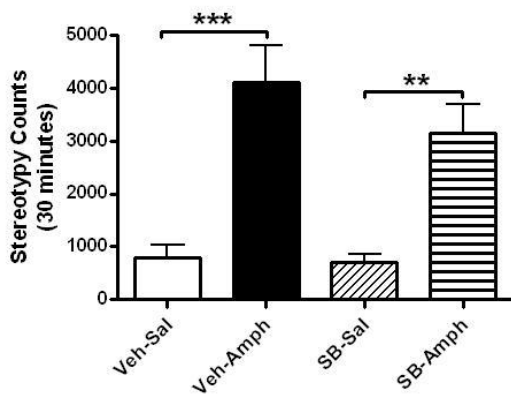


Figure 4. Amphetamine-induced sensitization to stereotypy in mice administered repeated amphetamine injections. All mice treated with repeated amphetamine developed significant sensitization to stereotypy compared to saline counterparts ( $**p < 0.01$ ,  $***p < 0.001$ ). Pretreatment with SB216763 (5 mg/kg) did not significantly alter amphetamine-induced sensitization.

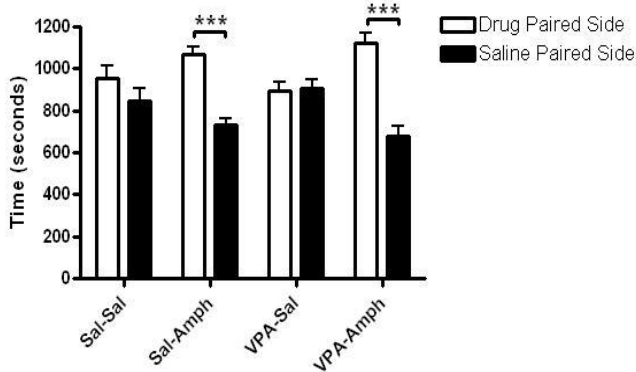


Figure 5. The effect of VPA on the development of amphetamine-induced place preference. All mice treated with amphetamine spent more time on the drug paired side of the chamber than saline paired side ( $***p < 0.001$ ). Pretreatment with VPA did not alter amphetamine conditioned reward.

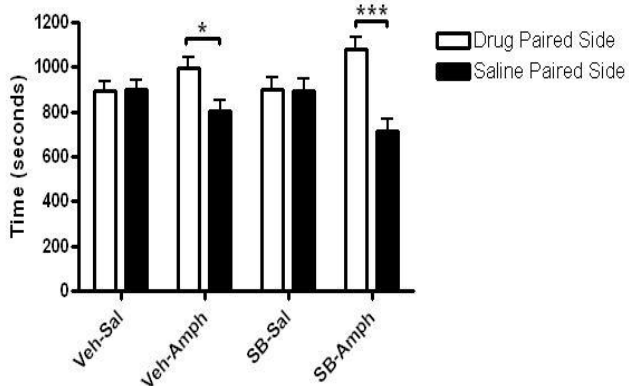


Figure 6. The effect of GSK3 inhibition by SB 216763 on the development of amphetamine-induced reward. All mice treated with amphetamine spent more time on the drug paired side of the chamber than saline paired side (\* $p < 0.05$ , \*\*\* $p < 0.001$ ). Pretreatment with SB 216763 did not alter amphetamine conditioned reward.

### **Research Project 7: Project Title and Purpose**

*Biomimetic Composite Design* - The purpose of this project is to refine analytical models of novel composites intended for use as dental restorative materials. The novelty of the composites lies in borrowing strengthening and toughening strategies from naturally occurring composites, i.e., seashells. The refined models will be useful for designing the new composites.

### **Duration of Project**

5/1/2009 - 5/31/2010

### **Project Overview**

We have been working on identifying and understanding the factors which limit the service lifetimes of tooth-colored dental restorative materials (dental composites). These materials, though esthetic and free of mercury, remain limited in their applications to single teeth, and clinically fail more rapidly than mercury-containing dental amalgam restorations. Our studies convinced us not only that composite toughness had to increase, but that the traditional methods of toughening composites had reached an effective limit, and that new means of toughening were needed.

In searching for these alternatives, we took note of naturally occurring biocomposites such as the abalone shell (nacre), which by virtue of its microstructure and composition has a toughness 8-3,000x (depending on measurement technique) greater than the primary constituent of the shell, aragonite (a form of calcium carbonate). It is also our belief that a key toughening component in nacre is the proteinaceous organic interphase layer, as this protein is able to absorb energy on deformation.

Specific tasks are:

1. Draw on our fracture mechanics experience and finite element modeling expertise to produce

a defensible and credible estimate of the potential toughening to be gained in both fiber- and particle-reinforced composites containing a nacre-protein-analogue interphase. The fiber-reinforced composite will be emphasized, as its microstructure more closely resembles that of nacre.

2. Extend the molecular dynamics modeling effort from single-chain polymers to polymer networks. The nacre-protein-analog interphase is in fact a network of polymer chains, and the jump in complexity from modeling a single chain is significant. A successful demonstration of network modeling capability will substantiate our rationale, provide additional preliminary data and publications, and contribute to the estimation of composite lifetime.

### **Principal Investigator**

George R Baran, PhD  
Associate Dean and Professor  
Temple University  
1947 N. 12<sup>th</sup> Street  
Philadelphia, PA 19122

### **Other Participating Researchers**

Wenhai Wang, PhD - employed by Temple University

### **Expected Research Outcomes and Benefits**

The expected outcome will be the development of a technique for extending our current work of modeling the mechanical behavior of single polymer molecules to the modeling of a polymer molecule network. The modeling will be accomplished using software that simulated molecular movement. The benefit of this outcome will be a more useful composite model, one that may be used to rapidly design and assess many different composite designs without the need to fabricate and test composites in the lab. In this way, we can more rapidly develop longer-lasting materials for treatment of diseased or missing teeth or bone.

### **Summary of Research Completed**

Our approach to composite design is inspired by the adhesive proteins of nacre that bind the inorganic component, aragonite. So far, we have conducted finite element modeling studies to determine if the toughening ascribed to the interphase proteins could be effective in a particle-reinforced composite. This modeling effort builds on the molecular dynamics modeling reported in last year's progress report.

### Model Setup

Fracture toughness and failure processes in particle/fiber reinforced composites are related to the basic problem of a crack interacting with a second phase particle or fiber. In this study, a small zone at the center of a typical single-edge notch 3-point bending specimen used in toughness measurements was selected as the area of interest. A detailed representation of microstructure is

shown in Figure 1, including particle, matrix and interphases. Two types of interphases are compared: nacre-protein-analogue material (beta-peptide), and traditional silane. The volume content of particles in the unit cell is 55%.

We use a progressive damage degradation material model to simulate crack propagation. As shown in Figure 2, this model includes an undamaged response, a damage initiation criterion, and a damage evolution response. Three parameters (Young's modulus, Poisson's ratio and yield strength) define the undamaged response of the material. A ductile damage initiation criterion was used in the simulation. The damage initiation strain under tensile load is derived from the fracture strain. For the matrix material, it is assumed to be 0.04. We are not aware of any specific reference in the literature that documents a direct measurement of fracture strain of silane. Therefore, its damage initiation strain is derived from fiber pull-out experiment force displacement curves shown in the references in Table 1. We chose the fracture strain in tension to be in the range of 2-7%.

The damage evolution law describes the rate of degradation of material stiffness once the corresponding initiation criterion has been reached. It manifests itself in two ways: reduction of the yield stress, and elasticity (stiffness). The rate of the degradation is controlled by another material parameter  $G_0$ , the energy required to open a unit area of crack. The  $G_0$  value varies in the range of  $0.05-0.1 \text{ Jm}^{-2}$  for polymer matrix-filler interphase bond failure. The matrix material property was set as  $0.1 \text{ Jm}^{-2}$  in the simulation. The  $G_0$  value for the silane interphase material was selected according to the critical energy release rate  $G_{ic}$  measured during fiber pull-out experiments.

The parameters chosen for newly developed beta-peptide interphase materials reflect the nanoscale mechanisms associated with organic layers (biopolymer) found in nacre. Experimental data (Smith et al. Nature, 399,761 1999) indicate that the force-extension behavior of biopolymer exhibited an irregular "saw-tooth" character. It has significant stretching capability and can maintain cohesion between nacre tablets over a large range during tablet sliding. This thin layer of biopolymer can be seen as a series of nonlinear springs that connect the faces of the tablets. Stretching of the springs (organics ligaments) controls the behavior of the interphase under tension and shear.

Note that the experimental data illustrate the large stretching capability of individual polymer chains, but might not be representative of the confined biopolymer at the interface. When a bundle of polymer chains is considered, the ensemble average constitutive response is likely to exhibit an approximately constant strength over the range of displacements. In the absence of further experimental data on the nanoscale mechanical response of the confined beta-peptide layer at the interface, it is reasonable to assume that the constitutive behavior of beta-peptide interphase can be derived from polymer network simulations. In this study, parameters used in the progressive damage material model are derived from a three-dimensional macromolecular network solid model analysis (H.J. Qi et al., Mechanics of Biological Tissues, p. 175 (2005)). This approach is briefly described below.

The force extension behavior of a single polymer chain can be represented by a free-jointed-chain (FJC) model or a worm-like-chain (WLC) model and can be derived based on single

polymer chain atomic force spectroscopy tests. Using statistical mechanics, the single polymer chain behavior can be incorporated into a three-dimension macromolecular "eight-chain" network. This network idealization captures the essential features of a random network in an "average" sense. The simulation for a macromolecular network shows that the stress-strain behavior of the material undergoes a nonlinear increase, then transitions to a plateau region, and finally increases again at large stretches. Our constitutive model well captures the first transition from a nonlinear increase to the plateau region which corresponds to triggering of the unfolding of individual polymer chains. According to the nominal stress *vs* stretch behavior in simple tension of a modular three-dimensional network representing the organic matrix in nacre (H.J. Qi et al., *Mechanics of Biological Tissues*, p. 175 (2005)), the damage initiation strain for beta-peptide interphase material is chosen to be in the range of 5-20 and the  $G_0$  value is chosen to be 1500-2000  $\text{Jm}^{-2}$ . Detailed parameter values are listed in Table 1.

The boundary conditions applied in the study zone are derived from a macroscopic 3-point bending simulation. We calculated the actual deformation gradient for a small square region in front of the crack tip during 3-point bending, then mapped onto current microscopic unit cell simulations as the displacement loading condition. A convergence study was carried out to ensure that the number of elements in the model was adequate. There are approximately 52000 nodes and 105000 elements in the final model.

## Results and Discussion

Our special interest area is the region surrounding the crack tip, where the energy is predominantly dissipated. Figure 3 compares the von Mises Stress as the crack propagates toward the embedded particles. The initial crack tip has a distance of  $r$  ( $r$  is the particle radius) away from the first particle. As shown in Figure 3a, as the crack starts to propagate in the composite with a beta-peptide interphase at 0.3 seconds, a stress concentration occurs only at the crack tip. Before the crack 'senses' the first particle, dissipation of energy by the creation of new surfaces relaxes stresses in regions other than at the crack tip. The beta-peptide interphase material provides continuous stress transfer between matrix and particle. As the crack approaches the first particle at approximately 0.44 seconds, a large stress concentration area between crack tip and the particle is built up. Even though the maximum stress is observed at the particle surface, the crack does not grow in that direction. Instead, it propagates within the matrix material and is deflected around the particle. Once the crack propagates forward again, the stress concentration in the area around the particle starts to decrease again. Once the crack passes the particle, it continues to propagate within the matrix. During this procedure, the crack propagation speed decreases dramatically when the crack interacts with the first particle. This is not observed in composites with the silane interphase. Even though the silane interphase also provides continuous stress transfer between particle and matrix, a large stress concentration area is not observed when the crack approaches the first particle. Comparing the crack length at the final stage (1.0 seconds), the composite with a beta-peptide interphase (Figure 3a) leads to a lower crack growth distance than that the composite with a silane interphase (Figure 3b) under the same loading conditions.

As shown in Figure 4, normalized damage dissipation energy decreases when the crack starts to interact with particles in composites with a beta-peptide interphase. Composites with a silane

interphase do not show the same behavior. The normalized damage dissipation energy increases monotonically. The decrease of normalized damage dissipation energy observed in composites with beta-peptide interphases indicates that the growth of the crack is retarded.

### Summary

2D FEM unit cell simulation results indicate that particle-reinforced polymer composites with a more compliant and stretchable interphase will help absorbing local strain energy while remaining intact, causing less damage within the matrix. As a result, this type of interphase decreases crack propagation speed and results in an increase of fracture toughness.

Table 1. Material properties of composite components

Material	Young's modulus E (MPa)	Poisson's ratio	Yield stress (MPa)	Crack initiation strain under tensile load	$G_0(\text{Jm}^{-2})$	References
E-Glass particle	75000	0.24	N/A	N/A	N/A	C.J. Sun et al., Composites Part A, 38,80 (2007).
BisGMA/TEGDMA resin matrix	2000	0.35	70	0.04	0.1	D.L. Zhao et al., Dental Materials, 13, 198 (1997).
Interphase material A (Silane)	7000	0.32	70	2-7	20-40	R. Plonka et al., Composites Part A, 35,1207 (2007). S.K. Khanna et al., Transactions of the ASME, 125, 90 (2003).
Interphase material B (beta-peptide)	160-2000	0.35-0.45	750	5-20	1500-2000	H.J. Qi et al., Mechanics of Biological Tissues, p175 (2005). P.K.V.V. Nukala et al. Biomaterials, 26, 30 (2005).

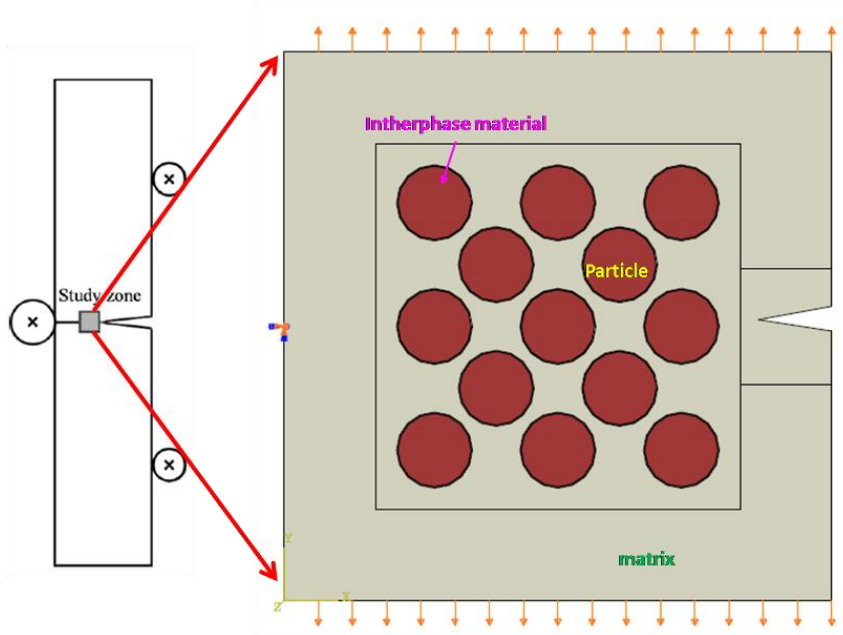


Figure 1. Schematic representations of 3-point bend specimen (left) and study zone (right).

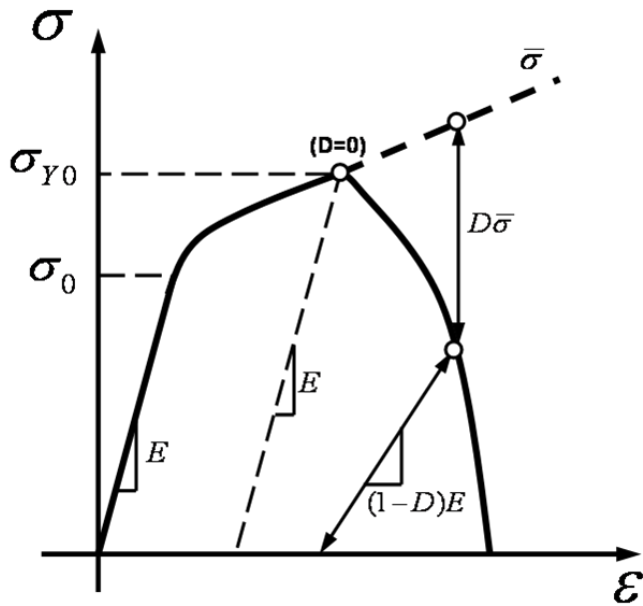
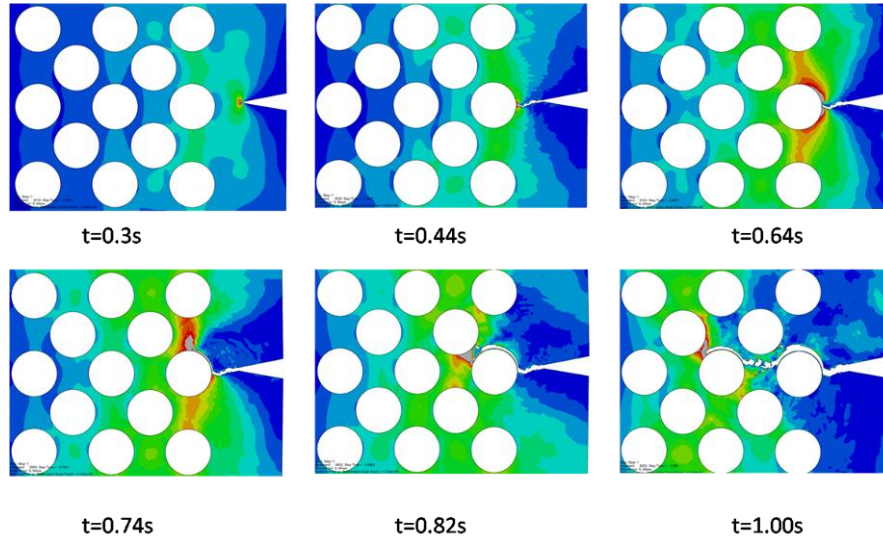


Figure 2. Stress-strain curves with progressive damage degradation used in the FEM simulation.

(a)



(b)

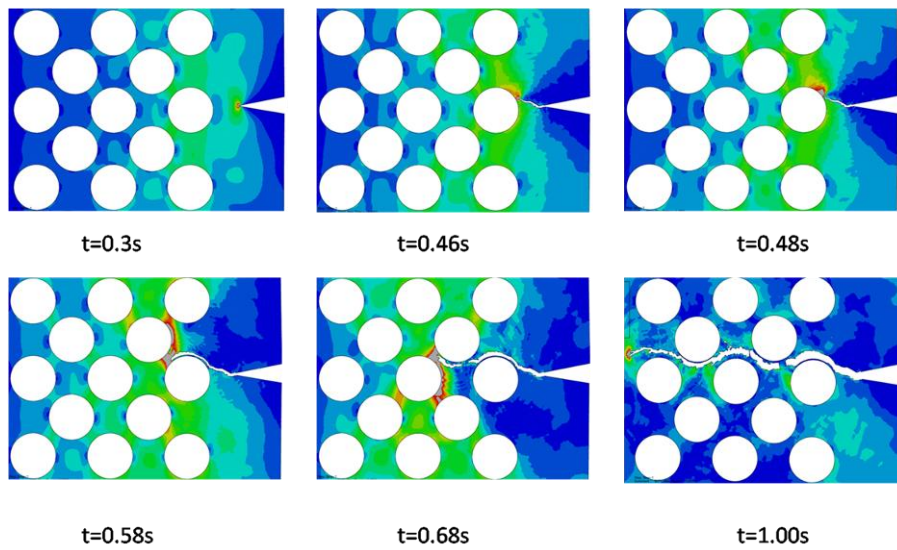


Figure 3. Von Mises stress evolution as the crack propagates around particles; (a) composite with beta-peptide interphase; (b) composite with silane interphase.

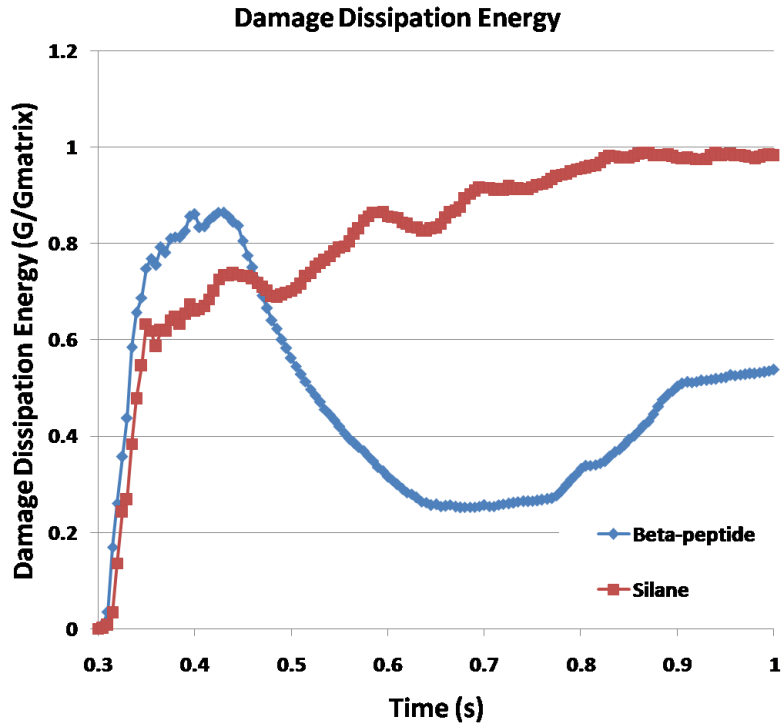


Figure 4. Normalized damage dissipation energy evolution as the crack interacts with particles.

**Research Project 8: Project Title and Purpose**

*Interactions Between Cytotoxic and Antiangiogenic Drugs* - Combination anticancer drug therapy is standard for most cancer types, yet the types of drugs that are combined in therapeutic regimens is changing. Rather than combining toxic drugs with severe and overlapping toxicities, new efforts seek to combine drugs not only with different and less severe toxicities, but also drugs with different cell and molecular targets or mechanisms of action. Antiangiogenic drugs are among a new portfolio of agents that may be referred to as targeted drugs that can interfere with the growth and spread of tumors by various mechanisms, and may compliment the action of more traditional cytotoxic drugs. The purpose of this project is to understand how two targeted drugs can be optimally combined with a cytotoxic drug in a preclinical brain tumor model.

**Duration of Project**

1/1/2009 – 8/30/2009

**Project Overview**

The advent of targeted anticancer drugs has harkened the age of molecular therapeutics with the ultimate goal to devise drug combination regimens that are more effective and less toxic. This alluring promise requires a multi-dimensional approach to develop new treatment schemes based on the use of targeted and standard cytotoxic drugs. A critical step to achieving novel and more

effective combination regimens is to understand the pharmacological basis of the combinations. This latter goal is the essence of this project. The pharmacological properties of a drug can be quantitated as a set of pharmacokinetic [PK] and pharmacodynamic [PD] characteristics that will assess whether drug combinations interact negatively or positively. The invasive spread of brain tumors requires active angiogenesis or neovascularization to provide blood and oxygen to the growing tumor, and makes antiangiogenic therapy a potentially important strategy. Many of the angiogenesis inhibitors target receptors on endothelial cells and effect different signaling pathways, such as the PI3K/AKT/mTOR pathway, that may either be dysregulated or promote feedback mechanisms that counteract their intended action, causing the cells to become drug resistant. Thus, one new strategy to overcome drug resistance and make the tumor more sensitive is to combine two targeted drugs and then combine these agents with a cytotoxic drug, like temozolomide.

#### Specific Aims:

1. Characterize the PK and PD properties of a combination of sunitinib, an angiogenesis inhibitor, and a PI3K inhibitor in a mouse orthotopic brain tumor model. Drug concentrations will be measured in plasma, normal brain and brain tumor, as well as PD endpoints including a vascular normalization index and expression of target proteins. Different drug doses and sequences will be used and PK/PD models will be developed.
2. Determine the PK characteristics of temozolomide in the presence of the optimal two drug combination regimen defined in Aim 1. Analogous experiments as in Aim 1 will be completed with a primary goal to determine if temozolomide penetrates brain tumors to a greater extent than when given alone or combined with a single targeted drug.

#### **Principal Investigator**

James M Gallo, PharmD, PhD  
Professor  
Temple University  
School of Pharmacy  
3307 N. Broad St.  
Philadelphia, PA 19140

#### **Other Participating Researchers**

Stephanie Zhou, PhD – employed by Temple University

#### **Expected Research Outcomes and Benefits**

The project will investigate new strategies to combine anticancer drugs into the most effective treatment schedules for a preclinical model of brain tumors. The expected outcome is to determine whether the selected three drug combinations have beneficial actions compared to single agent or dual combination therapy. The beneficial action will be measured in terms of different pharmacological measures that include enhanced drug distribution into tumors and improved inhibition of vascular growth or angiogenesis and tumor cell growth. The results from the preclinical investigations will be related or scaled to project how the different drug

combinations would behave in cancer patients. This would be beneficial to the drug development process and the use of anticancer drug combinations in patients since favorable combinations could be more readily translated to patients.

### **Summary of Research Completed**

We have concluded PK/PD studies of sunitinib and compound C in mice bearing orthotopic brain tumors. PD assays have determined that both pAKT and pS6 could serve as PD endpoints in tumor, and that there was no negative interaction with sunitinib.

### **Research Project 9: Project Title and Purpose**

*Control of Cellular and HIV-1 Gene Expression by Cellular CDK9, A Potential Target for HIV Therapeutics* - HIV is the causative agent of AIDS (Acquired Immunodeficiency Syndrome). Highly Active AntiRetroviral Therapy (HAART) is a drug combination currently used to reduce viral loads by neutralizing at least two different HIV proteins. However, because HIV mutates, viral strains resistant to current HAART drug combinations arise. It is believed that anti-HIV drugs directed to host cellular proteins that are essential for HIV replication may be a solution to this problem. Therefore, there is an urgent need for identification and validation of such cellular targets and the development of new high throughput assays to identify drugs against them. This project aims at both further characterizing a cellular kinase complex that is hijacked by an HIV-1 viral protein and to design strategies to identify drugs targeting this essential step on the HIV life cycle.

### **Duration of Project**

1/1/2009 – 6/30/2010

### **Project Overview**

The immediate objectives of this project are to further understand the cellular role of the cellular kinase complex, designated CDK9/cyclin T1, in the control of cellular host gene expression to determine whether there is a therapeutic window of opportunity that warrants development of drugs targeting this complex to inhibit HIV-1 replication. This one-year project will focus on two separate lines of related research aimed at generating strong preliminary data for submission of two separate R01 (or comparable) grant applications during the second half of the funding period or shortly after its completion.

#### **Subproject#1: Control of cellular and HIV-1 gene expression by CDK9.**

The CDK9/cyclin T1 complex is recruited by HIV-1 Tat to promote productive viral transcription and is essential for HIV-1 replication. CDK9 is the catalytic subunit of the transcription elongation factor b (P-TEFb) and is required for transcriptional elongation *in vitro*. Experiments with cells treated with flavopiridol (FVP), a CDK inhibitor that potently inhibits CDK9, have led to the proposition that CDK9 is required for the transcription of most cellular genes by RNAPII. However, our preliminary data show that the effects of FVP in gene

expression are distinct to the effects of inhibiting CDK9 activity with a dnCDK9 mutant. Our hypothesis is that the role of CDK9 in cellular transcription is gene specific. A better understanding of the function of this essential HIV-1 cellular cofactor may facilitate developing of future anti-therapeutic interventions.

Specific Aim: To examine the selectivity of T-type cyclin/CDK9 complexes in regulation of gene expression in normal human cells. DNA microarray analysis will be performed using normal human cells transduced with dnCDK9, shRNAs and control viruses.

Subproject#2: To develop a high throughput cellular reporter assay to identify inhibitors of HIV-1 transcription with no cellular toxicity.

HIV-1 transcription is an essential step in the viral cycle and is dependent on viral and host transcription factors. We hypothesize that selective inhibition of HIV-1 transcription, and hence replication, should be feasible if the small compound specifically targets a viral protein essential for productive transcription (i.e.: Tat), a required cellular cofactor non-essential for cellular transcription, or if it interferes with the interactions among viral and cellular cofactors without altering cellular functions.

Specific Aim: To generate and characterize dual reporter cell lines to simultaneously monitor HIV-1 and cellular transcription in vivo in multi-well tissue culture plates.

### **Principal Investigator**

Xavier Graña, PhD  
Associate Professor of Biochemistry  
Temple University School of Medicine  
AHP Bldg. Rm. 308  
3307 North Broad St.  
Philadelphia, PA 19140

### **Other Participating Researchers**

Judith Garriga, PhD, Alison Kurimchak, BS – employed by Temple University

### **Expected Research Outcomes and Benefits**

This project is aimed at obtaining additional evidence supporting the hypothesis that a particular cellular protein complex is a suitable target for anti AIDS therapeutic intervention and to devise strategies to screen for new drugs that halt the HIV-1 live cycle in infected cells. These studies also seek to generate strong preliminary data to support longer-term grant applications to the NIH or other agencies. While work over the past years by our lab and others using transformed cell lines has led to hypotheses that cellular CDK9 is a valid target for developing therapies for AIDS and other malignancies, knowledge on the particular cellular genes that are more sensitive to inhibition of particular CDK9 complexes is lacking for normal cells. Comparison on the effects of inhibiting a subset of CDK9 cellular complexes on host and HIV-1 gene expression may allow definition of a window of therapeutic opportunity. In addition, we will generate a

panel of dual reporter cell lines to be used in high throughput screening of small compound libraries to identify compounds with the ability to inhibit HIV-1 gene expression without affecting cellular function and viability.

Therefore, if successful this project is expected to: (a) expand our knowledge on the function of a family of important transcription factors (CDK9 cellular complexes) in the control of cellular gene expression and HIV-1 replication; (b) allow the generation of reagents to start developing novel anti-HIV therapies; and (c) generate the necessary strong preliminary data required to justify long term grant applications to the NIH or national/international private foundations.

## **Summary of Research Completed**

### *Control of Cellular and HIV-1 Gene Expression by Cellular CDK9, A Potential Target for HIV Therapeutics*

The immediate objectives of this project were to further understand the cellular role of the cellular kinase complex, designated CDK9/cyclin T1, in the control of cellular host gene expression to determine whether there is a therapeutic window of opportunity that warrants development of drugs targeting this complex to inhibit HIV-1 replication. The one-year project focused in two separate lines of related research aimed at generating preliminary data for submission of two separate R01 (or comparable) grant applications during the second half of the funding period or after its completion. This grant was extended through the end of this fiscal year (6/30/10), as the project is still active. We are actively collecting preliminary data with the aim of submitting one R01 proposal in the short term.

#### Subproject#1: Control of cellular and HIV-1 gene expression by CDK9.

The CDK9/cyclin T1 complex is recruited by HIV-1 Tat to promote productive viral transcription and is essential for HIV-1 replication. CDK9 is the catalytic subunit of the positive transcription elongation factor b (P-TEFb) and is required for transcriptional elongation *in vitro*. Experiments with cells treated with flavopiridol (FVP), a CDK inhibitor that potently inhibits CDK9, have led to the proposition that CDK9 is required for the transcription of most cellular genes by RNAPII. However, our preliminary data show that the effects of FVP in gene expression are distinct to the effects of inhibiting CDK9 activity with a dnCDK9 mutant. Our hypothesis is that the role of CDK9 in cellular transcription is gene specific. A better understanding of the function of this essential HIV-1 cellular cofactor may facilitate developing of future anti-therapeutic interventions.

Specific Aim 1: To examine the selectivity of T-type cyclin/CDK9 complexes in regulation of gene expression in normal human cells. DNA microarray analysis will be performed using normal human cells transduced with dnCDK9, shRNAs and control viruses. Our progress is summarized below.

*Ia.* This aim was based on preliminary data obtained from a series of DNA microarray profiling experiments performed with RNA obtained from human glioblastoma T98G

cells where CDK9 activity was downregulated via ectopic expression of a dominant negative form of CDK9. Unexpectedly, we found that a small number of genes/ORFs are downregulated (84) and upregulated (122), suggesting that CDK9 may both positively and negatively regulate gene expression and that the changes in gene expression are likely due to differential regulation of gene expression by CDK9 rather than a simple shutdown of general transcriptional elongation. This work was in preparation at the time of the application for this award. This study, which was partially funded through this award, was completed and published (Garriga et al, 2010).

*2b.* As outlined in the original proposal we have performed microarray analysis in normal human fibroblasts using BJ fibroblasts immortalized with hTERT (human Telomerase Reverse Transcriptase) where we modulated CDK9 activity by different means. BJ-T fibroblasts were transduced with inducible adenoviruses directing expression of dnCDK9 (Tet-off system), cyclin T1 and CDK9 combined or a combination of control adenoviruses. We also treated cells with FVP, a pharmacological inhibitor with significant selectivity for CDK9, in cells that had been transduced with control adenoviruses in the presence of Tetracyclin (no transgene expression). This ensured that the effects of FVP and the effects of the transgenes expressed following transduction with inducible adenoviruses were comparable. We also performed a series of microarray analyses with RNA probes obtained from cells where CDK9 was knocked-down via siRNA transfection. The results of these microarray analyses are shown in Fig. 1. As in the case of the experiments previously performed using T98G cells, FVP effects are consistent with a rapid block in transcription leading to time-dependent downregulation of many genes. However, there were also a large number of upregulated genes. Interestingly, among the upregulated transcripts there were various genes that are known to be highly inducible and short lived, including FOS, JUNB and EGR1 (see next section). Under the refined conditions of these experiments, expression of dnCDK9 resulted in changes in gene expression that appeared more comparable to the effects of FVP, as compared to the previous results obtained with T98G cells (Fig 1A). This is more obvious when we compare transcripts that are upregulated/downregulated more than 2 fold by dnCDK9 (Fig. 1B). We were also surprised to see that there was poor correlation between the effects of dnCDK9 with siCDK9 in BJ-T fibroblasts (Fig. 1C). These could be potentially explained by the difference in kinetics of inhibition of CDK9 and/or because dnCDK9 may sequester complexes with effects in transcription that are not a direct consequence of inhibition of CDK9 activity.

*3b.* While this work was in progress a report was published demonstrating the recruitment of P-TEFb to primary response genes in response to LPS stimulation (Hargreaves et al., 2009). Having seen potent upregulation of FOS, JUN and EGR1 transcripts upon FVP treatment for 8 and 24 h, we considered the possibility that the early effects of FVP on the expression of these genes could be in sharp contrast to what is seen at late time points. Therefore we treated BJ-T cells with FVP and collected cells at early time points (0, 0.5, 1 and 2 hrs) in addition to the time points that we had used in the microarray expression analysis. Transcript levels were measured using q-RT-PCR and specific Taqman probes. Interestingly, we found that most primary response genes tested are downregulated very rapidly upon FVP treatment. However, the expression of some

of these recovered transcripts was expressed potently at later time points (i.e. EGR1, JUNB and GADD45B). We also observed primary and secondary response genes with unchanged or upregulated expression by FVP at all time points. This was unexpected for secondary response genes whose expression is thought to be dependent on the expression of primary response genes that are expressed early and sharply downregulated. Finally, there were also secondary response genes that were downregulated less sharply, but their levels remained low through the remaining time course. With these results, we performed a new set of experiments with focus on genes that are known to be induced by mitogens as primary or secondary genes. BJ-T cells were serum starved for 3 days and subsequently stimulated with serum in the presence of FVP or vehicle (control). We observed that the FVP treatment effectively blocked cell cycle re-entry from quiescence (data not shown). We also observed that FVP effectively blocked the expression of several primary response genes though the 22 h time course. However, other genes were upregulated in these conditions including JUNB and cyclin D1. Our data with FVP suggest that expression of both primary and secondary response genes exhibit heterogeneous dependency on CDK9 activity. We are currently testing several shRNA lentiviral constructs targeting CDK9, cyclin T1, cyclin T2, to determine the specific effects of eliminating these subunits in the mitogenic response that stimulates the G0/G1 transition in normal cells. We are also setting up conditions to analyze promoter occupancy by CDK9, T- type cyclins and RNAPII (processive and non processive forms) in the primary and secondary response genes under study to start deciphering the mechanism that explains the complex role of CDK9 in the expression of these genes. These preliminary data are shaping up for the submission of an R01 proposal in one of the upcoming submission cycles.

*Subproject#2: To develop a high throughput cellular reporter assay to identify inhibitors of HIV-1 transcription with no cellular toxicity.*

HIV-1 transcription is an essential step in the viral cycle and is dependent on viral and host transcription factors. We hypothesize that selective inhibition of HIV-1 transcription, and hence replication, should be feasible if the small compound specifically targets a viral protein essential for productive transcription (i.e.: Tat), a required cellular cofactor non-essential for cellular transcription, or if it interferes with the interactions among viral and cellular cofactors without altering cellular functions.

Specific Aim 2: To generate and characterize dual reporter cell lines to simultaneously monitor HIV-1 and cellular transcription in vivo in multi-well tissue culture plates.

We made several attempts to generate HeLa cells with dual reporters directed by a Tat-dependent HIV-1 LTR promoter and a housekeeping like promoter (MSCV promoter). As reporters we utilized dEGFP and RFP for strategy 1, and firefly and renilla luciferases for strategy 2. We were successful in generating clones that expressed dEGFP or firefly luciferase under the control of the HIV-1 promoter in a Tat dependent manner. This was accomplished by the sequential introduction of appropriate plasmids as follow. First, transfection of the LTR-reporter plasmid, followed by selection of clones resistant to antibiotics but lacking reporter activity in the absence of exogenously transduced/transfected Tat. Second, transfection with a Tat expression plasmid, followed

by antibiotic selection and identification of clones with reporter activity. Third, transfection of the second reporter under the control of the MSCV promoter (Fig. 2a). We were successful in introducing and selecting clones for the first two steps (Fig. 2 and Fig. 3), but in both strategies introduction of the MSCV-reporter (RFP or renilla luciferase) resulted in toxicity leading to slow growth and inability to maintain stable clones. While these problems could have likely been worked out by reducing plasmid copy numbers, we obtained in collaboration with Dr. Olaf Kutsch Jurkat cells with the desired properties. These cells were generated as described in strategy 1 but using retroviral transduction strategies followed by cell sorting. It appears that Jurkat cells are better suited than HeLa cells to stably co-express several exogenous proteins. We also established a collaboration with Dr. Kutsch to perform two high throughput screens aimed at identifying small compounds with the ability to inhibit HIV-1 transcription, without altering cellular transcription. We dispensed in 96 well plates a library of about 3200 small compounds generated by our collaborator Dr. Premkumar Reddy. Alison Kurimchak, the graduate student assigned to this project traveled to Dr. Kutsch's lab (University of Alabama at Birmingham), where she performed the two fluorescent-based screens. One screen was flow cytometry-based and the other utilized a fluorescence plate reader. The screens were performed in Dr. Kutsch lab, as he had the required flow cytometric equipment and had extensive expertise in this innovative type of screen. The screens were completed within a week, and the data was analyzed in our lab. While the control compound, Ro24-7429, a known inhibitor of HIV-transcription validated both screens, we did not find potent inhibitors of HIV-1 transcription that were not also inhibitors of cellular transcription or toxic to cells. However, the library of small compounds that we used was relatively small. Thus, these results are not completely unexpected. Given the successful validation of both screens, it appears feasible to screen larger libraries of small compounds (>100,000). Submission of a grant application to support high throughput screens with large libraries of small compounds is being evaluated.

## References

Garriga, J., Xie, H., Obradovic, Z., and Graña, X. (2010). Selective control of gene expression by CDK9 in human cells. *J Cell Physiol* 222, 200-208.

Hargreaves, D. C., Horng, T., and Medzhitov, R. (2009). Control of inducible gene expression by signal-dependent transcriptional elongation. *Cell* 138, 129-145.

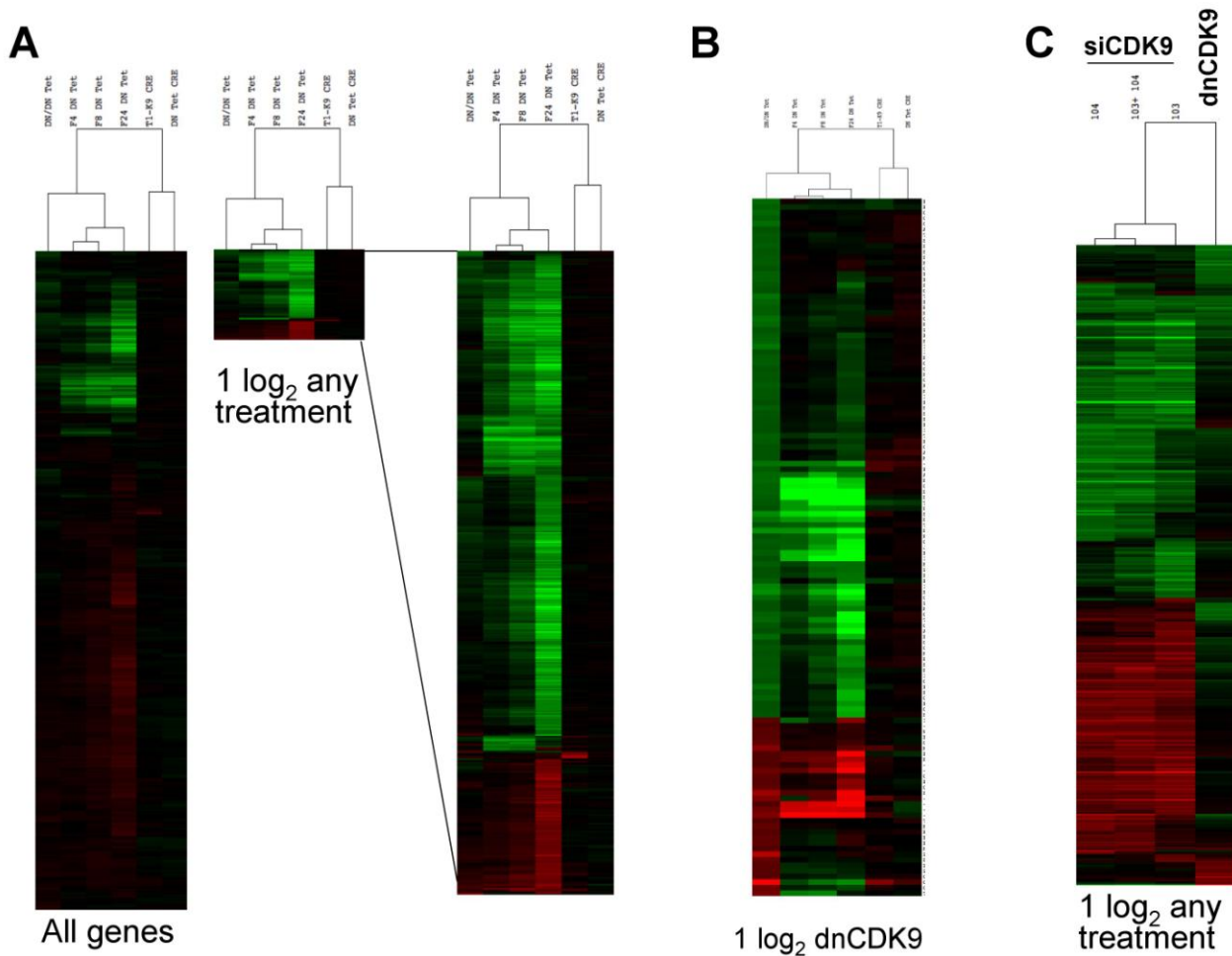


**Fig.1. Hierarchical clustering analysis of microarray expression data.** BJ-T fibroblasts were infected with tet-repressible adenovirus in the presence (control) of absence (dnCDK9 expression) of tetracycline and treated with FVP or left untreated as indicated in the text (F4, FVP 4 hrs, F8, FVP 8 hrs; F24, FVP 24 hrs). BJ-T fibroblasts were also transduced with adenoviruses expressing cyclin T1 and CDK9 in combination or CRE control adenoviruses. Expression data used for clustering was obtained included the log<sub>2</sub> ratios of treatment vs. control combinations. Log<sub>2</sub> expression ratios were clustered using Cluster analysis v 3.0 software using correlation uncentered, average linkage. Data was visualized with Java TreeView. Green represents downregulated genes. Red represents upregulated genes. Data were analyzed essentially as described in Garriga et. al., 2010. Black are non-modulated genes. (A) Clustering of transcript expression data for all genes in the Affymetrix Human Gene 1.0 ST Array (~29000)(left). The middle panel shows the fractions of genes in which the expression changes 1 log or more ( $|\log_2| > 1$ ). The right panel is a blow out of the middle panel. (B) Hierarchical clustering analysis for genes modulated by dnCDK9 more than 1 log. (C) Hierarchical clustering analysis for genes modulated more than 1 log by dnCDK9 or CDK9 siRNAs (103, 104 or 1003 + 104; scrambled siRNA was used as control)..

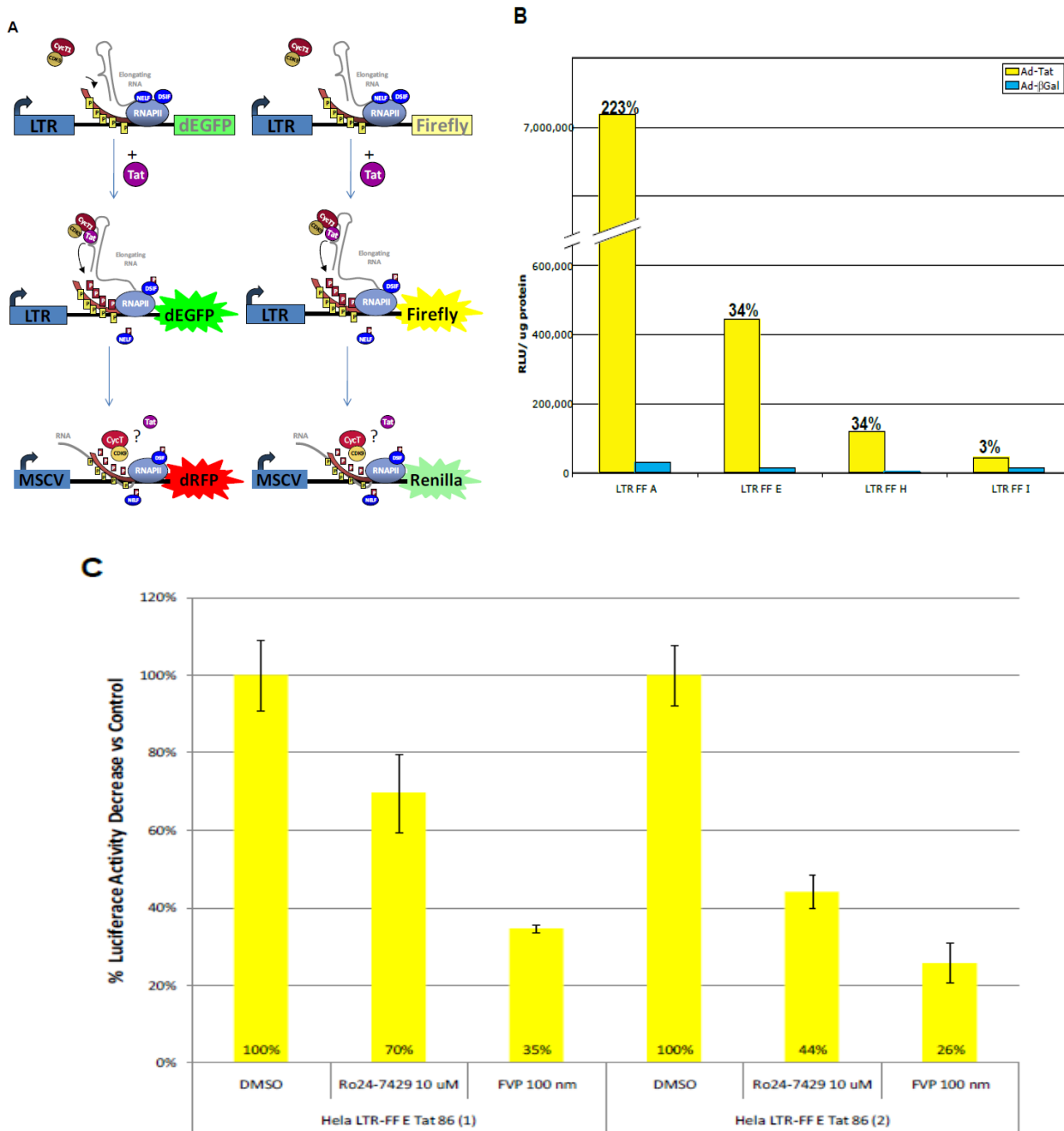
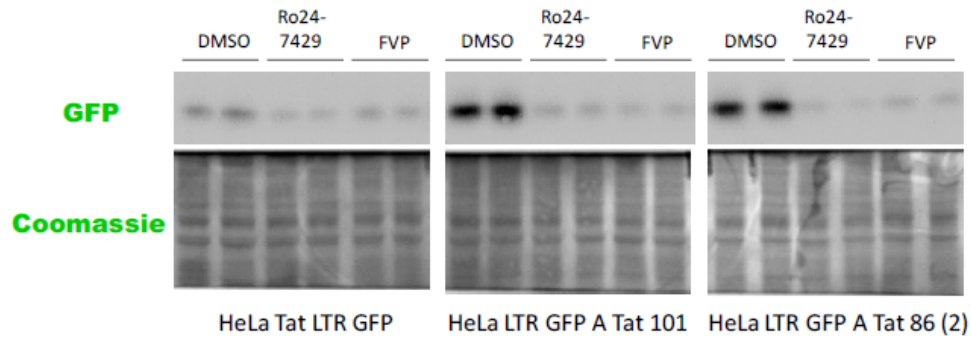


**Figure 2. Generation of Cell Lines.** (A) Schematic for generating HeLa based fluorescent and luciferase reporter cells. (B) Percent induction of LTR-FF activity in the absence or presence of Tat. Cells were infected with 50 MOI Ad-Tat or Ad-beta-gal and harvested 48 hours later and lysed. Firefly luciferase assays were performed, activity is normalized per microgram of protein. Percentages indicate fold increase over beta-gal control. (C) Effect of HIV transcriptional inhibitors in HeLa LTR-FF Tat dependent clones. Cells were treated with the indicated inhibitors and concentrations in duplicates for 48 hours, then harvested and lysed. Luciferase assays were performed using five micrograms of protein per sample. Chart shows percent decrease in luciferase activity over the control.

**A**



**B**

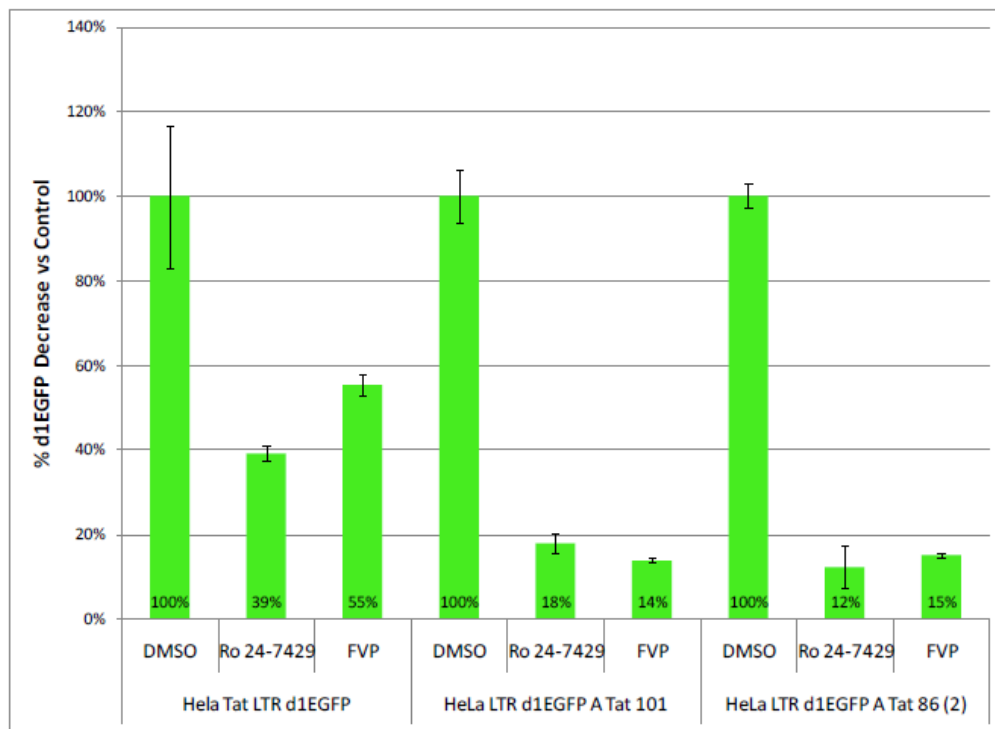


**Figure 3. Effects of HIV-1 Transcription Inhibitors in HeLa Tat LTR d1EGFP and HeLa LTR d1EGFP Tat Cells.** (A) d1EGFP western blot analysis of three cell lines treated with 10 microM Ro24-7429 or 100 nm flavopiridol. The cells were harvested and lysed. Twenty micrograms of protein were resolved in a 10% SDS-PAGE gel, transferred to a PVDF membrane and probed for d1EGFP. Bottom panels show Coomassie stained membranes for loading control. (B) Densitometric analysis of d1EGFP western blot bands shown in (A) normalized to the DMSO control using AlphaChemQ software.

## **Research Project 10: Project Title and Purpose**

*Data Analysis of Cognitive-Behavioral Therapy as an Augmentation Strategy for Social Anxiety Disorder* - We have completed a study of the efficacy of cognitive-behavioral therapy in the augmentation of response to the antidepressant paroxetine for patients with social anxiety disorder. The study was conducted at two sites (Temple University and the New York State Psychiatric Institute). Data files have been constructed at each site but funding expired prior to the initiation of formal data analysis suitable for professional publication. Therefore, the purpose of this project will be the construction of the final merged and cleaned dataset and the conduct of the statistical analysis for this project.

### **Anticipated Duration of Project**

7/1/2009 – 12/31/2010

### **Project Overview**

Social anxiety disorder is the third most common mental disorder in the US. Its symptoms include anxiety and avoidance of social situations and/or situations in which one might have to perform in front of others. It is associated with significant impairment in social, educational, and occupational functioning, as well as increased risk for other disorders that carry their own significant burdens, e.g., major depression and alcohol and substance abuse disorder. Viable treatments exist, but most patients complete trials of these treatments with significant residual impairment. Therefore, the study of augmentation treatment strategies is of great importance.

The broad objective of this project is to ready the data files necessary for analysis and conduct the analyses of the outcomes of our recently completed study of the efficacy of cognitive-behavioral therapy (CBT) as a method to augment the response of patients with social anxiety disorder who showed less than complete response to treatment with the selective serotonin reuptake inhibitor paroxetine. This research was funded by a grant from the National Institute of Mental Health, but expired before primary data analyses could be conducted. The final dataset has not been compiled and the sophisticated statistical analyses, based on hierarchical linear modeling that is the current standard in our field, have not yet been conducted. These essential analytical steps comprise the specific aims of this project.

### **Principal Investigator**

Richard G. Heimberg, PhD  
Professor of Psychology  
David Kipnis Distinguished Faculty Fellow  
Director, Adult Anxiety Clinic of Temple University  
Department of Psychology  
Temple University  
1701 North 13<sup>th</sup> Street  
Philadelphia, PA 19122-6085

## **Other Participating Researchers**

Carlos Blanco, MD, PhD, Henian Chen, PhD, Andrew B. Schmidt, LCSW – employed by New York State Psychiatric Institute

## **Expected Research Outcomes and Benefits**

Final and complete analyses of the data from the study of CBT augmentation of paroxetine treatment of social anxiety disorder will have several important (inter-related) outcomes and benefits. First, and most immediate, is that these analyses will serve as supporting data for a grant application to be submitted in 2009 to the National Institute of Mental Health (NIMH) that will further examine the nature and utility of augmentation treatments for social anxiety disorder. Second, completion of the data analysis will allow us to publish a paper in a top-tier journal and give our findings significant exposure, which should result in an increased interest in/utilization of CBT approaches in general and augmentation strategies in specific.

## **Summary of Research Completed**

The end date for this project was extended due to the loss of the project statistician; however, we were able to retain a replacement statistician several months later and are now progressing toward our goals.

We were in fact able to conduct preliminary statistical analyses of the partial dataset, sufficient to meet the first goal of supporting the writing and submission of a revised application for funding. This application, “Mirtazapine and CBT Augmentation of SSRI Treatment for Social Anxiety Disorder” was submitted to the NIMH a few days in advance of the deadline. The data analysis that was conducted and reported in that grant application is reproduced below.

The second goal of this project was to complete the dataset so that we could ultimately publish these promising findings in a top-tier journal in our field and give our findings significant exposure, which should result in an increased interest in/utilization of CBT approaches in general and augmentation strategies in specific. The requirements of this dataset are more stringent than required for the grant submission, and its completion has been hindered by the personnel changes noted above. However, the dataset is now in second draft and should be completed in sufficient time to conduct the necessary data analyses and prepare the manuscript for publication.

## **Grant Report**

This recent study assessed the efficacy of two treatments assigned at random for SAD patients who showed at least minimal response after an Acute Treatment Phase of 12 weeks of open treatment with paroxetine: (1) paroxetine continued as monotherapy or (2) paroxetine continuation augmented by individual CBT (as described in the preceding section) for 16 weeks. After the 16-week Augmentation/Continuation Phase, all treatments were discontinued and patients were followed up 24 weeks later (Follow-up Phase). This study and the proposed study share the design elements of open label paroxetine followed by augmentation with CBT. Preliminary analyses reported here therefore focus on results that best inform the proposed study. The analysis is limited to primary continuous and categorical outcome measures for patients who

have entered and completed the Acute and Augmentation/Continuation Phases (or dropped out prematurely).

Patients. 150 patients (94 NY, 56 Temple) who entered the study are the subject of this analysis.

Acute Treatment Phase Results. Analyses of acute outcomes were based on the intent-to-treat (ITT) sample, defined as patients who signed consent and provided data on the relevant measures during the Week 0 baseline assessment (with the exception of Clinical Global Impression Improvement Scores, CGI-I, which requires that at least one further assessment be administered after baseline for admission to the ITT sample, and for which the numbers are necessarily lower).

CGI-I scores were available for 122 patients. Of these patients, 79 (64.8%) were classified as responders (CGI-I score of 1 or 2). Twenty-nine of these patients (23.8% of the total) received a CGI-I score of 1. Twenty-seven (22.1%) patients received a score of 3. Sixteen (13.1%) patients received a score of 4 or higher.

We also examined changes achieved by patients in open paroxetine treatment on the clinician-administered Liebowitz Social Anxiety Scale (LSAS) and CGI-Severity Scale, as well as several self-rating measures. Significant changes were noted in the ITT sample for all of these measures.

Progression from Acute Phase to Augmentation vs. Continuation Treatment Phase. To progress to this phase, patients had to complete Phase I with at least 10% improvement on the LSAS. Fifty-two patients dropped out during Phase I, and 6 more patients dropped out when notified of their randomization (3 in each condition). We were most interested in the treatment of partial responders, and so we also excluded from the analyses to follow patients who met criteria for remission ( $n=23$ , 15.3%). Our criterion for this was a Week 12 CGI-I score of 1 and an LSAS score of less than 30. This cut-off score was found in our previous research (see Mennin et al, 2002) as the score that best discriminated between patients with SAD and normal controls in a receiver operating characteristics analysis (ROC). The ITT sample for Phase II included 29 patients who received paroxetine continuation and 32 who received paroxetine continuation augmented by CBT.

Augmentation vs. Continuation Treatment Phase Results. We looked at CGI-Improvement scores in two ways. First, we examined the proportion of patients in each randomized treatment who achieved remission, defined for this analysis as a CGI-Improvement score of 1 (we considered the Mennin et al. cut-off criterion to be appropriate in selection of patients for Phase II because it assured that patients with remaining symptoms would be included; however, we consider it to be too conservative for assessing outcome in Phase II, as its ROC analysis had compared patients to controls who could not meet criteria for any mental disorder, a “supernormal” group). Among partially responding patients who were continued on paroxetine alone, 3 of 29 (10.3%) were classified as remitters at Week 28. The corresponding number for the group receiving paroxetine augmented by CBT was 11 of 32 (34.4%), also significant, Fisher’s Exact Test,  $p = .034$ .

Second, we conducted the traditional responder-nonresponder analysis, in which a score of 1 or 2 denoted responder status. Among patients who were continued on paroxetine alone, 17 of 29 (58.6%) were classified as responders at Week 28. The corresponding number for the group

receiving paroxetine augmented by CBT was 28 of 32 (87.5%), and the difference between groups was significant, Fisher's Exact Test,  $p = .018$ .

We next looked at response to several other measures. There were no significant differences between treatment conditions at Week 12 with the exception of the Brief Fear of Negative Evaluation Scale,  $t(57) = -2.23$ ,  $p = .03$ , with higher scores reported by those patients reported by patients randomized to receive paroxetine continuation ( $M = 34.72$ ,  $SD = 7.92$ ) versus those randomized to receive paroxetine augmented by CBT ( $M = 30.47$ ,  $SD = 6.74$ ). For each measure, we then conducted an analysis of covariance, using the Week 12 score on the measure as the covariate, to examine whether there were differences between groups in residual change from Week 12 to Week 28. There were no significant differences between groups on the LSAS, Liebowitz Self-Rated Disability Scale, or Beck Depression Inventory. However, group differences were significant on the Social Phobia Scale,  $F(1,58) = 5.62$ ,  $p = .021$ , and the Brief Fear of Negative Evaluation Scale,  $F(1,58) = 4.24$ ,  $p = .044$ . The difference between groups approached significance on CGI-Severity,  $F(1,58) = 3.39$ ,  $p = .071$ , and the Social Interaction Anxiety Scale,  $F(1,58) = 3.36$ ,  $p = .072$ . In each case, differences favored the group receiving paroxetine augmented by CBT.

Finally, we examined within-group change for each treatment in Weeks 12-28. Statistical significance suggests further improvements during Phase II, whereas lack of significance reflects maintenance of gains for the specific group as a whole (individuals, of course, could get better or worse). Table 1 presents these data for the group receiving paroxetine alone and shows that patients in this group generally maintained their gains across measures, without further improvement. Table 2 presents the data for the group receiving paroxetine augmented by CBT; this group demonstrated additional change in Phase II on five of seven measures.

Summary of Findings. Open label treatment with paroxetine (Phase I) resulted in a high rate of response and significant changes from Week 0 to Week 12 on all measures. In Phase II, which focused on partial responders to Phase I treatment, continuation of paroxetine alone resulted in maintenance of gains, both on categorical measures of response and continuous clinician-administered and self-rated measures. However, there was little evidence for further change over the course of Phase II for these patients.

During Phase II, augmentation of paroxetine treatment with CBT was associated with further improvement. Improvement was significantly greater than for paroxetine alone for two measures and nearly so for two more. Further, this group improved significantly from Week 12 to Week 28 on 5 of 7 continuous measures, suggesting the efficacy of combined paroxetine/CBT for partial responders to an initial trial of paroxetine alone.

*Table 1. Week 12 to Week 28 Change on Measures of Social Anxiety, Depression, and Disability Among Patients Receiving Paroxetine Alone*

Measure	Wk 12 Mean	Wk 12 SD	Wk 28 Mean	Wk 28 SD	<i>t</i>	<i>df</i>	<i>p</i>
CGI Severity	4.00	0.77	3.85	1.27	0.66	27	.515
Liebowitz Social Anxiety Scale	49.45	19.23	44.86	20.75	1.24	28	.225
Brief Fear of Negative Evaluation Scale	34.72	7.92	33.07	8.43	1.48	28	.150
Social Interaction Anxiety Scale	39.31	12.97	37.03	12.70	1.47	28	.153
Social Phobia Scale	21.31	13.00	20.72	14.72	0.38	28	.707
Liebowitz Self-Rated Disability Scale	8.18	5.49	7.73	5.28	0.89	28	.381
Beck Depression Inventory	10.38	9.71	11.28	10.57	-1.2	28	.233

*Table 2. Week 12 to Week 28 Change on Measures of Social Anxiety, Depression, and Disability Among Patients Receiving Paroxetine Augmented by CBT*

Measure	Wk 12 Mean	Wk 12 SD	Wk 28 Mean	Wk 28 SD	<i>t</i>	<i>df</i>	<i>p</i>
CGI Severity	4.00	1.06	3.35	1.11	3.42	30	.002
Liebowitz Social Anxiety Scale	44.63	13.60	38.19	15.54	2.33	31	.026
Brief Fear of Negative Evaluation Scale	30.47	6.74	27.20	5.94	3.04	29	.005
Social Interaction Anxiety Scale	36.44	12.80	30.88	11.82	2.72	31	.011
Social Phobia Scale	17.25	10.52	12.78	8.69	3.16	31	.003
Liebowitz Self-Rated Disability Scale	6.55	4.34	6.72	4.25	-.35	31	.728
Beck Depression Inventory	7.97	7.30	8.30	8.53	-.25	29	.804

### **Research Project 11: Project Title and Purpose**

*RAD51 Causes Genomic Instability in Chronic Myeloid Leukemia* - BCR/ABL kinase-positive leukemia cells display genomic instability leading to the resistance to imatinib mesylate and malignant progression of the disease to fatal blast crisis. We reported previously that BCR/ABL enhances homologous recombination repair (HRR) of DNA double strand breaks (DSBs) due to stimulation of expression and tyrosine phosphorylation of RAD51. However, the fidelity of HRR is compromised in leukemia cells. We will investigate in depth the role of unfaithful DNA polymerase beta, BCR/ABL-RAD51 interaction, and constitutive tyrosine phosphorylation of RAD51 in compromising the fidelity of HRR eventually leading to genomic instability in leukemia cells.

## **Anticipated Duration of Project**

1/1/2009 – 12/31/2010

## **Project Overview**

The unifying hypothesis for this project is that BCR/ABL oncogenic tyrosine kinase causes overexpression of RAD51 protein, directly interacts with RAD51 and phosphorylates RAD51 on Y315 resulting in stimulation of unfaithful homologous recombination repair (HRR). This mechanism may contribute to genomic instability in chronic myeloid leukemia (CML) generating BCR/ABL mutants resistant to small molecule inhibitors such as imatinib, dasatinib and nilotinib, and producing chromosomal aberrations facilitating malignant progression of the disease from chronic phase (CML-CP) to fatal blast crisis (CML-BC).

We are planning to obtain preliminary evidence that RAD51 overexpression, interaction with BCR/ABL and/or tyrosine phosphorylation plays an important role in genomic instability in CML. To achieve our goals we will target BCR/ABL-induced overexpression of RAD51, BCR/ABL-SH3 - RAD51-PP functional interaction, and BCR/ABL-mediated constitutive phosphorylation of RAD51 on Y315 (RAD51-pY315).

RAD51 overexpression will be downregulated by previously validated commercially available RAD51-specific siRNA (Dharmacon); siRNA against non-coding sequence will be used as control. BCR/ABL-RAD51 interaction will be blocked by peptide aptamers containing proline-rich (PP) fragments of RAD51 (Genemed Synthesis, San Antonio, TX). Enhanced activity of RAD51-pY315, which probably depends on facilitated interaction with partner proteins and/or DNA substrates (to be examined in this project), will be abrogated by the aptamers containing phospho-Y315 of RAD51. Then, leukemia cells will be irradiated and chromosomal instability will be evaluated in surviving cells by spectral karyotyping (SKY) and by G-banding analysis to minimize the possibility of a false-positive result in SKY.

In addition, our preliminary data implicated a few polymerases possibly responsible for this effect; the primary suspect is DNA polymerase beta, which is overexpressed in leukemia cells and co-localizes with RAD51 nuclear foci. Therefore, polymerase beta will be downregulated by the expression plasmid carrying the shRNA and fidelity of HRR products will be determined by sequencing.

## **Principal Investigator**

Tomasz Skorski, MD, PhD  
Professor  
Temple University, School of Medicine  
3400 N. Broad Street, MRB 548  
Philadelphia, PA 19140

## Other Participating Researchers

Artur Slupianek, PhD – employed by Temple University

## Expected Research Outcomes and Benefits

We expect to obtain preliminary data about: (1) the role of unfaithful DNA polymerase beta in resistance to imatinib mesylate, (2) the role of BCR/ABL-RAD51 interactions contributing to chromosomal aberrations in CML. This information may be useful for planning novel strategies preventing/delaying the development of resistance to imatinib mesylate and blast crisis in CML patients.

## Summary of Research Completed

Our previous studies implicated BCR/ABL-mediated RAD51 Y315 phosphorylation as an essential event in enhanced recombination (Slupianek et al., Mol.Cell, 2001). We employed a peptide aptamer strategy targeting phospho-Y315 of RAD51. Peptides corresponding to the RAD51 fragment containing phospho-Y315, but not these with Y315F substitution reduced homeologous recombination repair (HomeoRR) activity by approximately 2-fold in BCR/ABL-positive leukemia cells (Fig. 1).

Altogether, it appears that phospho-Y315 stimulates abundant nuclear localization of RAD51 on DSBs, which disrupts the mechanisms responsible for preventing recombination using divergent templates resulting in unfaithful HomeoRR in BCR/ABL-positive leukemia cells. In summary, BCR/ABL-RAD51 interaction promotes survival and accumulation of chromosomal aberrations of CML cells expressing BCR/ABL kinase. We hypothesize that targeting BCR/ABL-RAD51 interaction may prevent/delay accumulation of secondary chromosomal aberrations and CML-BC progression.

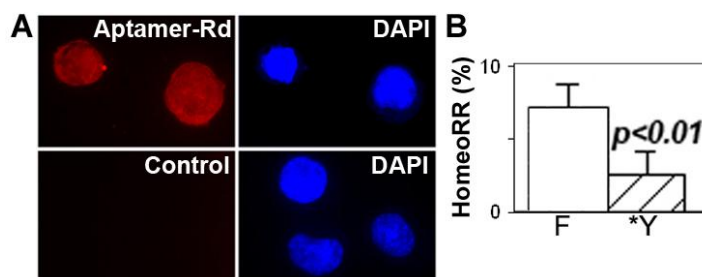


Fig. 1. RAD51 aptamers containing phospho-Y315 inhibit HomeoRR in BCR/ABL leukemia cells. (A) BCR/ABL-positive leukemia cells were incubated with 2mM of rhodamine (Rd)-labeled aptamer containing RAD51 phospho-Y315 (\*Y) fragment. Cellular uptake of the aptamer was detected by fluorescence after 4h incubation. (B) BCR/ABL-positive 32Dcl3 cells containing HomeoRR cassette were treated with 2mM of rhodamine (Rd)-labeled aptamer containing RAD51 phospho-Y315 (\*Y) or RAD51 Y315F (F) mutant fragments. Recombination activities in cells treated with \*Y or F aptamers was examined as described in Fig. 5. Results represent percent of G418-resistant clones (HomeoRR)  $\pm$  SD in I-SceI transfected cells. Statistical significance was calculated using Student *t* test.

## **Research Project 12: Project Title and Purpose**

*Enhancing Diabetic Foot Education by Viewing Personal Plantar Pressures* - The purpose of this project is to examine the efficacy of a novel patient education strategy, compared to a standard diabetic foot education. The proposed diabetic foot care education uses personal computer-animated plantar pressure data to educate patients on why and how they should care for their feet. The effectiveness of the diabetic foot education will be examined by looking at the following: (1) personal daily foot care as measured by foot-self care behavior scores; (2) subject understanding of peripheral neuropathy as assessed by the Patient Interpretation of Neuropathy Questionnaire; (3) occurrence of foot complications; and (4) peak barefoot plantar pressures.

### **Anticipated Duration of Project**

1/1/2009 – 12/31/2010

### **Project Overview**

In this project, the efficacy of an enhanced patient education strategy, compared to a standard diabetic foot education, will be investigated in a randomized control trial. The proposed enhanced diabetic foot education uses personal, computer-animated, multicolored, plantar pressure maps. The project will include 30 high-risk diabetic subjects. All subjects will receive a conventional foot care education and plantar pressure measurements. However, subjects randomized to the test group will receive the additional, enhanced diabetic foot education based on their footprints. A presentation of abnormal barefoot plantar pressure and how that pressure may be alleviated with proper shoes is postulated to motivate high-risk diabetic patients with peripheral neuropathy (loss of feeling in the feet) to take a more active role in caring for their feet. All participants will be monitored prospectively for a year along with quarterly palliative foot care and customary diabetic shoes. However, this project will focus on baseline, 1-month, and 3-month follow up evaluations. If the proposed visual diabetic foot education yields a more effective strategy, the subjects in the test group, as compared to the control group, are anticipated to show (1) better personal daily foot care, (2) greater understanding of peripheral neuropathy, and (3) fewer foot complications and (4) greater reductions in peak dynamic plantar pressure at follow up visits. The proposed diabetic foot education has a great potential to be an effective educational tool especially for those underserved minority communities, where health literacy is often a major challenge.

### **Principal Investigator**

Jinsup Song, DPM, PhD  
Director, Gait Study Center  
Temple University School of Podiatric Medicine (TUSPM)  
Gait Study Center, 2<sup>nd</sup> Floor  
148 North 8<sup>th</sup> Street  
Philadelphia, PA 19107

## **Other Participating Researchers**

Guenther Boden, MD, Gary Foster, PhD, Bradley Collins, PhD, Alexandra L. Hanlon, PhD, Carol J. Homko, RN, PhD, CDE – employed by Temple University

## **Expected Research Outcomes and Benefits**

This project targets methods of preventing diabetic foot complications. Effective diabetic foot care education is an important component in combating serious consequences of diabetic foot problems. This is an especially critical issue where health literacy is a concern. If the proposed education, which is personal and more visual than the traditional method, yields improved patient understanding and compliance, it can lead to significant reductions in the number of foot complications and health care costs. In addition, it may improve the quality of life of patients and their families. In this project, 30 participants who have diabetes and are at risk of developing foot complications are evaluated for three months to test the feasibility of the novel diabetic foot education. Participants may benefit directly by gaining a greater understanding of diabetic foot problems, improving their daily foot care, having periodic access to podiatric diabetic foot care, and preventing serious diabetic foot complications. In addition, any knowledge that is gained on efficacious educational strategies will be beneficial to others diagnosed with diabetes and will hopefully lead to a reduction in diabetic foot complications.

## **Summary of Research Completed**

Since our last reporting period we have been actively recruiting study participants and completing the study protocol. We have met our target enrollment of 30 subjects. Of the first 30 subjects enrolled, 3 were withdrawn due to clinical outcomes, and one was withdrawn due to noncompliance of study procedures. We've enrolled an additional 4 subjects at this time to accommodate for the 4 subjects withdrawn. Currently, we are in the process of completing the third and final visit for this project for the last 10 subjects. If the visits go according to schedule, all of the subjects will have completed visit 3 by the end of July 2010.

Data analysis has been started. A formal statistical analysis will be conducted when the data collection is completed.

## **Research Project 13: Project Title and Purpose**

*Tactile Imaging Sensor and Hyperspectral Data for Early Breast Cancer Detection* - The purpose of this project is to investigate the feasibility of a novel portable tactile and hyperspectral system for early breast cancer detection. A portable system would dramatically increase the probability of detecting breast cancer early, especially in remote areas. We propose to develop a tactile imaging sensor for breast cancer detection. When an object touches the sensor, the light will be diffused in varying amounts, which can be captured with a camera. Furthermore, we propose to integrate the tactile sensor image with the hyperspectral camera image to generate more accurate diagnosis of the breast cancer. Hyperspectral camera images allow health care providers to see in “different” colors—bands. The material composition of an

object can be identified using a hyperspectral camera. This system will allow minimally trained health care providers to detect breast cancer.

### **Anticipated Duration of Project**

7/1/2009 – 5/31/2011

### **Project Overview**

Objectives and Specific Aims. The broad objective of this research is to investigate the use of a tactile image sensor and hyperspectral images to detect breast cancer. Specific aim one is to develop a tactile imaging sensor that will image the touch sensation of the breast. This will enable the system to detect the palpable breast cancer tumors. Specific aim two is to develop a hyperspectral imaging subsystem with a novel light source to detect the calcification of the breast tissues. This will enable the detection of non-palpable breast cancer detection.

Research Design and Methods. We propose to develop a tactile imaging sensor that will quantify the touch sensation. Tactile sensation (palpation) is one of the most reliable methods of detecting breast tumors. We hypothesize that the healthy tissues will have similar elasticity throughout, and unhealthy tissues will have different elasticity. Thus, we will measure the softness/hardness of the tissues. Utilizing total internal reflection principle, the tactile imaging subsystem will quantify the breast tissues' elasticity, which in turn can be used to determine breast tumors.

Another subsystem consists of the hyperspectral camera subsystem, lighting subsystem, and processing subsystem. Hyperspectral camera is a combination of charge-coupled-device (CCD) camera with spectral information in each pixel. We propose to use high intensity light emitting diodes and a liquid crystal tunable filter. We will identify which band will be most effective in detecting calcification. We will also test different LEDs to determine the wavelength that will have the largest penetration. The processing subsystem will identify and characterize the calcification of the breast tissues.

### **Principal Investigator**

Chang-Hee Won, PhD  
Assistant Professor  
Temple University  
1947 N. 12<sup>th</sup> Street  
Philadelphia, PA 19122

### **Other Participating Researchers**

Dina Caroline, MD - employed by Temple University

## **Expected Research Outcomes and Benefits**

Early and reliable detection of breast cancer is an important issue. Utilizing multiple modalities will improve the reliability of breast cancer detection and decrease false alarms. A novel tactile sensor subsystem will detect tumors by palpation, and a novel hyperspectral subsystem will detect calcification of the breast tissues. We propose to investigate the feasibility of such a system. If successful, a portable system will detect cancer cells with high accuracy in almost real-time. This will allow breast cancer screening to be performed in nonhospital settings. If this preliminary project is successful and a system can be developed, then the impact will be in three areas: breast cancer early detection, detection from a remote location, and intraoperative tool.

One of the most common reasons for irregular breast cancer physical examination is procrastination. People are simply too busy to make an appointment to see a doctor for a potential problem that may or may not be there. One of the impacts of this project is to solve this problem by providing a Tactile and Hyperspectral System near the patients. For example, this system could be checked out from the local library.

Tactile and Hyperspectral system can be used in remote locations, where breast cancer specialists are not available. For example, in a rural area where there are no major hospitals nearby, a small pharmacy may have a Tactile and Hyperspectral System to detect breast cancer.

Tactile and Hyperspectral System provides almost real-time information about the breast cancer cells. So, Tactile and Hyperspectral System can be used as an intraoperative tool. During an operation surgeons can view the progress of their surgery by viewing tactile and hyperspectral images on a screen. After the surgery, the surgeon can verify that all the cancer cells have been removed by scanning for potential problem areas. This intraoperative tool will reduce wrong site surgery, excessive removal of the healthy tissues, and insufficient removal of the cancerous cells.

## **Summary of Research Completed**

We developed an optical tactile sensor based on the single layer silicone elastomer and the total internal reflection principle. We have built a sensor and performed the normal force computation from the tactile images. Then we determined the material composition using a hyperspectral camera.

*Tactile Sensor Design.* We have developed a simple prototype tactile sensor using a single layer silicone, a light emitting diode (LED), a camera, and a computer. The waveguide was made of transparent polydimethylsiloxane silicone elastomer. The refractive index of the silicone is 1.43. The light source is a cool white micro LED with a diameter of 1.8 mm. We used a complementary metal-oxide-semiconductor (CMOS) camera with 768 x 492 pixels with 8.4  $\mu\text{m}$  x 8.4  $\mu\text{m}$  pixel size. This system was developed to test the feasibility of imaging the tactile sensation. The resolution, sensitivity, and specificity were not optimized.

We pressed the sensor with varying force and as the force was increased the brightness of the image also increased.

Normal Force Determination. We have results in computing the normal force using the optical tactile images. Figure 1 shows three images with varying grayscale values. The first image on the left in Figure 1 is the image of a spherical indenter pressing on the sensor with 0.620N. The second image was taken after pressing with 1.12N and the third with 1.43N of normal force.

We hypothesized that we can estimate the normal force from the grayscale values. In order to verify our hypothesis, we performed an experiment with many different normal forces and obtained the corresponding images. We used a stainless steel indenter with a spherical shaped tip with the diameter of 3mm. Then we integrated the gray scale values to obtain the graph shown in Figure 2. The black dots are the experimental data points. We note that the data fit in a linear line. Even though more careful measurements and analysis must be performed, we suspect that the grayscale values are linearly related to the normal force.

The results were presented in the following conference.

Jong-Ha Lee, Chang-Hee Won, "High Resolution Tactile Imaging Sensor for Inclusion Detection and Identification," *The First AMA-IEEE Medical Technology Conference on Individualized Healthcare*, Washington DC, March 21-23, 2010.

### Hyperspectral Imaging System for Breast Calcification Characterization

Hyperspectral imaging system (HIS) is a novel method to generate a spectral characteristic map of region of interest based on the chemical composition. In our system we replaced the CMOS camera with a hyperspectral camera to create HIS. Previously, HIS has been used in non-medical applications including satellite investigation to find minerals on the ground or to access the condition of agriculture fields. Recently, HIS has been applied to the investigation of pathological changes in living tissue of animal and human. It has proven that HIS can provide valuable information as to the health or disease of tissue that sometimes other modalities are unavailable. HIS is a remote sensing technology to create 2-dimensional image having spectral information in each pixel. This information can be interpreted as the gradient map of species. It means HIS is a method of imaging spectroscopy combining the chemical specificity of spectroscopy with spatial information of imaging.

Biological tissues have optical signatures that reflect their chemical characteristics. The primary compositions in human tissue are oxyhemoglobin (HbO<sub>2</sub>) and deoxyhemoglobin (Hb). The Hb further breaks down into melanin, lipids and water (oxygenation). Total hemoglobin (HbT) indicates the combined quantities of HbO<sub>2</sub> and Hb. In near infrared (NIR) region, HbO<sub>2</sub> and Hb are major sensitive spectrum absorber. Since many diseases have specific effects on tissue oxygen and blood supply, tissue oxygenation and total hemoglobin concentration are major indicators of viability and tissue health. Thus in this paper, we mainly focus on the NIR region, particularly the short wavelength NIR of 650 to 1100 nm. By comparing the acquired spectrum absorption measurement in NIR region, information about type, location and relatively concentration of chemical composition about the tissue can be quantified. As far as we know, non-invasive, real time, local measurement of tissue oxygenation and total hemoglobin is still not commercially available. In this project, we constructed an HIS system capable of detecting photons in the NIR wavelength region to characterize the tissue condition. HIS has several advantages compare to other modalities such as CT and MRI. It penetrated into biological tissue

without radiation exposure such as CT, thus functional imaging with non-invasive and non-radioactive in real time is available. In addition it is simple, portable, and low cost compared to MRI.

The object of this work is to design HIS and investigate the ability of detecting calcification (Hydroxyapatite) in the breast. HIS is integrated with charged coupled device (CCD) and liquid crystal tunable filter (LCTF) to automatically capturing the spectrum information of Hydroxyapatite. LCTF controller is tuned to scanning from 650 nm to 1100 nm bands with 5 nm steps.

For the breast calcification characteristic experiments, Microcrystalline Hydroxyapatite 1200 mg is prepared. Totally 91 spectral band images, each image of  $1392 \times 1040$  pixels in size was obtained within 23 seconds. The 500W lighting source is used for illumination. Fig. 3. shows the spectrum characteristic of Microcrystalline Hydroxyapatite. It reveals the peak of 760 nm, 805 nm, 855 nm, 905 nm, and 960 nm. Thus, we conclude that we can detect calcification (hydroxyapatite) using a hyperspectral camera.

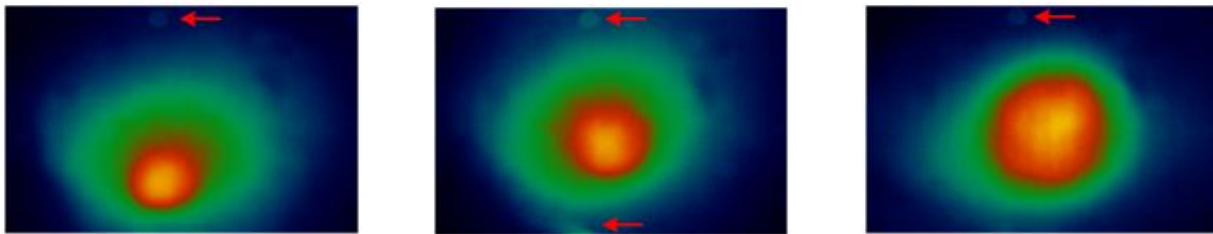


**Figure 1.** Tactile image with 0.620N, 1.12N, 1.43N normal force (from left to right). We integrate the grayscale values to obtain the forces. The arrows show impurities of the silicone elastomer.

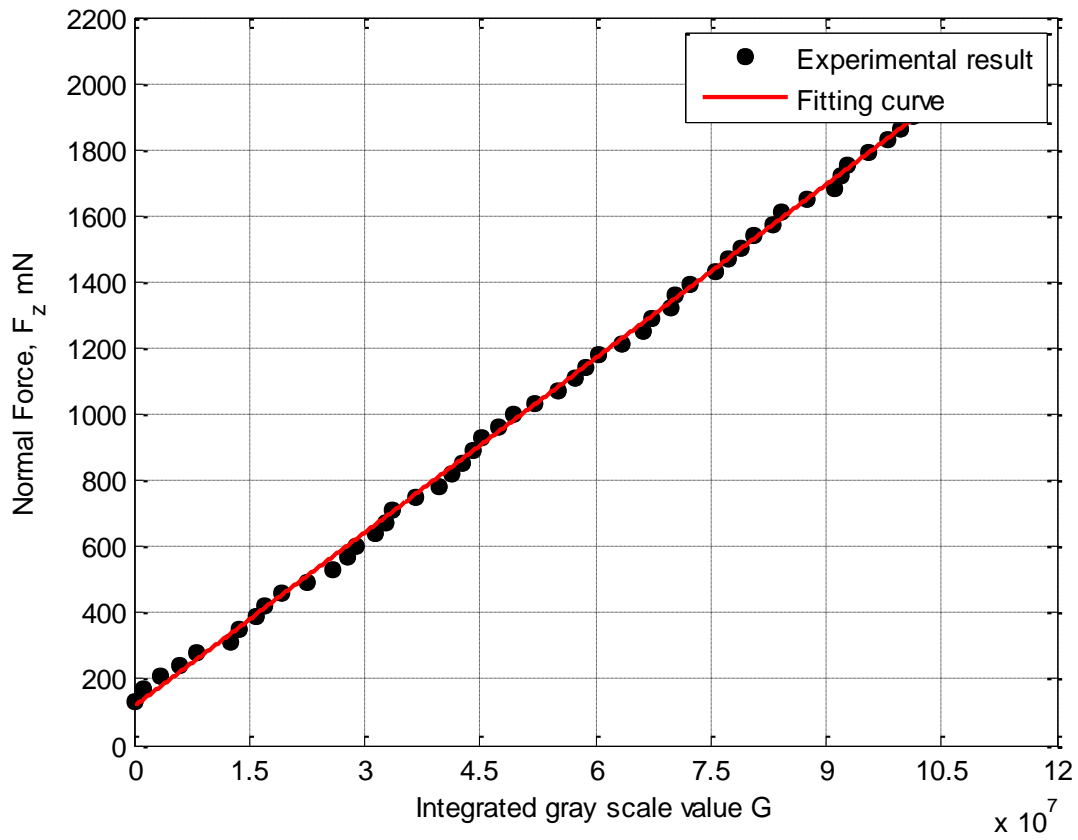


Figure 2. The normal force versus integrated gray scale values.

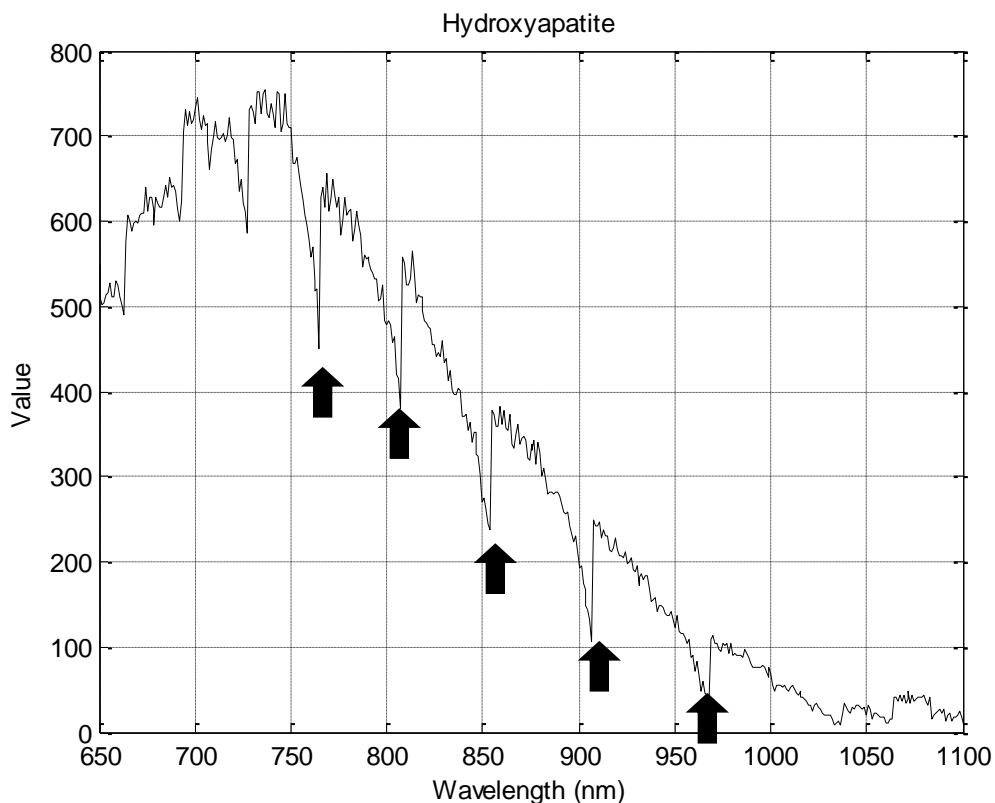


Figure 3. The NIR spectrum of Hydroxyapatite. Measured spectra within the region of area are averaged and plotted. Spectrum contains an absorption peak of 760 nm, 805 nm, 855 nm, 905 nm, and 960 nm.

### **Research Project 14: Project Title and Purpose**

*Small Animal Model of Medulloblastoma for Translational MR Neuroimaging at 3 Tesla* - This project will support the acquisition of a customized mouse brain coil which will allow us to adapt our brand new state-of-the-art human 3 Tesla MRI scanner for small animal neuroimaging. We will utilize the mouse brain coil for imaging of our transgenic mouse brain tumor model of medulloblastoma. The ability to perform high resolution neuroimaging and longitudinal studies of our mouse model of medulloblastoma on a human 3 Tesla magnet will give us the ability to directly translate our findings to non-invasive diagnostic, molecular, and therapeutic neuroimaging in the clinical setting.

### **Anticipated Duration of Project**

7/1/2009 – 7/31/2010

### **Project Overview**

Medulloblastomas and primitive neuroectodermal tumors (PNETs) are highly cellular malignant primary brain tumors representing the most common solid tumors arising in children. The major

limitations of the current state of the art clinical Magnetic Resonance Imaging and Spectroscopy to diagnose this disease include the inability to clearly define the parenchymal interface between normal and tumor regions; to differentiate tumoral edema from infiltration; to diagnose small primary or metastatic lesions; and to differentiate medulloblastomas or PNETs from other primary central nervous system (CNS) neoplasm.

Currently, to our knowledge, realistic animal models to study these medulloblastoma tumors are lacking. It is therefore necessary to develop and study the imaging characteristics of these CNS tumors using spontaneous brain tumor animal models that mimic human disease, as well as develop image processing tools to quantitatively analyze these tumors to improve diagnostic accuracy. Spontaneous tumor models in mice are generally thought to be more realistic models of human cancer than xenografts, and the lesions these animals develop present special challenges for imaging.

We will use high field Magnetic Resonance (MR) imaging to develop optimal characteristics to image these spontaneous CNS tumors. Quantitative methods for tissue segmentation based on fuzzy connectedness and medical image data mining techniques will be developed and tested to analyze these tumors. The imaging and image post processing methods will be validated using histological staining and immunohistochemistry for the transgene T-antigen, the viral oncoprotein expressed in these tumors.

Such a unique spontaneous brain tumor model will be useful for validation of the novel quantification methods proposed in this project. The long-term goal of this project will be to use these tools for validation and quantitation of tumor-specific contrast agents and therapeutics for medulloblastoma in children. These methods of imaging and quantification may be useful for in vivo imaging, diagnostics, and monitoring of response to tumor-specific therapy in other human CNS cancers. The magnetic resonance imaging (MRI) coil and accessories acquired through this project will allow us to use a human MRI to scan our small animal model of human medulloblastoma brain tumors at high power. In vivo imaging of this model will allow us to test and validate non-invasive novel diagnostic and therapeutic strategies that can be directly used in the clinic.

### **Principal Investigator**

Kamel Khalili, PhD  
Professor and Chair  
Department of Neuroscience  
Temple University School of Medicine  
Bio-Life Sciences Building, MS 015-96  
1900 N. 12th Street, Room 203  
Philadelphia, PA 19122

### **Other Participating Researchers**

Scott Faro, MD, Jennifer Gordon, PhD, Feroze Mohamed, PhD – employed by Temple University

## **Expected Research Outcomes and Benefits**

In addition to its role in chronic central nervous system (CNS) demyelination, JC virus (JCV) induces medulloblastomas in several experimental animal models. Morphologically, the medulloblastomas induced in transgenic mice are indistinguishable from human medulloblastomas. Of particular interest is recent evidence demonstrating the association of JCV with human medulloblastoma and the detection of the viral early protein, T-antigen, in a significant number of these childhood tumors. It is therefore suggested that JCV may serve as a tool for the development of an animal model to study the molecular mechanisms of tumor formation and to further investigate the molecular mechanisms by which JCV may induce cellular transformation. This information is critical for devising and implementing safe and effective therapeutic protocols for brain tumor treatment. In this project, we will utilize a state-of-the-art 3 Tesla human MRI for translational research to develop and test novel imaging techniques for accurate identification, delineation, and quantification of CNS tumors in a unique spontaneous transgenic mouse medulloblastoma model. The goal of this project is to develop sensitive and specific procedures for *in vivo* imaging of our transgenic mouse model of human medulloblastoma. The availability of high resolution MR images will assist us with disease diagnosis, detection of recurrent disease prior to clinical signs or symptoms, and evaluating the efficacy of therapeutic modalities during treatment.

## **Summary of Research Completed**

We are utilizing the JCV T-antigen transgenic mouse model which spontaneously develop medulloblastomas in the brain to closely mimic development and progression of human medulloblastoma. Optimal MR imaging conditions and protocols are employed to maximize image resolution and contrast-to-noise ratio in this animal model. We will investigate the role of the developed image post-processing techniques for tumor classification and volumetric analysis of the tumor data. Furthermore these imaging and image post processing methods are validated using histological correlations and a blinded investigation of the tools that are developed are used to analyze a group of mouse brain images without prior knowledge of pathology.

After MR scanning, the brains of the animals are perfusion-fixed and the morphological evaluations are performed on their tissue in collaboration with Core B. Tissue for histological analysis is fixed in paraformaldehyde. Drs. Gordon and Mohamed review the scans for abnormalities, fiduciary markers and anatomical landmarks then evaluate any apparent gross pathological changes. Tissues are then orientated for cutting in the proper plane (i.e., sagittal, coronal, etc.). Histological staining is performed first. Dr. Gordon then reviews the slides to identify the appropriate regions for further analysis. Additional histological staining and immunohistochemistry are then performed as needed using antibodies which recognize T-antigen or cellular markers. Dr. Gordon is very familiar with the T-antigen transgenic mouse brain tumor models developed in collaboration with Dr. Khalili.

Initially a neuroradiologist reviewed all the MR images (T2-weighted and pre- and post-gadolinium T1 weighted images) and characterized the normal and tumor areas of the mouse brain images. This is primarily be based on the signal characteristics of the tumor visualization

on various imaging sequences used (T2, pre and post T1), as well as morphological characteristics of the normal and abnormal structures in the mouse brain. Signal-to-noise ratio (SNR) of the tumor area compared to the non-tumor area is also measured using ROI measurements at the scanner console. The images are then sent to the MRI/DEN Laboratory for further post-processing. The semi-automated segmentation techniques based on fuzzy-connectedness are used to accurately identify the tissues and delineate the tumor margins. The neuroradiologists based on MRI and histopathological data identifies the seed points for typical characteristic tumor regions such as viable tumor, edema, necrosis, tumor margins, and normal brain tissue with blood vessels as well as visualization and delineation of the tumor margins. Different tissues types are identified and classified from the segmented images. Next, features are extracted from these segmented ROI data using concentric circles methods, vector quantization, and fractal mass dimension methods to quantitatively characterize tumor masses. MR imaging results as well as the automated segmentation and texture analysis results are then correlated with the histological findings and tabulated.

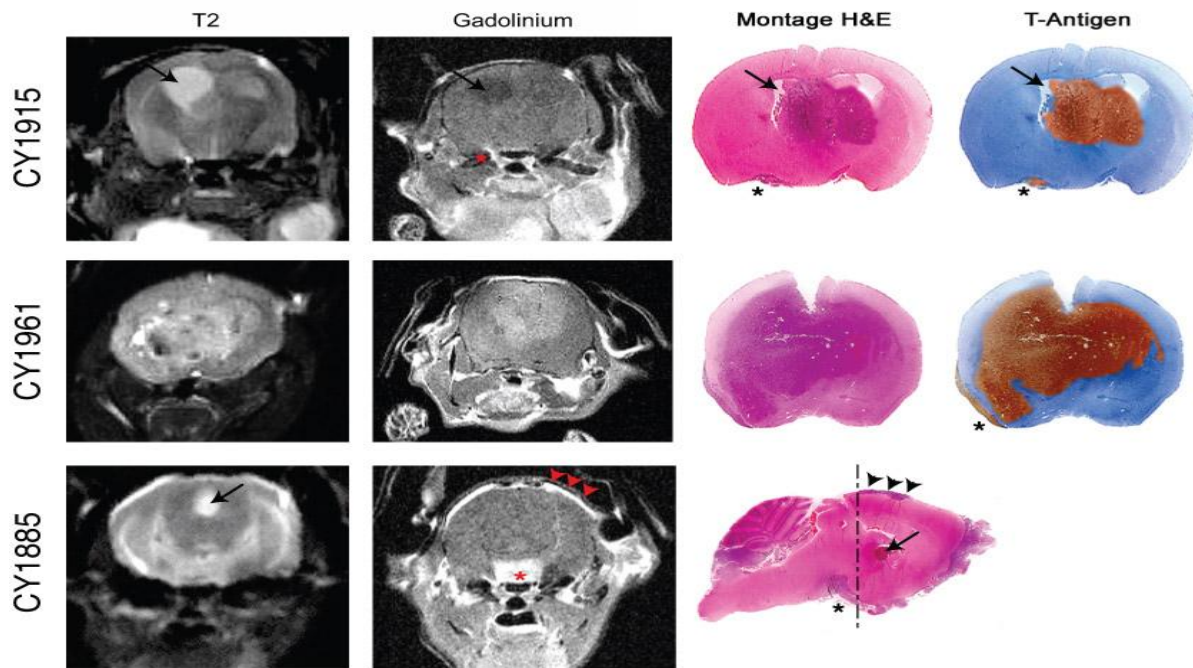


**Figure 1. Co-registration of MR images and histological features of PNETs.** Animals were imaged prior to injection of contrast material, removed from the scanner, injected intravenously with gadolinium, then repositioned and imaged again. Brain tissue was formalin fixed, paraffin embedded, sectioned coronally\*, and stained with hematoxylin and eosin (H&E) or immunostained which recognizes the transgene, T-antigen, then counterstained with hematoxylin. Representative MR images post gadolinium and pre T2 scanning were used to orient fixed brain tissue for co-registration by microscopic classification. Areas of solid tumor, tumor with extensive blood vessels, normal brain, necrosis, and edema were identified radiologically and histologically and scored, Unusual features were also identified including CY1885: arrow: hemorrhage, asterisk: extra-axial tumor mass, arrowheads: subarachnoid

spread of tumor; CY1915: asterisk: contrast enhanced tumor, arrow: dilated ventricle; CY1961: asterisk, subarachnoid spread of tumor mass. \*Note that CY1885 was sectioned sagittally, dotted line represents approximate plane of coronal MR images.

## **Research Project 15: Project Title and Purpose**

*Developing Radiological Risk Communication for Low-literacy Populations* - Radiological exposure from a terror event has been identified by the Centers for Disease Control and Prevention (CDC) and the Office of Homeland Security as a potential threat worthy of significant national preparedness. Little research has been done, however, to develop risk communication strategies for those with limited literacy. The purpose of this project is to assess whether new approaches to designing risk communication are valid methods to develop emergency preparedness materials for people with low literacy. The project will pilot the use of health literacy measures as well as physiological measure tools (i.e., skin response, eye tracking and respiration) with General Internal Medicine Clinic patients at Temple University Hospital. These pilots will enable us to effectively use these evaluative tools with individuals with low levels of literacy.

### **Anticipated Duration of Project**

9/15/2009 – 8/31/2010

### **Project Overview**

The overall goal of these two pilot studies is to provide data to indicate the feasibility of proposed research in the re-submission of a National Institutes of Health (NIH) grant. PILOT ONE will show the feasibility in securing subjects with low literacy through Temple University's General Internal Medicine clinic and which literacy tool is easiest to administer. PILOT TWO will show the feasibility of using the psycho-physiological equipment with subjects who are of low literacy. This will allow us to understand the special needs of this population when using these research measures. Specific methodology will be used.

1. **PILOT ONE:** Conduct a pilot with 30 patients of the General Internal Medicine clinic at Temple University Hospital using both the Rapid Estimate of Adult Literacy in Medicine (REALM-R) (N=15) and the Short Test of Functional Literacy in Adults (S-TOFHLA) (N=15) to assess general literacy levels of patients as well as assess the feasibility of using both measures in the clinical setting. Patients who are waiting to see the doctor will be asked if they would be willing to participate in the study. Once consented, the subject will be asked to either read words (REALM-R) or circle the correct answers (S-TOFHLA) in the tool. When the subject is done, the participant will be given a \$10 gift card and the examiner will score the test. This pilot test will allow the investigator to provide data illustrating that she will be able to find sufficient numbers of people with low literacy to take part in the research as well as information about which measure is easiest to use in the setting.
2. **PILOT TWO:** Conduct a pilot (N=10) to assess the feasibility of using psycho-physiological measures with low-literate subjects. Because the equipment tracks eye movements

it will be important to be able to demonstrate that this equipment is not too difficult for low-literate subjects to use. Subjects will have sensors attached for skin resistance monitoring and heart-rate monitoring, and a headset for eye-tracking/pupil-dilation measures. Subjects will then be shown a colorectal cancer (CRC) screening decision aid while data from the sensors and eye-tracking measures are being recorded. Sensors and the eye-tracking headset will then be removed and subjects will complete a survey on their experience using the psycho-physiological measures and be given a \$30 gift card. This pilot will utilize an existing low-literacy level tutorial on colorectal cancer that has been developed for another project as a mechanism to evaluate the acceptability of the equipment as well as the validity of results in a low-literate population.

### **Principal Investigator**

Sarah Bauerle Bass, PhD, MPH  
Associate Professor of Public Health  
Temple University  
Ritter Annex, Room 927  
1301 Cecil B. Moore Ave.  
Philadelphia, PA 19122

### **Other Participating Researchers**

None

### **Expected Research Outcomes and Benefits**

Individual subjects will benefit in three ways: (1) the knowledge that they have contributed to the development of more effective health decision aids for those with low literacy; (2) knowing they have helped to develop more effective procedures for testing health decision aids and the development of more effective ways to communicate with the public about health issues; and (3) the knowledge and experience gained from having participated in a scientific study will contribute to their personal understanding of how scientific studies in general are conducted and, specifically, how eye-tracking and psycho-physiological assessments are done.

Society will benefit in two ways: (1) the development of more effective, literacy-appropriate health decision materials will make it easier for the public to learn about health issues and, in the case of the larger NIH proposal, prepare for radiological terror events; and (2) the development of more sophisticated assessment procedures, such as the combined perceptual mapping, eye-tracking, and psycho-physiological measures, which will lead to more valid and reliable research techniques. This information is critical for developing educational materials and communications that assist the public in preparing for or responding to public health situations.

## Summary of Research Completed

PILOT STUDY ONE of this project was to determine which health literacy tool (the REALM-R or the STOFHLA) is easier and most efficient to administer to General Internal Medicine Clinic patients, as well as which tool provides superior results for assessing health literacy.

The REALM-R, the mostly commonly used health literacy tool, takes less than 5 minutes to administer and score. The REALM-R is a word-recognition test comprising 11 medical terms, arranged in order of complexity by the number of syllables and pronunciation difficulty, starting with simple one-syllable words (e.g., pill) and ending with multi-syllable words (e.g., osteoporosis). Of these 11 words, 8 are scored. Patients read down the list, pronouncing aloud as many words as they can while the examiner scores the number of words pronounced correctly using standard dictionary pronunciation as the scoring standard. Scores on the REALM-R vary from 0 (no words pronounced correctly) to 11 (all words pronounced correctly.) A score of 6 or less is considered low health literacy.

The STOFHLA takes approximately 10 minutes to administer and score. The STOFHLA is a timed reading comprehension test that uses the modified Cloze procedure, in which every 5th to 7th word in a passage is omitted and replaced with a blank space. The patient must select a word to fit into the blank spaces from the 4 multiple-choice options provided for each space. The STOFHLA is scored on a scale of 0 to 36. Patients are categorized as having adequate health literacy if the STOFHLA score is 23–36, marginal health literacy if it is 17–22, and inadequate health literacy if the score is 0–16.

During the fiscal year, PILOT ONE of the project was completed. A summary of activities follows.

### *Subject Recruitment and Accrual*

During September and October 2009, thirty patients (N=30) ages 18 and over were recruited from the General Internal Medicine clinic located at Temple University Hospital in Philadelphia. The clinic primarily serves low income African Americans who have Medicare or Medicaid insurance, the majority of whom have low health literacy.

### *Research Procedure*

Research assistants used scheduling records to determine eligibility. A convenience sample of volunteers was obtained. Patients who refused typically cited that they could not stay after their visit because they did not have time, had to leave immediately to go to work or to another doctor's appointment, or were accompanied by a caretaker. Other patients declined because they were not interested or were focused solely on their health issues during the visit.

Two research assistants recruited patients and obtained informed consent prior to administering the health literacy instrument, the REALM-R or the STOFHLA, and socio-demographic questions. The directions were read aloud by the research assistants to the patients who were asked to either pronounce a set of words or fill in the word that best fit each sentence. The data

were collected prior to or after patients had been seen by the resident physicians. Administration of all research consent forms and instruments took from 5-10 minutes. Of the 30 patients, 15 were administered the REALM-R and 15 were administered the STOFHLA. Research assistants kept track of how much time each test took and scored the tests using the standard scoring rubrics. Each subject received a \$10 gift card and two SEPTA transit tokens as compensation.

The Temple University Institutional Review Board (IRB) approved use of both instruments, the patient recruitment plan and procedures for maintaining anonymity.

### *Demographic Distribution of Sample*

Table 1 illustrates the demographic description of participants. Statistics indicate the two groups were similar, with the majority of both groups African American and indicating they had either not graduated from high school (average of 40% for both samples) or had a high school diploma (average 53.4% of both samples) but had no college level education; thus, over 90% of the samples had no higher education. There were two differences between the two groups. One was gender distribution; those in the REALM-R group were equally divided between male (N=7; 46.7%) and female (N=8; 53.3%), while those in the STOFHLA group had more females (N=10; 66.7%) than males (N=5; 33.3%). The second was age; those in the STOFHLA group were slightly older, with 80% of the sample between the ages of 51 and 70, compared to 40% of the sample taking the REALM-R. The overall average age of the sample was 53, with a range from 21 years of age to 72. These differences are a limitation of the data but it is not believed to have significantly affected the data.

### *Health Literacy Testing Results*

Results indicate very low health literacy in the clinic population, despite half of the population reporting high school graduation. Those taking the REALM-R were able to pronounce on average only 5 of the 8 scored words with 93% falling in the “low” or “very low” literacy categories. The lowest score was a zero (meaning the subject was not able to pronounce/read any of the words) and the highest was an 8, meaning they could pronounce/read all the words (see Table 2).

Of those taking the STOFHLA, the average score was a 17.9 out of 36 points, with 86.7% falling in the “inadequate” or “marginal” literacy categories. The lowest score in the sample was a 10 out of 36 and the highest was a 33 (See Table 3).

Research assistants estimated the time it took each individual to complete the literacy testing. On average, it was found that the informed consent, protocol narrative, REALM-R test and demographic questions took on average three to four minutes to administer. On the other hand, the STOFHLA protocol tool on average 12 to 15 minutes. We also had many patients become frustrated by the STOFHLA test, feeling inadequate or unsure of how to answer the questions. We had no patients express concern about the REALM-R and patients did not question why we were asking them about the ability to read or pronounce words. These significance differences are crucial findings when designing a study that uses health literacy testing as an outcome.

*Conclusions*

Of the two measures, the REALM-R took less time (3-4 minutes vs. 12-15 for the STOFHLA) and patients felt less threatened or confused by what was expected of them. While the STOFHLA results showed slightly more variation by health literacy category and identified a few individuals who would be considered to have adequate literacy compared to the REALM-R, the negativity towards the STOFHLA and the amount of time it took most patients to take it indicate the REALM-R is a more practical health literacy assessment to use with this population. We found that using the STOFHLA would alienate our patients by making them feel marginalized. When working with a low-literacy population, you want to make all study protocols, interventions and materials accessible and appropriate; our findings indicate that the use of the STOFHLA would be counter-productive to that goal and we will be using the REALM-R in future studies.

*Table 1. Demographic Characteristics of Participants*

	REALM-R Participants N=15	STOFHLA Participants N=15
<b>Race</b>		
African American	12 (80.0%)	15 (100%)
Other	3 (20.0%)	0
<b>Hispanic Origin</b>		
Yes	3 (20.0%)	0
No	12 (80.0%)	15 (100%)
<b>Gender</b>		
Male	7 (46.7%)	5 (33.3%)
Female	8 (53.3%)	10 (66.7%)
<b>Education Level</b>		
Some High School	6 (40.0%)	6 (40.0%)
Graduated High School	7 (46.7%)	9 (60.0%)
Some College	1 ( 6.7%)	0
Graduated College	1 ( 6.7%)	0
<b>Age</b>		
20-30	3 (20.0%)	0
31-50	5 (33.3%)	2 (13.3%)
51-70	6 (40.0%)	12 (80.0%)
71+	1 (6.7%)	1 ( 6.7%)

*Table 2. REALM-R Results*

<i>Literacy Category</i>	<i>Number/Percent</i>
Literate	1 (6.7%)
Low Literacy	9 (60.0%)
Very Low Literacy	5 (33.3%)
<i>Words Pronounced (Average 5.1 words/8; 63.8%)</i>	
Minimum Words Pronounced	0
Maximum Words Pronounced	8

*Table 3. STOHFLA Results*

<i>Literacy Category</i>	<i>Number/Percent</i>
Inadequate Literacy	7 (46.7%)
Marginal Literacy	6 (40.0%)
Adequate Literacy	2 (13.3%)
<i>Scores (Average score 17.9/36 points; 49.7%)</i>	
Minimum score	10
Maximum Score	33

### **Research Project 16: Project Title and Purpose**

*Using a Telemedicine System to Promote Patient Care Among Underserved Individuals -* Hypertension (high blood pressure) affects more than 65 million people in the US with African Americans disproportionately affected. Untreated hypertension is associated with an increased risk for heart attacks, sudden death, stroke, and kidney failure. Home-measured blood pressure has become an important method of managing hypertension. This study will test the effectiveness of an Internet-based telemedicine system coupled with home-measured blood pressure to strengthen the patient-provider relationship and to educate and empower individuals with hypertension to take a more active role in their own health care.

### **Anticipated Duration of Project**

9/15/2009 – 8/31/2011

### **Project Overview**

Despite the importance of controlling hypertension and available therapy, inadequate blood pressure control remains all too common. For hypertension care, strategies are needed that support a Patient Centered Care (PCC) approach. We believe that telemedicine can provide a PCC model for hypertension care. We have established a telemedicine system for disease management, based on a personal health record and have used this system in diverse disease states (heart failure, cardiovascular disease (CVD) risk reduction, hypertension, diabetes). This research project will support PCC by increasing access, and automating care reminders and

feedback for both patients and health care providers. Urban underserved patients with uncontrolled hypertension (BP>140/90 mmHg) will be randomized to either usual care or telemedicine. Blood pressure, weight, blood glucose and lipids, and physical activity will be measured at baseline and at 6 months. The primary endpoint is the proportion of subjects who achieve goal blood pressure.

The specific aim of this Department of Health (DOH) funding is to recruit 82 additional subjects for this study. Our expanded recruiting efforts have required unanticipated personnel commitments that exceed budgeted personnel time. Additional funds of \$30,000 will allow recruiting efforts to complete the study on time.

Successful completion of the project will lead to new Agency for Healthcare Research and Quality (AHRQ) funding, approximately \$1,200,000 of direct funding, and 400,000 of indirect funding. Funding to provide wider dissemination is dependent on showing a positive effect of our telemedicine intervention for hypertension.

### **Principal Investigator**

Alfred A. Bove, MD, PhD  
Professor of Medicine  
Temple University Hospital  
Cardiology Section  
2401 N. Broad Street  
Philadelphia, PA 19140

### **Other Participating Researchers**

William P Santamore, PhD, Carol Homko, RN, PhD, Margaret Kerper, RN, Abul Kashem, MD, PhD, Philip Berger, BS – employed by Temple University

### **Expected Research Outcomes and Benefits**

DOH funding will support recruiting 82 subjects to extend our findings to a broader population, which includes type 2 diabetes. Effective chronic disease management requires: (1) patient participation in decision making; (2) active patient self-monitoring and self-management; (3) effective patient-provider communication; and (4) adherence to established guidelines and quality indicators. The telemedicine system addresses all these issues and supports patient's engagement in their own care. The patient's knowledge will be increased by the motivational/educational messages (covering all quality measures – advice on sodium, alcohol, exercise, weight loss, DASH diet), by the educational modules on the site, and by links to other websites. The cardiovascular knowledge questionnaire will be utilized to test this hypothesis.

The patient self-management and engagement in their self-care (Patient Centered Care) is supported by the system. The frequency of self-monitoring can be measured. The patient is sent automated reminders to send data and receives feedback and reinforcement when data is sent. Trend lines in blood pressure and physical activity are provided to both patient and physician.

The net result will be sooner and more frequent changes in medication; better control of hypertension; and timely office visits.

Thus for the underserved populations, the telemedicine system addresses the suboptimal control of blood pressure, and improves care in a cost effective manner. The telemedicine system can be rapidly updated as new national guidelines are developed, and offers the possibility of rapid dissemination throughout the U.S.

### **Summary of Research Completed**

Formula Funding was provided to allow us to complete recruiting in a program to manage hypertension in underserved urban subjects. The base funding for the program was supplied by a 3-year grant from AHRQ.

*Project Aim:* Reduce blood pressure from hypertension levels to pre-hypertension levels in 50% of subjects with hypertension using an internet-based Telemedicine disease management system.

We planned to recruit 252 subjects by February 15, 2010 to allow time for data analysis in August 2010. We used the Formula funds to intensify recruiting, and to add Christiana Medical Center, Wilmington, Delaware as a second recruiting site. Christiana began recruiting for the study in early December 2009. As of May 2010, we have recruited 2229 subjects (Temple 201, Christiana 28). We screened 536 subjects, 43% entered the study. 126 subjects have completed the 6 month study. We closed recruiting at Temple on March 1, 2010, and will continue to recruit at Christiana until September 2010. We expect to recruit 240-245 subjects vs. planned 252. The subjects recruited will provide adequate numbers for completing the statistical analysis. We presented an abstract on our baseline population at the AHA outcomes research meeting in Washington DC in May 2010. Formula funds were used to accelerate recruiting at our Temple site and to add Christiana Medical Center as a recruiting site. We also requested and received a one-year no-cost extension from AHRQ to allow us to process the data through 2011.

Summary of the progress to date:

Total number of screened patients: 536

Total number entered as of June 1, 2010: Temple-201, Christiana - 28

126 subjects completed the 6 month study.

Demographic data for the entire cohort are shown in the table below.

Male	36%
Female	64%
Caucasian	16%
African American	80%
Asian	1%
Hispanic,	3%
Age – years*	59.3
Ht – inches*	65.9
Wt – pounds*	208.1

BMI Kg/M <sup>2</sup> *	33.7
Income < \$25,000	51%
Education High School or above	87%
Internet at home	51%
Smokers	20%
Diabetes	26%
Hyperlipidemia	38%

\* mean value

## **Research Project 17: Project Title and Purpose**

*Control of Calcium Entry Mechanisms in Smooth Muscle* - An understanding of the molecular mechanisms of store-operated channels and the coupling interactions between Stim sensors and Orai channels has important implications in vascular SMC function and the development of therapies to treat contractile and growth diseases, including hypertension and atherosclerosis. The purpose of this project is to understand and clarify the basic pharmacology of the activation of these channels which may provide crucial new methods to control Ca<sup>2+</sup> in vascular smooth muscle cells.

### **Duration of Project**

9/15/2009 – 5/31/2010

### **Project Overview**

Ca<sup>2+</sup> entry signals in vascular smooth muscle is an integration of channels activated by a variety of stimuli including voltage, stretch, hormone receptors, and Ca<sup>2+</sup> store depletion. A new pathway involving two protein families, Stim and Orai, has been discovered to mediate “store-operated” Ca<sup>2+</sup> entry (SOCE) in most cells, including SMCs. Stim1 and Stim2 are ER Ca<sup>2+</sup> store sensors, and Orai1, Orai2, and Orai3 are highly Ca<sup>2+</sup>-selective plasma membrane (PM) store-operated channels (SOCs). Pharmacological control of SOCs is a crucial question. 2-aminoethoxydiphenyl borate (2-APB) is a powerful SOC modifier although its mechanism of action remains unknown. This project addresses two hypotheses: (a) that 2-APB functions to link specific functional regions of the Stim and Orai proteins together, and (b) that the linking of Stim and Orai proteins is controlled by Ca<sup>2+</sup> entering through Orai channels which may physiologically control SOC activation. The aims are to address these hypotheses in model cell systems (HEK293 cells) expressing Stim and Orai proteins specifically modified with fluorescent probes, using a combination of approaches including high-resolution fluorescence imaging, Förster Resonance Energy Transfer (FRET) analysis, and patch-clamp electrophysiology

## **Principal Investigator**

Donald L. Gill, PhD  
Professor and Chair  
Temple University  
Department of Biochemistry  
Kresge, Room 623  
3440 N. Broad St.  
Philadelphia, PA 19140

## **Other Participating Researchers**

Eunan Hendron, BSc – employed by Temple University

## **Expected Research Outcomes and Benefits**

1. Identify the minimum regions of Stim and Orai proteins required for 2-APB-induced interactions, involving (a) sequential dissection the C-terminal regions of YFP-labeled Stim proteins to assess the minimal regions for interaction with CFP-labeled whole Orai proteins, and (b) examination of small cytoplasmic domains of the Orai proteins, each CFP-tagged, to assess the effective interactions with Stim proteins
2. Assess whether clustering of STIM and Orai proteins is a pre-requisite for 2-APB-induced Stim-Orai interactions, involving a determination of whether the action of 2-APB is to multimerize the Stim or Orai fragments (cis-interactions) as a pre-requisite for trans-interactions between the Stim and Orai molecules.
3. To determine whether Ca<sup>2+</sup> entering through SOCs controls the interaction between STIM1 and Orai proteins, involving examination of the local Ca<sup>2+</sup> environment using a simple FRET-based measurement using the Ca<sup>2+</sup>-sensing yellow cameleon (YC3.1) linked to Orai1, as a direct probe for Ca<sup>2+</sup> in the restricted space in which Orai channels operate.

Completion of this work will provide a new insight into understanding how calcium entry mechanisms can be controlled in vascular smooth muscle, allowing for the identification and development of effective pharmacological modifiers of cardiovascular diseases including hypertension and atherosclerosis.

## **Summary of Research Completed**

Aim 1. To identify the minimum regions of Stim and Orai proteins required for 2-APB-induced interactions, involving (a) sequential dissection the C-terminal regions of YFP-labeled Stim proteins to assess the minimal regions for interaction with CFP-labeled whole Orai proteins, and (b) examination of small cytoplasmic domains of the Orai proteins, each CFP-tagged, to assess the effective interactions with Stim proteins.

Our experiments have provided important new information on function of the SOAR (STIM1 Orai-activating region) of STIM1. This region (Fig. 1) includes the 344-442 sequence of STIM1 including and surrounding the second coiled coil domain of the cytoplasmic domain of STIM1. This segment is significantly shorter than the “CAD” domain (342-448) defined by Lewis and coworkers. We confirm that there is large constitutive activation of  $\text{Ca}^{2+}$  entry when expressed in HEK293 cells stably expressing Orai1 (Fig. 2A). Addition of 2-APB caused little further  $\text{Ca}^{2+}$  entry and resulted in inhibition of entry. The peptide was almost totally attached to the PM (Fig. 2B) and addition of 2-APB did not change this (Fig. 2C). These results reveal that SOAR is fully constitutively associated with Orai1, and the inhibition by 2-APB is not a result of SOAR-detachment. These results contrast strongly with the larger C-terminal fragments of STIM1 and STIM2 which we revealed had little effect on Orai1 unless 2-APB was added in which case they bound avidly and reversibly to Orai1 causing complete channel activation.

When the C-terminus of SOAR was reduced by 17 amino acids, the peptide induced no constitutive  $\text{Ca}^{2+}$  entry nor did 2-APB activate this (Fig. 3A). This truncated peptide was expressed entirely in the cytosol (Fig. 3B), and no PM association was observed after 2-APB addition (Fig. 3C). This indicates that the C-terminal region of SOAR is required for coupling to Orai1. The result is important in continuing to pinpoint the small region of STIM1 involved in Orai channel coupling.

Aim 2. To assess whether clustering of STIM and Orai proteins is a pre-requisite for 2-APB-induced Stim-Orai interactions, involving a determination of whether the action of 2-APB is to multimerize the Stim or Orai fragments (cis-interactions) as a pre-requisite for trans-interactions between the Stim and Orai molecules.

Importantly, truncation of the N-terminal region of SOAR by removing 8 amino acids (342-349) gave rise to a peptide that did not activate Orai1 constitutively but was rapidly activated upon addition of 2-APB (Fig 4A). This reveals that these eight amino acids are required for the association of SOAR with the Orai1 channel. However, 2-APB can clearly substitute for these amino acids and result in full activation of the channel. This suggests that this N-terminal end of the SOAR molecule is unlikely to be involved in the actual Orai channel gating, but more likely assists the C-terminal region of SOAR by allowing association with the channel. As shown in Fig. 4B,C, CRAC channel activation results from 2-APB-induced activation by the SOAR fragment. Interestingly, when using the double LQ347/348AA double mutant of SOAR, exactly the same results were seen (Fig. 4D). This mutation was reported to be essential for Orai1 activation, however, we can now conclude that these amino acids are involved in interaction with Orai1 but 2-APB can substitute for their interaction and allow complete coupling and a gating of Orai1. Both the SOAR C-terminal truncation and double mutation can become associated with the membrane in the presence of 2-APB (Fig. 4E,F). However, we observe that both molecules appear to be associated in the form of larger and more punctate-like associations with Orai1. Thus, in comparison with intact SOAR which associates more uniformly on the membrane, the modified SOAR proteins appear to be involved in larger cluster formation.

The results shown here provide new information on the roles of discrete segments of the SOAR peptide. Our work will continue to truncate the N-terminus of SOAR to assess the minimal segment required for 2-APB-induced Orai1 coupling and hence determine the actual gating sequence. This work is significant in not only defining the STIM-Orai interactions but also

revealing an important pharmacological modification mechanism for the 2-APB molecule. As described in the main research plan, 2-APB may have actions to cause STIM-STIM association that results in STIM-Orai activation. We are also now expressing short N- and C-terminal fragments of the Orai1 protein and continuing to examine FRET-based interactions among and between the STIM and Orai fragments.

Aim 3. To determine whether  $\text{Ca}^{2+}$  entering through SOCs controls the interaction between STIM1 and Orai proteins, involving examination of the local  $\text{Ca}^{2+}$  environment using a simple FRET-based measurement using the  $\text{Ca}^{2+}$ -sensing yellow cameleon (YC3.1) linked to Orai1, as a direct probe for  $\text{Ca}^{2+}$  in the restricted space in which Orai channels operate. With respect to this aim, we made important progress with STIM1- and Orai1-tagged chameleons as proposed.

C-terminal STIM1-cameleon construct: We made two constructs – one tagged with the  $\text{Ca}^{2+}$ -sensing D2cpv cameleon ( $K_d \text{Ca}^{2+} 3 \mu\text{M}$ ) at the cytoplasmic-facing C-terminus (shown in Fig. 5), the other tagged with the lower affinity D1-cameleon at the ER luminal N-terminus (this construct is still in progress). The STIM1-D2cpv construct expressed and functioned identically to wt N-terminally YFP-labeled STIM1 used in our recent studies. This was important to assess since we could not be sure that the bulky cameleon would not interfere with successful coupling to Orai1 channels. Expressed in our stable Orai1-expressing HEK-293 cells, the distribution of STIM1-D2cpv was typically ER-like, both fluorophores (CFP, YFP) superimposable (Fig. 1A-C). STIM1-D2cpv activated large and typical CRAC currents in BAPTA-loaded cells (Fig. 1D, E), and was identical to wt-YFP-STIM1 in activating store-operated  $\text{Ca}^{2+}$  entry after store-emptying with ionomycin (Fig. 1F). Moreover, we undertook FRET analysis, measuring CFP ( $436_{\text{Ex}}/480_{\text{Em}}$ ,  $F_{\text{CFP}}$ ) and FRET<sub>raw</sub> ( $436_{\text{Ex}}/535_{\text{Em}}$ ,  $F_{\text{raw}}$ ) images every 20 sec in HEK Orai1 stable cells transfected with STIM1-D2cpv using our Leica DMI 6000B microscope and SlideBook 4.2 Software (2-channel corrected FRET was:  $\text{FRET} = (F_{\text{raw}} - F_d/D_d * F_{\text{CFP}}) / F_{\text{CFP}}$  where FRET is corrected total, and  $F_d/D_d$  is CFP bleed-through the YFP filter (0.592248)). As shown in Fig. 1G, a robust local  $\text{Ca}^{2+}$  signal can be observed upon  $\text{Ca}^{2+}$  addition after store-emptying with ionomycin. High resolution imaging reveals clear hotspots of local high  $\text{Ca}^{2+}$  (Fig. 1H).

N-terminal Orai1-cameleon construct: We also made the N-terminal D2cpv-tagged Orai1 proteins (Fig. 6). This also was highly successful. In stable STIM1-HEK293 cells, D2cpv-Orai1 was expressed in the PM as expected (Fig. 2A-C), and gives rise to large robust ionomycin-induced  $\text{Ca}^{2+}$  entry (Fig. 2D) and CRAC currents (Fig. 2E) exactly as for wildtype Orai1. Thus the large cameleon-tag had no detrimental effect on the function of the Orai1 protein. Moreover, as for STIM1-D2cpv, the D2cpv-Orai1 construct gave a robust and highly measurable FRET signal for  $\text{Ca}^{2+}$  entering after store-depletion (Fig. 2F). High-resolution FRET imaging revealed the cameleon sensed  $\text{Ca}^{2+}$  increases in discrete PM-localized areas that likely correspond with junctional clusters induced by coupling to STIM1 after store-depletion.

Figures

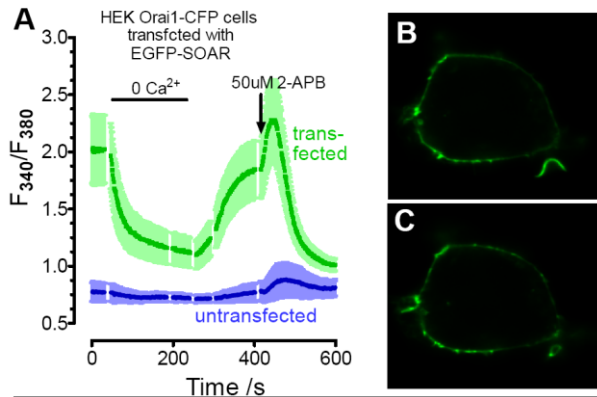
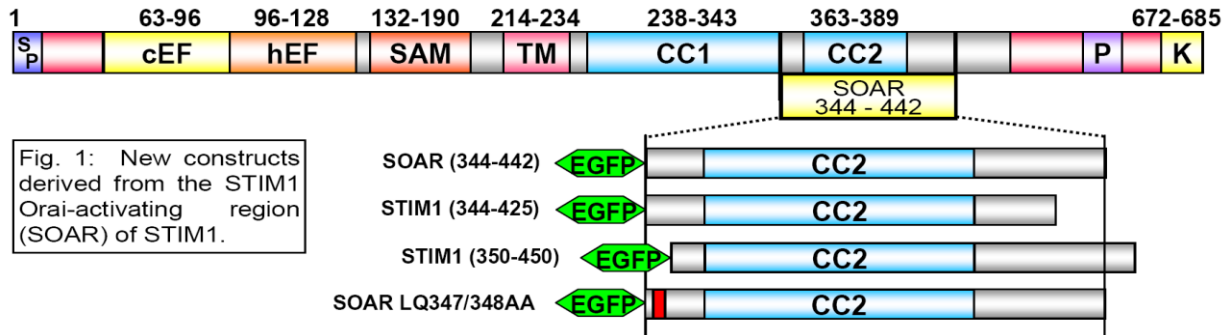


Fig. 2: SOAR activates large constitutive entry of Ca<sup>2+</sup> in HEK cells expressing Orai1 that is blocked by 2-APB (A). The SOAR fragment is constitutively expressed tightly associated with Orai1 at the PM (B) with no further effect of addition of 2-APB (C).

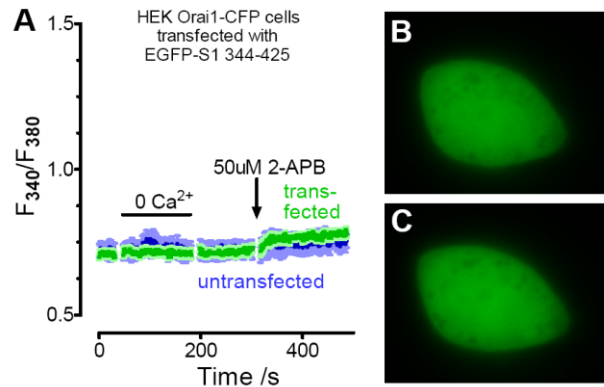


Fig. 3: Truncation of just the last 17 C-terminal amino acids from SOAR (344-425) results in a peptide that has no effect on Ca<sup>2+</sup> entry with or without 2-APB (A). The peptide is expressed in the cytoplasm exclusively and is unaffected by 2-APB (C).

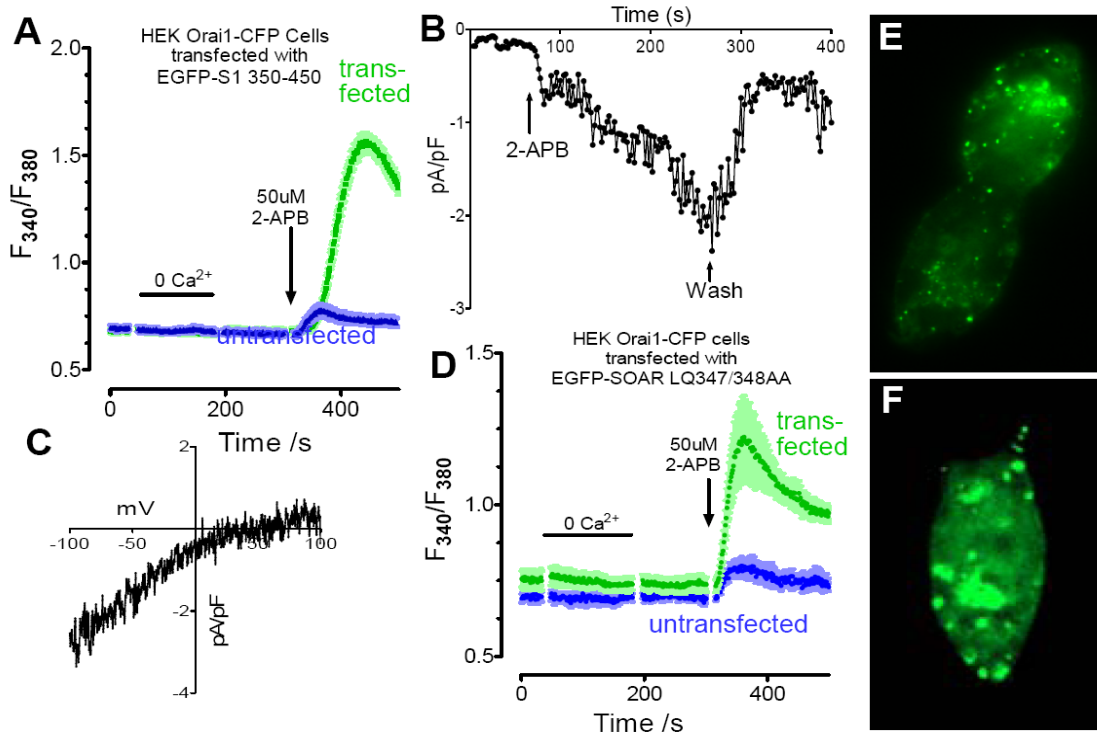


Fig. 4: Removal of 8 amino acids from the N-terminal domain of SOAR results in a peptide with no constitutive  $\text{Ca}^{2+}$  activation, but activated by 2-APB (A). 2-APB induces  $\text{Ca}^{2+}$ -selective current (B) with CRAC characteristics (C). Similarly, the LQ347/348AA double mutation results in a constitutively inactive peptide strongly activated by 2-APB (D). For both constructs there are large areas of puncta observed following addition of 2-APB.

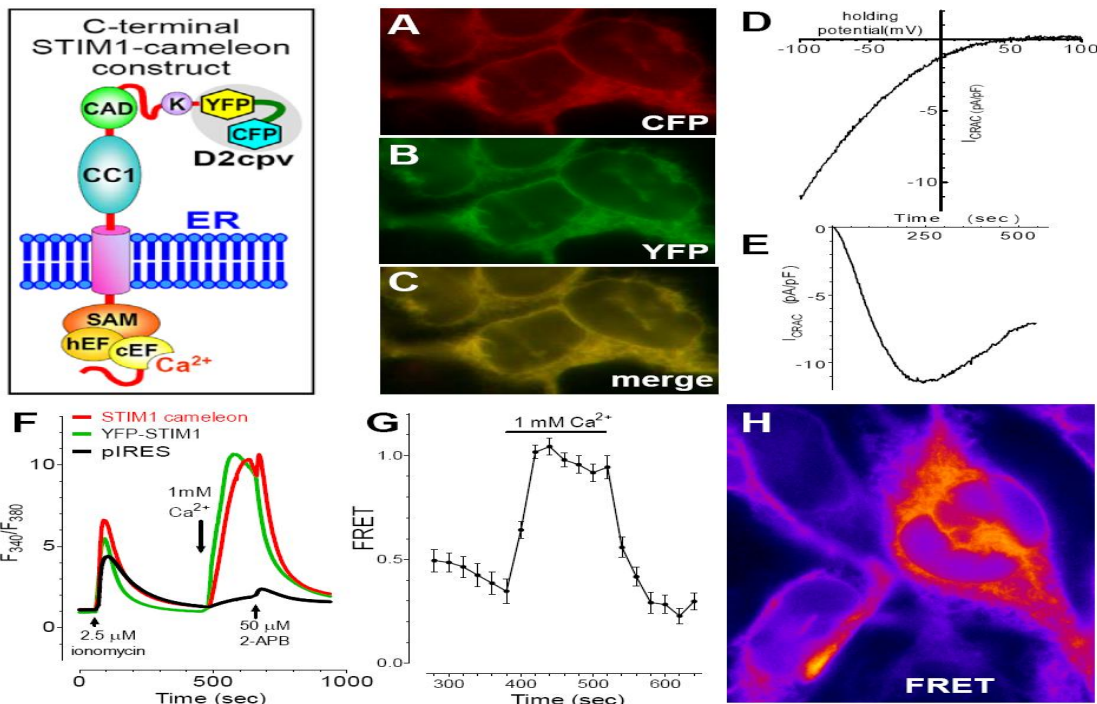


Fig. 5: Structure, expression and function of the C-terminal STIM1-cameleon construct in stable Orai1-expressing HEK293 cells.

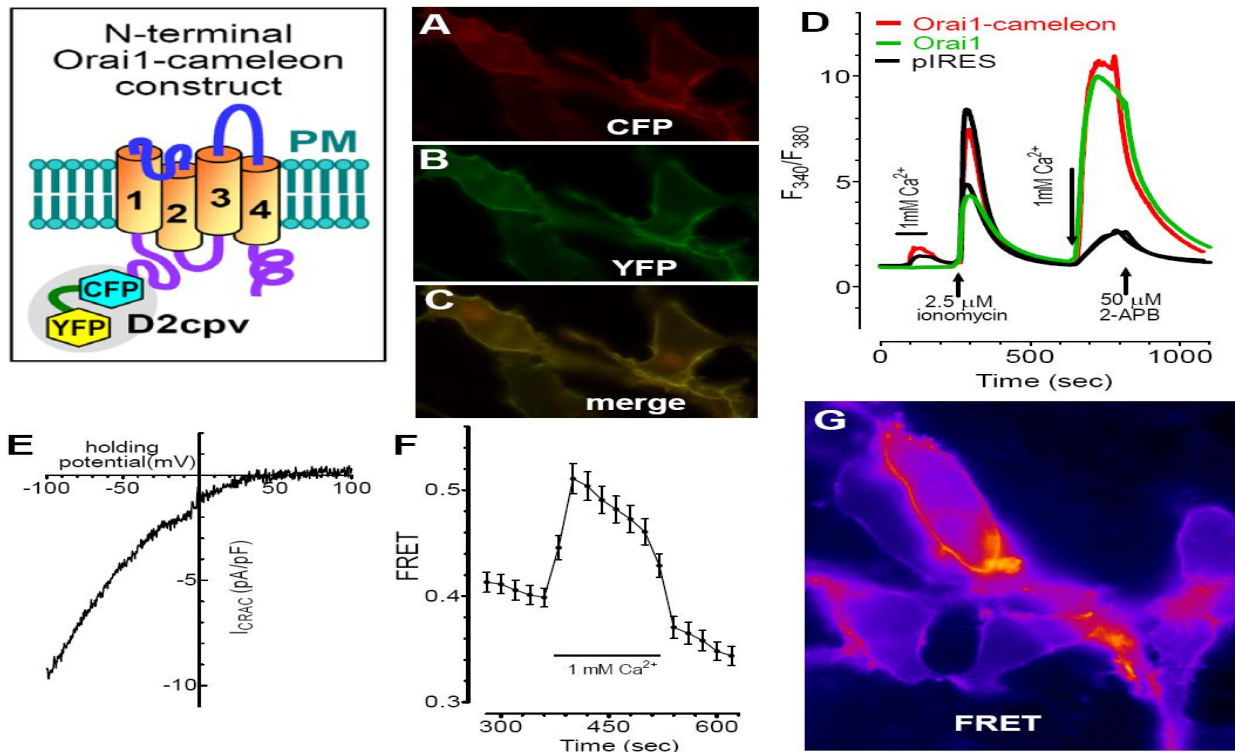


Fig. 6: Structure, expression and function of the N-terminal Orai1-cameleon construct expressed in stable STIM1 HEK293 cells.

### **Research Project 18: Project Title and Purpose**

*Assays to Identify Inhibitors of Cellular and HIV Transcription in Human Cells* - To develop assays to monitor inhibition of RNA polymerase II (RNAPII) activity and/or phosphorylation or other markers of transcriptional activity in human cells. Identification of compounds with the ability to inhibit particular events during a transcription cycle by RNAPII will generate tools to study the control of gene expression in vivo and in vitro. Further characterization of the selectivity of these compounds as C-terminal domain (CTD) kinase inhibitors in vitro will allow identification of their direct targets. Compounds with enhanced selectivity towards particular cyclin/CDK complexes, or with defined inhibitory potency towards a subset of CDKs may have enormous potential in the clinic for the therapeutic treatment of HIV, cardiac hypertrophy or even certain cancers.

### **Anticipated Duration of Project**

9/15/2009 – 8/31/2010

### **Project Overview**

HIV-1 transcription is an essential step in the viral life replication cycle and is dependent on viral and host transcription factors. Selective inhibition of HIV-1 transcription, and hence replication,

should be feasible if a small compound specifically targets a viral protein essential for productive transcription (i.e., Tat), a required host cofactor non-essential for cellular transcription, or if it interferes with the interactions among viral and cellular cofactors without altering cellular functions. Potential cellular indirect targets include RNA polymerase II (RNAPII) C-terminal domain (CTD) kinases, such as CDK9 or CDK2. However, developing pharmacologic inhibitors based on inhibition of kinase activity *in vitro* has disadvantages, as the compounds might exhibit poor selectivity, toxicity or fail to enter the cell. More robust screenings can be designed by measuring inhibition of HIV transcription or host cofactors in living cells. This project addresses strategies for developing assays for primary and secondary screening of libraries of small pharmacological compounds for selective inhibitors of site-specific kinases targeting the CTD of RNAPII, which might help in the identification and/or characterization of HIV-1 inhibitors. We will use fluorescence-based western blot analysis and/or “in-cell western assays” to measure differential inhibition of Ser-2/Ser-5 phosphorylation on the CTD of endogenous RNAPII. HeLa or other suitable human cell lines will be grown in 3 cm dishes or in 96-well plates and treated with compounds for predetermined periods of time. Subsequently, cells will be either (1) harvested for multiplex fluorescence-based western blot analysis or (2) fixed and permeabilized. Membranes or fixed cells will be incubated with antibodies specific for phosphorylated Ser-2 and Ser-5 followed by fluorescent-coupled secondary antibodies. Fluorescence will be measured and quantitated using a fluorescent imaging system to be acquired for this project. Assays will be developed using compounds known to inhibit CDKs, RNAPII CTD phosphorylation and HIV-1 transcription.

### **Principal Investigator**

Xavier Graña, PhD  
Associate Professor  
Temple University School of Medicine  
Fels Institute for Cancer Research and Molecular Biology  
AHP Bldg., Rm 308  
3307 N. Broad St.  
Philadelphia, PA19140

### **Other Participating Researchers**

Judit Garriga, PhD, Alison Kurimchak – employed by Temple University School of Medicine

### **Expected Research Outcomes and Benefits**

Recent advances in technology have resulted in development of instrumentation that allows acquiring more accurate and more quantitative protein expression and modification data than previously possible with hitherto antiquated detection methods. Through the acquisition of a state-of-the-art imaging equipment scanner, we intend to enhance our research capabilities through increasing the quality and the output of the results gained from current methodologies. Multiplex fluorescence detection will allow simultaneous monitoring of protein expression and phosphorylation data, or phosphorylation of two independent events that can be used as markers of cellular processes, in this case changes in cellular transcription. We plan to develop assay(s)

that should be amenable to developing primary and/or secondary screenings of libraries of small chemical compounds for inhibitors of particular processes in cellular transcription that are utilized by the HIV-1 virus. The same assays could be easily adaptable to perform other types of high throughput screening, provided that suitable markers are validated for the identification of compounds with therapeutic and or research applications.

### **Summary of Research Completed**

This grant started on September 15, 2009. All the funds in this grant (\$50,000) were budgeted for the purchase of a fluorescent imaging system that could be used for multiplex western blot analysis. Upon scheduling demos from three different vendors (Alpha Innotech, LI-COR Biosciences and Carestream Molecular Imaging) and performing a series of test western blots using both fluorescent and ECL coupled antibodies to be imaged and quantitated with the three systems, we decided to purchase a FluorChem Q imager from Alpha Innotech with fluorescent and ECL capabilities. This instrument was ordered, delivered and assembled by Alpha Innotech technicians in a room dedicated to imaging and gel documentation. We received basic training from Alpha Innotech technicians late in 2009. This imaging instrument forms part of the core instruments of the Fels Institute for Cancer Research and Molecular Biology.

The instrument has been set up by a Senior Associate Scientist (Dr. Judit Garriga) and a student (Prachi Patel) and it is also being utilized by other labs that are participating in its set up.

ECL-based western blot approaches are working producing data of high quality. In our hands, imaging with the FluorChem Q imager is superior to conventional western blot analysis using X-ray film. This is because the data appears linear over more orders of magnitude and because its easiness and speed of quantification. However, the development of fluorescent based-approaches requires further experimentation. This experimentation is carried out with my grant funds from other sources, as the budget for this grant only covered equipment. Therefore, the set up of this instrument for fluorescent detection and quantitation is progressing more slowly with only part-time dedication to the project. Progress will be reported in the next cycle, as the project is still active.

### **Research Project 19: Project Title and Purpose**

*Smoking Cessation in Homeless Shelters: Benefits of Physical Activity and Support* - The purpose of this project is to pilot test protocols for a future trial that will provide evidence of the efficacy of delivering a smoking cessation intervention in conjunction with an existing physical activity program vs. cessation alone with the homeless population. Further, this project will examine whether any differences between the two interventions are mediated by social support to inform intervention components for the future trial. To date, this project represents a first attempt at examining the efficacy of smoking cessation intervention combined with physical activity with a sample of homeless individuals. Findings from this project will advance knowledge and understanding of tobacco use behaviors among the homeless, a population that smokes at a rate three times greater than the general population yet is generally overlooked in tobacco related research.

## **Anticipated Duration of Project**

9/15/2009 – 12/31/2010

## **Project Overview**

This project will expand an existing collaboration between Temple University investigators and a community organization, Back on My Feet (BOMF), a non-profit that promotes psychosocial and physical health through an organized running program for residents of homeless shelters. This project is significant in that it will examine the feasibility and efficacy of evidence-based smoking cessation treatment in a non-traditional setting by comparing outcomes between residents who have been physically active in BOMF and non-BOMF residents. By embedding smoking cessation services within a larger existing community-based health promotion program, the BOMF-cessation approach could be a model for increasing the capacity of community programs to promote smoking quit rates and reduce risk of tobacco-related morbidity and mortality. The BOMF-cessation approach should facilitate access and adherence to tobacco intervention services, and it will increase knowledge and understanding of tobacco use behaviors and physical activity – smoking cessation associations. This project will improve our understanding of barriers to substance abuse behavior change and will explore if social facilitation and contingent support for smoking cessation through group physical activity promotes smoking behavior change in an underserved population. Our overarching aim is to test preliminary protocols for recruitment, retention, and intervention delivery to guide future studies. The primary aim is to test the efficacy of smoking cessation treatment in combination with the existing program, BOMF, which promotes psychosocial and physical health. We will recruit homeless individuals from the Ridge Shelter, and enroll consenting, volunteer smokers in cessation treatment that includes 8 weekly behavioral counseling sessions and nicotine gum. All participants will receive the same health and eligibility screening provided by the BOMF program, excluding participants with major medical and psychiatric disorders. All participants will receive counseling and gum, but separate group sessions will be available for smokers who have actively participated in BOMF, and smokers who are not in BOMF. We hypothesize that the BOMF smokers will have higher quit rates, longer abstinence, and higher participant retention at 8-week end of treatment than the no-BOMF group. Our second aim is to improve our understanding of physical activity-smoking cessation associations and the mechanisms that affect smoking behavior change in this population, such as pretreatment nicotine dependence, fitness, and psychological factors.

## **Principal Investigator**

Jeremy S. Jordan, PhD  
Assistant Professor  
Temple University  
1700 N. Broad St. 316-F  
Philadelphia, PA 19122

## **Other Participating Researchers**

Bradley N. Collins, PhD, Jennifer K. Ibrahim, PhD – employed by Temple University

## **Expected Research Outcomes and Benefits**

This project focuses on gaps in substance abuse treatment access by testing the feasibility of implementing evidence-based smoking treatment in homeless shelters– a nontraditional site for substance abuse intervention. Smoking rates in homeless populations triple rates observed in the general population. Homeless smokers rarely choose to quit smoking through traditional channels, although evidence indicates that many individuals want to quit. Thus, examining this project’s innovative implementation of evidence-based intervention is expected to create substantial impact. For example, we expect improved understanding of factors that facilitate smoking behavior change and factors that may improve substance abuse treatment retention in this population. Smoking cessation treatment provides an adaptable model to other substance abuse treatment in this setting. This project also presents the opportunity to examine the relationship between physical activity and substance abuse behavior change while improving understanding of behavioral mechanisms that influence cessation and maintained abstinence. To our knowledge, this would be the first research project to examine the role of physical activity in promoting substance abuse treatment (smoking cessation) in a homeless population. While a full randomized clinical trial (RCT) design is beyond the scope of this project, results obtained from this project will inform us of program feasibility and provide proof of concept for conducting a fully randomized trial.

## **Summary of Research Completed**

A series of focus groups were conducted with shelter residents who are members of Back on My Feet (BOMF). The purpose of these focus groups was to determine unique aspects of the homeless population that might impact the design of the smoking cessation interventions. The need to obtain qualitative data from this population regarding perceived effectiveness of a standard evidence based smoking intervention was identified by reviewers of a previous grant application who questioned whether a standard cessation protocol would be effective with subjects who were experiencing homelessness. Therefore, prior to implementation of the smoking cessation intervention, focus groups were conducted with members of BOMF to obtain data related to key components of the smoking cessation intervention. Specifically, key components covered in the focus groups included information regarding quit attempts, smoking cessation strategies previously used, transportation strategies to maximize retention, and participants’ views for designing an intervention program that included opinions on content, format, and length of the intervention. Some of the general comments from the participants consisted of having a cessation program that encompassed basic health education and awareness such as the dangers of smoking and carcinogens present in cigarettes, urge management and reduction, education and use of NRTs (patch or gum), and preference for group counseling sessions over individual sessions.

Based on information obtained from the focus group sessions, a tailored smoking cessation intervention has been developed that is appropriate for this population. Currently all project

related staff are being trained on the specifics of the altered cessation intervention and a pilot test of the protocol will commence on June 1, 2010. A group of 8-10 BOMF members who are currently smokers will participate in an eight week cessation program described below.

Cessation treatment will be provided in weekly modules including: 1. Group Support for Quitting and a Healthy Lifestyle; 2. Dealing with Stress without Smoking; 3. Managing Craving and Urges to Smoke; and 4. Benefits of Quitting and Preparing a Successful Quit. Participants will cycle through these four modules twice to complete eight weeks of group cessation counseling. These modules will continue to repeat throughout the intervention phase of the project, allowing new participants on the waiting list to start treatment in any module after a participant completes their eight weeks. Participants can start their treatment with any of the four modules, but will be encouraged to complete all four modules twice. At the beginning of each session, new participants will receive nicotine gum with instructions about proper usage (e.g., urge management, “chew and park”) and instructions for self-monitoring. All participants will alternately review their smoking activity through self-monitoring forms and discuss successes and challenges during the previous week. New participants will review why they are interested in quitting smoking and their level of confidence (a target the group will attempt to bolster in each member each week.)

At the beginning of each session, participants will provide expired CO through a breathalyzer to provide them with feedback about their progress (or lack thereof). Counselors will model strong positive reinforcement for participants who have low CO levels (indicating progress with quitting), while modeling encouragement and support for those who continue to struggle with quitting (as evidenced by elevated CO). Throughout treatment, counselors will model positive social support for smoking behavior change through the shaping of social contingencies around smoking behavior change (e.g., group praise for demonstrating urge management skills; or praise or “points” toward a session incentive for successful completion of weekly self-monitoring, etc.). “Negative support” will be defined for participants as friendship or encouragement that maintains smoking behavior (e.g., offering a cigarette when noticing a co-participant is experiencing distress). Other behavioral strategies will be employed throughout sessions, such as role playing urge management, stress and mood management training, homework that includes practicing pleasant activities other than smoking, urge delay, and stimulus control (e.g., limiting smoking situations and locations while practicing urge management in new non-smoking locations). Participants will also be encouraged to share cell phone numbers with one another to facilitate achievement of intersession smoking behavior change goals. Participants will be asked to participate in the breathalyzer analysis at baseline, end of the eight week treatment and then return for a three month follow-up.

#### Dependent Measures:

1. *Enrollment and Retention:* Retention will be measured through eight-week end of treatment (EOT) and at 3-month follow-up as the proportion of enrolled participants completing post-treatment assessments.
2. *Self-reported Quit Status:* At EOT and 3 month follow-up, participants will provide self-reported seven-day point prevalence estimates of their quit status.

### Independent Measures:

1. *Demographics*: age, gender, marital status, education, employment, smoking history, number of close friends that are smokers and previous NRT use.
2. *Nicotine Dependence*: measured by the Fagerström Test for Nicotine Dependence (FTND), which has adequate internal consistency ( $\alpha = .64$ ) and high test-retest reliability ( $r = .88$ )
3. *Readiness to Quit or Intention to Quit*: Participants' intention to quit using the Biener Contemplation Ladder.
4. *General Social Support*: Perceived availability of social support will be assessed using the Interpersonal Support Evaluation List (ISEL). The 40-item ISEL measures the perceived availability of: (a) appraisal, or emotional, support (perceived availability of someone with whom one can discuss personal problems); (b) belonging support (perceived availability of people with whom one can do activities); (c) tangible support (perceived availability of material aid from others); and (d) self-esteem support (perceived availability of praise from others or positive social standing).
5. *Perceived Stress Scale*: 14-item Perceived Stress Scale (PSS) is a global measure of the degree to which individuals find their lives unpredictable, uncontrollable, and overloaded.

The feasibility of the smoking cessation trial will be measured in terms of participant retention through eight weeks of treatment, and qualitative information from participants at the end of each session from discussions about ideas to improve treatment and retention of participants. We will ask participants about location, access, timing, comfort level, and content of the session.

Examination of 24-hour quit attempts during eight weeks of treatment, percent of participants abstinent at the end of eight weeks of treatment, and at 3 month follow-up as defined by 7-day point prevalence abstinence verified by CO levels measured by breathalyzer. Analysis of descriptive statistics will be examined to determine trends over time and bivariate comparison to look at associations between smoking/quit status and possible mediators or moderators, including demographics, nicotine dependence, intent to quit, social support and perceived stress.

### **Research Project 20: Project Title and Purpose**

*Cellular Transformation and Transcriptional Regulation of JC Virus in a Human Brain Tumor Model* - Human medulloblastoma is a malignant pediatric brain tumor that is refractory to treatment. Our model of medulloblastoma induced by the human polyomavirus, JC virus, will allow us to study the mechanisms involved in transcriptional regulation of JC virus and investigate a novel splicing pathway which may play a role in cellular transformation and tumor progression.

### **Duration of Project**

9/15/2009 – 6/30/2010

## **Project Overview**

Cerebellar medulloblastoma is the most common malignant brain tumor in children and the prototypical embryonal neuroblastic neoplasm of the central nervous system. Although a minority of medulloblastomas is associated with heritable abnormalities predisposing to tumorigenesis, most are sporadic and at present their pathogenesis remains elusive. Recently, we have developed an experimental transgenic animal model of medulloblastoma using the human JC virus oncogenic protein, T-antigen. Histologically, brains from these mice harbor cerebellar tumors resembling human medulloblastomas in appearance, expression of neuronal marker proteins, and anatomical location. JC virus (JCV) is a neurotropic polyomavirus infecting more than 80% of the human population early in life. The early genome of this virus, which encodes for the regulatory protein T-antigen, is critical for the productive viral lytic cycle. This protein also possesses transforming ability in cell culture and its expression induces tumors in several laboratory animals. In addition, we and other laboratories have reported the association of the JCV genome with expression of its early protein, T-antigen, in several human medulloblastomas. To further understand the involvement of JCV with medulloblastomas, JCV T-antigen transgenic mice harboring medulloblastomas and cells derived from tumors formed in the transgenic animals will serve as a model for our mechanistic studies.

## **Principal Investigator**

Kamel Khalili, PhD  
Professor and Chair, Department of Neuroscience  
Temple University School of Medicine  
Bio-Life Sciences Building, Room 203  
1900 North 12<sup>th</sup> Street, MS 015-96  
Philadelphia, PA 19122

## **Other Participating Researchers**

Jennifer Gordon, PhD, Ilker Sariyer – employed by Temple University

## **Expected Research Outcomes and Benefits**

We have previously demonstrated that the JC virus oncogenic protein, by associating with several key cellular proteins involved in the control of cell proliferation and apoptosis, promotes the formation and progression of medulloblastoma brain tumors in transgenic animals expressing JCV T-antigen. In humans, several studies have shown the presence of the JCV genome and expression of the viral early protein, T-antigen, in different types of brain tumors including cerebral medulloblastoma. Thus, it is evident that activation of the JCV early genome results in expression of the viral oncogenic protein and that results in uncontrolled cell proliferation. In a more recent study we have investigated the regulation of JCV gene transcription by cellular regulatory proteins and have identified ASF/SF<sub>2</sub>, a known splicing factor as a negative regulator of the JCV genome. In this project we will employ molecular and cellular approaches to determine the molecular mechanisms involved in the regulation of JCV gene expression and investigate the potential use of ASF/SF<sub>2</sub> as an inhibitor of gene expression. The outcome of this

study will provide further evidence of the oncogenic role of JCV in tumorigenesis and the potential utility of a novel therapeutic agent for human medulloblastoma.

### **Summary of Research Completed**

The human neurotropic virus, JCV, is the etiologic agent of a demyelinating disease of the CNS, progressive multifocal leukoencephalopathy (PML). PML is primarily seen in immunocompromised individuals, most notably AIDS patients. JCV replicates almost exclusively in glial cells and its promoter sequence, which has tissue-specific characteristics, tightly modulates transcription of the viral genome in appropriate cell types. Here we identified the alternative splicing factor, SF2/ASF, as a potential regulator of JCV as its expression in glial cells suppresses viral gene expression and replication. Unexpectedly, down-regulation of JCV by SF2/ASF is mainly mediated at the transcriptional stage, thus ascribing a novel role for SF2/ASF in the control of promoter activity. SF2/ASF suppresses both viral early and late gene transcription by direct association with a specific DNA motif within the viral bi-directional promoter. Further mapping studies revealed that the RRM1 domain of SF2/ASF is responsible for this effect. Interestingly, down-regulation of SF2/ASF in both primary human fetal and adult astrocytes increased the propagation of the virus suggesting that SF2/ASF expression might be a critical factor in the control of JCV progression. These observations open a new avenue for investigating the mechanisms involved in reactivation of the JCV genome in glial cells during the course of immunosuppression and suggest a novel approach for suppressing JCV replication in humans.

Alternative splicing of primary transcripts is a widely used mechanism to increase the coding capacity of the genes in mammalian cells. Several protein factors play important roles in the complex regulation of pre-mRNA splicing. Among these factors, the Ser/Arg-rich proteins (SR proteins) are phylogenetically conserved proteins originally identified for their regulatory roles in alternative and constitutive splicing of mRNA precursors. SF2/ASF (splicing factor 2/alternative splicing factor) is a prototypic member of this family, and is one of the key regulators of alternative splicing. Depending on splice site selection, SF2/ASF can negatively or positively regulate splicing. Beside the roles of SF2/ASF in the regulation of gene expression through the modulation of pre-mRNA alternative splicing, it has also been shown to be an inducer of translation initiation by suppressing the activity of 4E-BP1, an inhibitor of cap-dependent translation. SF2/ASF has also been shown to be an essential host protein since SF2-deficient mice show embryonic lethality. In addition to its role in gene expression through the regulation of splicing and translation, SF2/ASF is also up-regulated in various human tumors, including lung, kidney, colon, pancreas, small intestine, and thyroid. Up-regulation of SF2/ASF in tumor cells indicates a possible role in malignant transformation. Furthermore, over-expression of SF2/ASF is sufficient to transform NIH- 3T3 and Rat1 fibroblasts, and its transforming activity is related to aberrant splicing of the tumor suppressor, BIN1, and the kinases, MNK2, and S6K1.

Not surprisingly, SF2/ASF is utilized by many viruses (i.e., adenovirus, human papillomavirus, Rous sarcoma virus, influenza virus, herpes simplex virus, and HIV-1) in order to regulate their gene expression upon infection of host cells. It has been shown that SF2/ASF binds the human papillomavirus type 16 late RNA control element, HPV-16 NRE and its expression is up-regulated by viral E2 protein during the differentiation of epithelial cells infected with the virus.

Gene expression of HIV-1 is also influenced by SF2/ASF. The 9kb full-length HIV genomic transcript undergoes a series of posttranscriptional modifications that generates viral mRNAs that produce viral structural and regulatory proteins. SF2/ASF binds to exonic splicing enhancers (ESEs) downstream of the Tat-, Rev-, Env splice sites and promotes exon definition. Therefore, SF2/ASF is thought to play a major role in the regulation of HIV-1 pre-mRNA splicing and has been proposed as a novel target for the inhibition of HIV replication.

SF2/ASF was first discovered as a cell-type specific regulator of SV40-early gene expression at the post-transcriptional level. Early studies using *in vitro* transcribed SV40-early primary transcript and cellular extracts have suggested that SF2/ASF enhances the usage of small t antigen splice site at the expense of the Large T antigen site. However, *in vivo* studies have revealed that over-expression of SF2/ASF inhibited not only Large T but also small t, and caused accumulation of un-spliced RNA. These studies suggest that alternative splicing of polyomaviruses transcripts, and their regulation by alternative splicing factors, particularly by SF2/ASF, might be a critical determinant of a successful viral replication.

Here, we investigated the possible impact of SF2/ASF on propagation of human polyomavirus, JC virus, in glial cells. Our results indicate that SF2/ASF might be an important cellular protein in control of JCV infection, since its expression in glial cells completely blocked viral propagation. Surprisingly, JCV gene expression is inhibited by SF2/ASF mostly at the transcriptional stage of the gene expression rather than posttranscriptional. This provides evidence for SF2-mediated transcriptional regulation in addition to its roles in alternative splicing and translation, and suggests a novel approach for the suppression of JCV propagation.

JC virus infection commonly occurs in early childhood, and establishes a latent infection in healthy individuals for the rest of their life. Under immunosuppressive conditions, such as AIDS and lymphoproliferative diseases, the virus reactivates from the latently-infected tissues, transmitted through the blood (possibly by B-cells), and reaches the brain, where it preferably infects and replicates in glial cells. Although JCV can enter/infect almost all types of different organs and tissues, it can only complete its life cycle in the CNS. The mechanism of JCVs tropism to the CNS, specifically to the glial cells, has not yet been clarified. Most research has been focused on the identification of glial specific transcription factors. As an outcome of these studies, many transcription factors have been identified, such as *pur-alpha*, YB-1, NF-1, GF-1, SP1, and c-jun. However, none of these transcription factors were neither glial specific nor able to explain the viral tropism. Another interesting feature of the JCV is the slow progression of replication cycle in the primary fetal glial cultures, PHFG, the only primary cell culture system to grow virus *in vitro*. Upon infection of PHFG cells, JCVs early protein expression can be detected after several days, and the virus completes its replication cycle in several weeks. On the other hand, expression of viral early proteins of simian polyomavirus, SV40, starts around 8-10 h post-infection and completion of the viral life cycle occurs in as early as 48 hours in CV-1 cells. Absence of glial specific /JCV specific transcription factors and slow progression of JCV even in the glial systems suggest that JCV gene expression might be also controlled by other cellular factors which suppress or slow the viral propagation.

We show here that SF2/ASF limits the replication and progression of JC virus in glial cells. Overexpression of SF2/ASF during JCV infection resulted in a great reduction of viral

replication and gene expression. SF2/ASF is a well characterized alternative splicing factor. Therefore we hypothesized that the observed suppression of JCV replication could be due to a posttranscriptional block to the viral primary transcripts. We developed an RT-PCR based approach to address this question in vivo. JCV early genes were expressed under the control of either JCVs own promoter or a CMV promoter. As hypothesized SF2/ASF suppressed the splicing, and caused an accumulation of the viral early pre-mRNA when expressed from pCDNA3.1 expression plasmid. Surprisingly, SF2/ASF not only suppressed the splicing but also broadly inhibited the formation of the viral primary transcripts when expressed under the control of JCVs own promoter. In addition, SF2/ASF also caused an extinction of Large T antigen and small t antigen expression in JCV-transformed tumor cell lines, BSB8 and HJC2. On the other hand, overexpression of SF2/ASF in SVG-A cell line, a glial cell line transformed by SV40, did not cause an inhibition of SV40 Large T antigen expression. These results strongly indicated that SF2/ASF could be specifically regulating JCV transcription rather than posttranscriptional regulation. In order to further characterize the SF2-mediated suppression of JCV transcription, we utilized a CAT-based reporter gene assay. Consistent with the observations from splicing experiments, SF2/ASF showed a strong inhibition of not only JCV-early but also -late promoter activities. Furthermore, SF2/ASF did not show any inhibition on CAT activities driven by the E2F-1 promoter or the BKV early and late promoters.

Specific inhibition of JCV transcription but not SV40 or BKV by SF2/ASF suggested that it could be directly involved in regulation of the JCV transcription. We showed that SF2/ASF was able to precipitate JCV regulatory region (JCV-RR) assessed by a ChIP assay in vivo. In order to test the direct interaction between SF2/ASF and JCV-RR, we incubated radiolabeled oligonucleotides spanning the 98 bp repeated region of JCV Mad-1 strain with recombinant SF2/ASF (GST-SF2). Interestingly, SF2/ASF specifically interacted with only the CR3 region of the viral promoter. We further characterized the interaction of SF2/ASF with CR3 oligonucleotide by gel shift assays, and showed that SF2/ASF formed a complex with this unique region of the JCV promoter. Removal of RNA from the nuclear protein extracts before the binding studies greatly improved the binding efficiency of SF2/ASF to the CR3 oligonucleotide. Even though, DNA binding activity of an RNA binding protein is a rare event, SF2/ASF has been recently shown interacting with a dsDNA motif within a human rDNA replication origin. Our DNA binding studies, by using either nuclear extracts or recombinant proteins as a source of SF2/ASF, suggested that it also directly binds to a motif within the JCV promoter region, which represents the second report of the DNA binding activity of SF2/ASF. While the exact mechanism responsible for the inhibition of JCV transcription by SF2/ASF remains to be elucidated, it is likely to involve a dose dependent competition with some other transcription factors which are required for transcriptional activation of the virus. On the other hand, interaction of SF2/ASF to the viral promoter might also interfere with the initiation and/or elongation of the transcription complex. Further studies of the action of SF2/ASF on transcriptional regulation of JC virus through interaction with the viral promoter will provide more insight into this novel regulatory role of SF2/ASF.

SF2/ASF exhibits a modular structure consisting of two copies of RNA binding motifs (RRM1, RRM2), followed by an Arginine-Serine-rich (RS) domain. While RRM1 and RRM2 domains determine the RNA-binding specificity, RS domain interacts with the core splicing components. In order to characterize the functional DNA binding module of SF2/ASF, we sequentially created

truncated forms of the protein, and performed a ChiP assay. We found that RRM1 domain was mainly responsible for the interaction with JCV genomic DNA. We also tested the functional role of this interaction by CAT reporter assays. Consistent with the DNA binding studies, RRM1 domain of SF2/ASF was also mainly responsible for the suppression of JCV transcription. These observations strongly suggest that direct interaction of SF2/ASF with JCV regulatory region through RRM1 domain is required for the suppression of viral transcription.

In addition to those gains of the function studies, we also analyzed the impact of SF2/ASF on JCV propagation by loss of function studies. First we compared the endogenous expression of SF2/ASF in primary human fetal (PHFA) and adult (PHAA) astrocytes, and U87 MG cells. Interestingly, SF2/ASF expression was ~2 and ~4 fold higher in PHAA cells than U87 MG and PHFA cells, respectively. PHFA cells are the only primary culture system which support viral multiplication, and used by us and others as a model system of JCV infection. On the other hand, JCV infection of PHAA cells has not yet been established. Here we additionally demonstrated that PHAA cells could also suit JCV infection with a ~ 6 to 10 fold lower efficiency than PHAA cells. Furthermore, downregulation of SF2/ASF expression resulted in a significant increase of JCV propagation in PHFA and PHAA cells, respectively. Further studies should address the functional importance of the differential expression of SF2/ASF in PHFA and PHAA cells, and its role of the reactivation of JCV from latency period and contribution to the pathology of the PML.

In conclusion, the data represented here provides the first report of transcriptional suppression of JC virus, by an unusual candidate, SF2/ASF, a cellular alternative splicing factor. Our results suggest a novel role of SF2/ASF as a transcriptional inhibitor of JC virus. These observations may suggest a novel mechanism of JCV reactivation and a new approach for suppression of JCV infection.

### **Research Project 21: Project Title and Purpose**

*The Role of Mucin in Promoting Survival of CA-MRSA and Streptococcus mutans*- The purpose of these studies is to understand the role of mucin in survival of Community-Associated/Acquired Methicillin Resistant *Staphylococcus aureus* (CA-MRSA) and *Streptococcus mutans*. Mucin is found in saliva and on mucosal surfaces such as the inside of the nose and throat. We found survival of both CA-MRSA and *S. mutans* requires nutrients. *S. mutans* is the major agent of dental caries (cavities) and mucin found in saliva prolongs its survival from days to months. CA-MRSA is the cause of lethal infections in young, healthy student athletes. We found mucin allows for survival of CA-MRSA on artificial turf, suggesting “snotting” by CA-MRSA carriers could deposit CA-MRSA on the artificial turf, where it remains alive for >60 days serving as a reservoir of CA-MRSA for subsequent athlete infections. The goal of these studies is to determine if mucin is providing sugars necessary for the survival of these pathogens.

### **Anticipated Duration of Project**

9/15/2009 – 11/30/2010

## **Project Overview**

Many Gram-positive pathogens and normal flora survive in the pharynx. Mucin is a major component of the pharyngeal mucosal linings and of saliva. We found mucin prolongs the survival of two major pathogens; *Streptococcus mutans* and Community Associated/Acquired Methicillin resistant *Staphylococcus aureus* (CA-MRSA). *Streptococcus mutans* is a facultative member of the oral plaque community and its production of acid during sugar fermentation is associated with dental decay. In the oral plaque, *S. mutans* is subjected to a “feast or famine” life style, making it necessary for the bacteria to survive short-term starvation. In addition, *S. mutans* located deep in the dental plaque may be subject to longer-term starvation due to sugar limitation and competition. We found survival for longer than 3 days is dependent on nutrients. Mucin can prolong survival to >30 days. In an unrelated study on the survival of CA-MRSA in artificial turf, we found mucin allowed for the survival of significant numbers of CA-MRSA. Much of the evidence linking MRSA to athletes comes from sporadic outbreaks, but it is agreed that CA-MRSA infections among athletes represent a growing public health problem. Artificial turf is generally thought to increase the degree of skin injury following football trauma. This may account for the predisposition of football players to CA-MRSA infection. We determined that CA-MRSA could survive >60 days in high numbers on artificial turf, that survival depended on nutrients, and that mucin could serve as a nutrient source. Bacteria in mucin could be present if an athlete that was a CA-MRSA carrier deposited nasal secretions onto the field. The striking observation that two generally different pharyngeal pathogens could use mucin as a nutrient source for survival, leads to the hypothesis that mucin may be a source of metabolic sugars for Gram-positive pathogens. This hypothesis will be tested by two specific aims. The first specific aim is to determine if mucin is degraded during incubation with *S. mutans* or CA-MRSA. The second specific aim is designed to determine if mucin can serve as a source of carbohydrates. Mucin contains fucose, mannose and galactose residues. To determine the contribution of these sugars to survival, the enzymes necessary for utilization of these sugars will be mutated and the ability of the mutants to survive in mucin will be compared to the parental strain. These studies will lay the groundwork for future studies on regulation of mucin metabolic pathways in *S. mutans* and for epidemiologic studies on the survival of CA-MRSA in nasal secretions on artificial turf.

## **Principal Investigator**

Bettina A. Buttaro, PhD  
Associate Professor  
Temple University School of Medicine  
Department of Microbiology and Immunology  
3400 N. Broad St.  
Philadelphia, PA 19140

## **Other Participating Researchers**

Phillip Ranglin, Deepa Mothey – employed by Temple University

## Expected Research Outcomes and Benefits

The expected outcomes and benefits will fall into three broad categories; (1) general bacteriology, (2) *S. mutans* and dental caries and (3) CA-MRSA survival on artificial turf as a risk factor for student athletes.

(1) General Bacteriology. Recently there has been increasing interest in understanding the basic metabolic properties of pathogens in the host as opposed to grown in laboratory medium. The metabolism of mucin has been studied in only a few organisms and the use of gluconate residues by *E. coli* is one of the only metabolic pathways that has been worked out. If mannose and/or galactose from mucin are being used by two diverse pharyngeal pathogens, this will provide a new metabolic scheme for the utilization of mucin and may have wide implications for both intestinal and naso-oral pathogens.

(2) Production of acids by *S. mutans* results in the dissolution of enamel and the eventual formation of cavities. The proposed metabolism of mannose residues by *S. mutans* results in the production of acetate and may allow for the continued production of acids even deep in the biofilm and in the absence of dietary sugars. These results could have significant impact on our understanding of dental caries, especially in patients with a good diet that are still prone to cavities.

(3) The presence of CA-MRSA on surfaces has been shown to be a risk factor for infection of healthy athletes. Artificial turf would be both a potentially abrasive surface and a source for CA-MRSA. The demonstration of mucin as a source of nutrients for survival of CA-MRSA on artificial turf leads to the hypothesis that one potential source for CA-MRSA infections is nasal secretions deposited by carriers. These results would be the basis for epidemiological studies on the survival of CA-MRSA in nasal secretions deposited on artificial turf fields by CA-MRSA carriers.

## Summary of Research Completed

### Specific Aim 1. Degradation of mucin during survival of *S. mutans* and CA-MRSA.

Due to the amount of mucin in the medium and the small number of surviving bacteria (1:1000), it was difficult to examine bulk changes in the mucin present in the medium as originally proposed. A collaboration has been initiated with Charles Grubmeyer, Department of Biochemistry, Temple University School of Medicine to use mass spectroscopy to examine the degradation of mucin during survival.

### Specific Aim 2. Mutation of genes in the mannose and galactose utilization pathways.

The vectors necessary for mutation of the genes in the mannose and galactose operons are being constructed in *E. coli* and are almost ready to be introduced into CA-MRSA and *S. mutans*.

During the course of experiments, new data was obtained suggesting a pivotal role for the *pdh* operon (pyruvate dehydrogenase complex) in the utilization of and response to mucin in *S.*

*mutans*. Previous data has shown the *pdh* operon has a significant effect on survival of *S. mutans* during carbohydrate starvation in the presence of mucin. In recent studies, using a *Ppdh*-GFP fusion, we have found that *pdh* is expressed in only a subpopulation of cells (0.1-1.0% of the cells). Early in starvation (~24 hrs), this subpopulation of cells is present as single cells or in short chains. Later in starvation, these cells produce long chains, suggesting the *pdh* subpopulation is surviving and replicating (Busuioc, Buttaro and Piggot *et al.*, J. Bacteriol., in press). These studies were done in medium containing amino acids and a hexose carbohydrate source that was metabolized to various triose endproducts by the end of exponential growth. Both the amino acids and the sugar endproducts could be used as alternate carbon sources after the primary sugar had been depleted.

Since mucin is a glycoprotein that could provide both a fermentable sugar source (e.g. galactose) and amino acids, experiments were done to determine the effect of mucin in the absence of amino acids. For these experiments, *S. mutans* containing the *Ppdh*-GFP fusion was grown in medium lacking amino acids and containing limiting glucose or sucrose, such that the sugar was depleted by the end of exponential growth, leaving only fermentation endproducts such as pyruvate and lactic acid. The *pdh*-expressing cells were a slightly smaller subpopulation of the total cells and the chains did not grow as long in late stationary phase (Table 1). These data suggest that the absence of amino acids slowed cell growth during early stationary phase and that amino acid metabolism may contribute to continued growth in stationary phase. When mucin was added under these conditions, the percent of *pdh*-expressing chains increased as well as overall chain lengths in the culture. These data were similar to results obtained from experiments in the presence of amino acids suggesting mucin could compensate for the lack of amino acids. At later time points (20 days), the percent of fluorescent chains and the number of fluorescent bacteria increased, consistent with replication of the GFP bacteria in the chains. Preliminary data showed that at time points >20 days the fluorescent *pdh*-expressing chains continued to elongate to chains of >25 cells, whereas, non-fluorescent chains did not continue to elongate. These data were consistent with *pdh* mutant data that indicated *pdh* is essential for viability after about 20 days.

In the above experiments, although hexoses were depleted, the spent medium still contained fermentation endproducts such as pyruvate and lactate. To determine the effect of more stringent starvation conditions on survival, cells were washed and resuspended in fresh CDM lacking amino acids and any sugar source. The cells were grown on coverslips. In the absence of a carbohydrate source the bacteria did not form biofilms, but survived as adherent cells. Under these conditions of severe nutrient deprivation, *pdh* is expressed in all of the cells at 24 hrs rather than just a subpopulation (Fig. 1). These results suggest that severe starvation conditions (e.g. amino acid and carbohydrate depletion) induced expression of *pdh* sooner than in cells when the endproducts from hexose metabolism were present. At later time points, while all of the cells remained fluorescent and only a subpopulation grew into longer chains (Fig. 1). This suggests that while *pdh* is expressed in all cells under extreme nutrient starvation, still only a subpopulation, were able to survive and grow.

Days starvation	Chain Length without Amino Acids							Total Chains	% GFP Chains	Total Bacteria	% GFP Cells
	1	2	3	4	5	6	>10				
Day 1	1779	299	46	27	0	0	0	2151	<b>0%</b>	2623	<b>0%</b>
<b>GFP</b>	<b>0</b>	<b>0</b>	<b>0</b>	<b>0</b>	<b>0</b>	<b>0</b>	<b>0</b>				
Day 9	1807	634	96	9	5	1	0	2553	<b>0.04%</b>	3435	<b>0.03%</b>
<b>GFP</b>	<b>0</b>	<b>0</b>	<b>0</b>	<b>0</b>	<b>0</b>	<b>0</b>	<b>1</b>				
Day 22	1800	847	142	16	0	0	0	2808	<b>0.11%</b>	4000	<b>0.08%</b>
<b>GFP</b>	<b>0</b>	<b>0</b>	<b>0</b>	<b>0</b>	<b>2</b>	<b>1</b>	<b>0</b>				
	Chain Length without Amino Acids + Mucin										
Day 1	958	899	211	319	87	93	0	2572	<b>0.2%</b>	5671	<b>0.23%</b>
<b>GFP</b>	<b>1</b>	<b>2</b>	<b>0</b>	<b>2</b>	<b>0</b>	<b>0</b>	<b>0</b>				
Day 9	946	432	117	128	57	36	18	1737	<b>0.17%</b>	3379	<b>0.739%</b>
<b>GFP</b>	<b>0</b>	<b>0</b>	<b>0</b>	<b>0</b>	<b>1</b>	<b>0</b>	<b>2</b>				
Day 22	400	613	70	83	10	36	0	1212	<b>1.1%</b>	2552	<b>4.6%</b>
<b>GFP</b>	<b>0</b>	<b>0</b>	<b>0</b>	<b>0</b>	<b>0</b>	<b>3</b>	<b>10</b>				

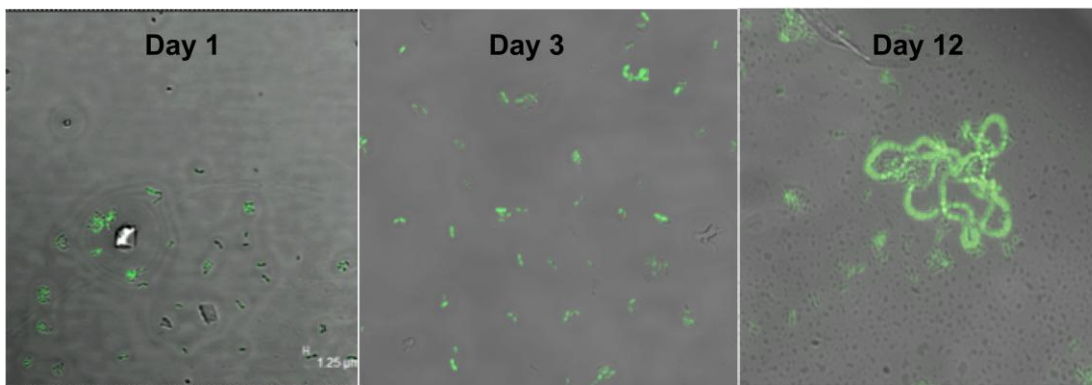


Fig. 1 The *pdh* operon expression in the absence of fermentation byproducts and amino acids (stringent starvation conditions). *S. mutans* UA159 containing a *Ppdh-mut3b*\*GFP fusion was grown overnight in CDM containing glucose and amino acids. The cells were washed and used to inoculate wells of a 24 well plate containing glass coverslips. At indicated time points a coverslip was removed and imaged using confocal microscopy. Images shown are merged images of the DIC and GFP fluorescent images.

Publications submitted:

Revised 08/19/10: K.N. Waninger, T.P. Rooney, J. Miller, J. Berberian, A. Fujimoto, and B.A. Buttaro, CA-MRSA Survival on Artificial Turf Substrates, *Medicine and Science in Sports & Exercise*

## **Research Project 22: Project Title and Purpose**

*Active Owls: Promoting Active Commuting and Physical Activity at Temple University* - The Active Owls project seeks to evaluate a multi-pronged project aimed at promoting physical activity, primarily via cycling. Phase I will assess a social marketing campaign (“Bike Temple”) designed to promote active commuting via cycling among Temple University community members. Phase II will evaluate an intervention aimed at college students using an adapted web-based program that includes both online gaming and social networking through the use of Facebook (“social gaming”). Finally, Phase III will assess child participant and college student perceptions (using focus groups) of a local non-profit neighborhood program designed to promote cycling (“Earn-a-Bike”).

### **Anticipated Duration of Project**

11/18/2009 – 1/30/2011

### **Project Overview**

We seek to evaluate the preliminary efficacy of programs designed to promote physical activity (PA) among members of the Temple University and North Philadelphia communities. The primary objectives of this proposal are to: 1) Determine the efficacy of a social marketing campaign (Bike Temple) designed to increase active commuting via cycling among members of the Temple community. Participants (1000 faculty/staff, 2000 students) will be recruited to complete pre and post questionnaires online, which will assess use of active commuting, perceptions of cycling, and knowledge of the campaign. 2) Design and evaluate the effect of a social networking intervention (using Facebook) for PA and weight gain prevention among college students who are at risk of weight gain. Research participants will be 180 normal and overweight (BMI: 20-30kg/m<sup>2</sup>) college students (ages 18-25) who will be randomly assigned to one of two 6-month conditions (Facebook Intervention or Wait-list Control). Participants will complete measures at baseline and follow-ups (months 3 and 6). Intervention participants will complete PA modules based on the existing iOTA program and compete for prizes by uploading their PA stats to the Facebook group over a 12 week period. 3) Assess the usability of ActiPed technology, a novel monitoring strategy that will automatically transmit physical activity data to the Facebook application via a small device worn on a participant’s shoe. A subsample of intervention participants will wear an ActiPed. Their data will be compared to participants who are instructed to self-monitor and enter data using a standard pedometer. 4) Evaluate participant knowledge of, and interest and engagement in, the Earn-a-Bike program, as well as interest in having Temple University students volunteer with the program. Qualitative data will be obtained via pre/post focus groups held with Earn-a-Bike participants (n = 10) and a single focus group held with Temple University students (n = 12).

## **Principal Investigator**

Melissa A. Napolitano, PhD  
Associate Professor  
Temple University  
3223 N. Broad Street Suite 175  
Philadelphia, PA 19140

## **Other Participating Researchers**

Robert Gage, MSPH, Sharon M. Hayes, MS – employed by Temple University

## **Expected Research Outcomes and Benefits**

Hypotheses: 1) A social marketing campaign (Bike Temple) will be successful in increasing knowledge, attitudes, and behavior about cycling to Temple University 2) A Facebook-based social gaming intervention will be successful in increasing time spent in physical activity compared to a control group. 3) By month 6, participants in the Facebook Approach will remain weight stable, while participants in the Wait-list Control will gain 2.0 pounds. 4) The ActiPed will show high rates of concordance with other measures of physical activity outcomes, thus making it a useful tool to implement in other physical activity trials as an objective measure of activity. 5) The Earn-a-Bike focus groups are exploratory in nature. However, based on anecdotal data and Neighborhood Bike Works self-study results, we predict that participant feedback will be generally positive.

Benefits: 1) Bike Temple survey participants may benefit from learning more about their own behavior, as well as from receiving physical activity referrals. Data from this research will help to inform future health promotion campaigns that have the ability to reach broad populations in at-risk groups. 2) Our proposed physical activity intervention study addresses an important public health need (i.e., promoting physical activity and preventing weight gain) among a priority population of young adults using an innovative gaming strategy with high dissemination potential, using the existing platform of Facebook. Although long-term benefits are unknown, it is possible that intervention participants may decrease their chance of gaining weight during study participation. The anticipated benefits to society-at-large are great, insofar as the results will be used to further our understanding of the social and cognitive processes of the game play experiences related to health. 3) There are no known direct benefits attributable to participation in the focus group. However, the anticipated benefits to society-at-large are great, insofar as the results will be used to the further understanding of the factors related to the efficacy of community-based physical activity promotion programs in urban settings.

## **Summary of Research Completed**

During this reporting period, we have made substantial progress toward meeting our research goals.

### Phase I

Phase I progress consisted of designing and developing a survey to assess physical activity behavior, perceptions and attitudes towards cycling, and knowledge of the Bike Temple campaign. With input from researchers at Temple University and International experts in the field, we designed and developed a survey to be distributed at two time points: a) prior to advertisements regarding the Bike Temple campaign; b) four weeks following the initial survey. We obtained University approval to distribute this survey to a random subsample of Temple University faculty, students and staff. Project staff also attended health fairs, posted flyers and recruited potential participants via other electronic media. As of May 1, 2010, 469 baseline surveys have been completed, and participants will be contacted for follow-up beginning May 7, 2010. We will plan an additional survey distribution for Fall 2010. Given that the survey is on-going, results are not available at this time.

### Phase II

In Phase II, the project goals consist of designing, developing and evaluating a social networking intervention (using Facebook) for PA and weight management among college students who are at risk of weight gain. Progress on this phase has included conducting literature reviews in the area to identify scientific gaps, evidence-based practice, and relevant content. Additionally, existing Facebook applications have been identified and summarized for effective key components. Based on this formative work, the study team has identified the active ingredients necessary to adapt and develop a Facebook platform for weight management among college students. The Principal Investigator and her team are scheduled to have a conference call with Dr. Gary Bennett (Consultant) and the computer programmers on May 20, 2010 to discuss the key components and finalize programming plans for the Facebook application. Implementation of the program and recruitment of participants is planned for Fall 2010.

### Phase III

The goal of Phase III of the project is to evaluate participant knowledge of, and interest and engagement in, the Earn-a-Bike program. To meet this project aim, we proposed conducting focus groups with approximately 10 youth participating in the Neighborhood Bike Work's (NBW) Earn-a-Bike program in North Philadelphia, PA. To date, we have conducted two focus groups (n=6; n=3), with children whose ages range from 8 to 13 years old. Another focus group session is scheduled for late June.

While the focus groups are on-going and have not been analyzed fully, some preliminary impressions are reported here. First, a majority of the participants learned about the program while walking by the NBW location, and about half entered the program for the primary reason of receiving a bike upon completion. All participants wished that the program was held every day during the week. All of the participants had heard of Temple University and thought it would be a good idea if students were a part of the program to help them learn more about bikes. They all agreed that they would not ride their bicycles to school for fear of parts being stolen. Follow-up data indicated that they enjoyed the program and that they would recommend it to their friends. The participants reported learning bike safety rules and the basics to fixing flat tires, chains, and helping others fix bicycles. The majority of boys planned to ride their bicycles every day.

## **Research Project 23: Project Title and Purpose**

*The Role of Osteoactivin (OA) as a Downstream Mediator of Osteoblast Differentiation Induced by BMP2* - Osteoactivin (OA) is a downstream mediator of osteoblast differentiation induced by BMP2. OA expression is regulated by BMP2 through the Smad1 signaling pathway. We hypothesize that OA acts a downstream mediator of BMP2-induced osteoblast differentiation and function, and this effect is mediated by the recruitment of Smad1, homeodomain proteins, and the CBP co-activator to the OA promoter to modulate the induction of its activity during osteoblast differentiation. We will determine whether OA acts as a downstream mediator of BMP2-induced osteoblast differentiation using primary osteoblasts derived from WT, OA KO and OA Tg mice and examine BMP2 responsiveness and Smad signaling. Subsequent analysis to examine the mechanism of activation and regulation of OA transcription by Smad1, Dlx3, Dlx5 and CBP during osteoblastogenesis.

### **Anticipated Duration of Project**

11/18/2009 – 10/31/2010

### **Project Overview**

#### Specific aims:

1) To examine the role of OA as a downstream mediator of osteoblast differentiation induced by BMP2

Objective A: OA acts as a downstream mediator of BMP2 induced osteoblast differentiation

Objective B: The effects of absence (OA KO) or over-expression (OA Tg) of OA in osteoblasts on Smad signaling induced by BMP2

2) To examine the effect of BMP2 treatment on the recruitment of Smad1, Dlx3, Dlx5 and CBP proteins to the OA gene during osteoblast differentiation

We will first confirm and expand our analysis to determine whether OA acts as a downstream mediator of BMP2-induced osteoblast differentiation using primary osteoblasts derived from WT, OA KO and OA Tg mice and examine BMP2 responsiveness and Smad signaling. Next we will expand our analysis to examine the mechanism of activation and regulation of OA transcription by Smad1, Dlx3, Dlx5 and CBP during osteoblastogenesis.

This project represents an expansion of and next steps in research funded with previous CURE Formula Grants.

## **Principal Investigator**

Fayez F. Safadi, PhD  
Associate Professor  
Temple University School of Medicine  
Department of Anatomy and Cell Biology  
3400 N. Broad Street  
610 OMS  
Philadelphia, PA 19140

## **Other Participating Researchers**

Maneet Singh, MS, Steven N. Popoff, PhD – employed by Temple University School of Medicine

## **Expected Research Outcomes and Benefits**

OA is expected to have a direct and important role in the process of cellular differentiation and in skeletogenesis as a whole. We expect that OA will act as a down-stream mediator of BMP-2 induced osteoblast differentiation.

The work should enhance our understanding of how stem cells differentiate into cartilage and bone. Currently in the United States, 10 million people suffer from osteoporosis and a further 20 million suffer from osteoarthritis. Although current therapies to treat these diseases are met with only limited success, there is much potential in stem cell therapy as a possible cure. To use stem cells for therapy, an intimate understanding of skeletogenesis is required in the hopes to manipulate stem cell differentiation to cure diseases. By understanding the role of factors that regulate the differentiation of stem cells, this work will bring us one step closer to using stem cells to cure skeletal diseases such as osteoarthritis and osteoporosis.

## **Summary of Research Completed**

1) To examine the role of OA as a downstream mediator of osteoblast differentiation induced by BMP2

*Objective A:* OA acts as a downstream mediator of BMP2 induced osteoblast differentiation

*Objective B:* The effects of absence (OA KO) or over-expression (OA Tg) of OA in osteoblasts on Smad signaling induced by BMP2

Experiments proposed in this aim are still underway. We are in the process of isolating primary osteoblasts from OA OK and OA Tg mice. Once osteoblasts are isolated we will then examine their ability to respond to BMP2-mediated effects on osteoblast differentiation and function.

2) To examine the effect of BMP2 treatment on the recruitment of Smad1, Dlx3, Dlx5 and CBP proteins to the OA gene during osteoblast differentiation

1. Cloning of Osteoactivin (OA) proximal promoter: We cloned 1 Kb of OA proximal promoter using liver DNA specific primers. The PCR product was sequenced and blasted using web-based sequence analysis software (figure 1).

2. BMP-2 dependent stimulation of Osteoactivin promoter: In order to identify whether BMP-2 stimulates Osteoactivin promoter activity, rat primary osteoblasts were transfected with Osteoactivin promoter vector, as described in figure 1. Renilla expression vector was co-transfected as transfection control. Twenty four hours post-transfection osteoblasts were treated with BMP-2 (100ng/ml) and the luciferase activity was assayed 24 hours after BMP-2 treatment. BMP-2 treatment had no change in the promoter activity of empty vector (used as a negative control) and no significant changes were observed for a constitutively active promoter with different concentrations of BMP-2. Osteoactivin promoter showed a dose-dependent increase in promoter activity with BMP-2 treatment (figure-2).

3. Time dependent effect of BMP-2 treatment on Osteoactivin promoter activity: Rat primary osteoblasts transfected with Osteoactivin promoter (as described above) were treated with BMP-2 for different time periods and assayed for promoter activity. BMP-2 treatment for 24 hours showed a maximal promoter activity and this time duration was used for future experiments (figure 3).

4. Osteoactivin promoter activity in different cell systems: Evidences indicate osteoactivin to be expressed in different tissues in which it plays varying roles. In order to test whether BMP-2 stimulates Osteoactivin in different cell systems, we transfected Osteoactivin promoter in mouse pluripotent mesenchymal cell line, C3HT10 T1/2 and pre-osteoblast cell line MC3T3-E4, C2C12 cell lines. Human non-osteoblast cell lines, Hela and HEK-293 cells, were treated in the same manner as described above for rat primary osteoblasts. BMP-2 enhanced Osteoactivin promoter activity in all the cell systems. However, a maximal enhance of endogenous and BMP-2 stimulated Osteoactivin promoter activity was observed in rat primary osteoblasts. Also, mouse pre-osteoblast cell lines showed increase in osteoactivin with BMP-2 treatment. HEK-293 cells showed a minimal increased in promoter activity both endogenous and with BMP-2 treatment. However, Hela cells showed both basal and endogenous Osteoactivin promoter activity similar to rat primary osteoblasts. Also, literature evidences indicate that Hela cells are deficient in Runx2 expression. Thus, in order to elucidate mechanism of Osteoactivin promoter activity in Hela cells, we will first measure the relative expression of varying transcription factors in varying cell systems, both endogenously and with BMP-2 treatment. This will give us a clear picture of transcription factors regulating osteoactivin expression. It is also possible that other non-osteoblast-specific transcription factors in Hela cells could enhance Osteoactivin promoter activity. For this purpose, we will test the effect of knock down of osteoblast-specific transcription Dlx3 and Dlx5 knockdown on Osteoactivin promoter activity in Hela cells and rat primary osteoblasts (figure-4).

5. Effect of deletion of consensus transcription factor binding on Osteoactivin promoter: Osteoactivin promoter sequence was analyzed using MatInspector and found to contain consensus sequences that interact and bind to DNA-binding domain of various osteoblast specific transcription factors as indicated in table 1. In order to examine the effect of these sequences on Osteoactivin promoter activity, we designed a deletion mutant for Osteoactivin

promoter (figure 5a) that lacked a few consensus transcription factor binding sites and transfected them in rat primary osteoblasts and assayed endogenous and BMP-2 stimulated osteoactivin promoter activity. Loss of consensus transcription factor binding sites decreased both basal and BMP\_2 stimulated Osteoactivin promoter activity (figure 5c).

6. Effect of site-directed mutagenesis in consensus transcription factor binding sites in Osteoactivin promoter activity: Osteoactivin mutant constructs were transfected in rat primary osteoblasts and stimulated with BMP-2 and assayed for promoter activity. Site-directed mutagenesis in Runx2 and Homeodomain transcription factor binding sites significantly decreased both basal and BMP-2 induced Osteoactivin promoter activity (figure 6).

7. Effect of Knock down of Smad1 and Smad4 on Osteoactivin promoter activity: Osteoactivin promoter contains multiple consensus Smad1 and Smad4 binding sites. Rather than mutating each of the consensus Smad1 and Smad4 transcription factor binding sites, we studied the effect of Smad1 and Smad4 on Osteoactivin promoter activity by depletion of Smad1 and Smad4 using specific siRNA for Smad1 and Smad4. Smad1siRNA (100nM) decreased the Smad1 expression significantly and this dose of Smad1-siRNA was used for luciferase assay to study the effect of Smad1 depletion on Osteoactivin promoter activity (figure 7).

#### Summary and future directions:

Our laboratory identified Osteoactivin in bone, a secreted glycoprotein that promotes osteoblast differentiation and function. Previous studies suggest that Osteoactivin expression is regulated by Bone Morphogenetic Protein-2 (BMP-2), an osteogenic growth factor, through Smad1 signaling. Furthermore, we have shown that Osteoactivin acts as a downstream mediator of BMP-2 effects on OB differentiation and function. BMP-2 is required for the initial commitment of osteoblast progenitor cells and promotes their differentiation into mature osteoblasts. BMP-2 mediates these osteogenic effects by recruiting transcription factors, namely Runx2, Homeodomain (HD), (Dlx3 and Dlx5), Smad1 and Smad4 to the promoter region of osteoblast specific genes and induces their transcription. The goal of this study is to identify osteoblast-specific transcription factors that regulate BMP-2 induced Osteoactivin transcription. In order to study the regulatory effects of BMP-2 on Osteoactivin promoter activity, we cloned 1kb upstream of rat Osteoactivin gene in a luciferase expression vector and have shown that BMP-2 stimulated Osteoactivin promoter activity in a dose- and time-dependent manner. Using deletion mutants of this Osteoactivin promoter lacking one or more of the consensus binding sites for Runx2, HD, Smad1 and Smad4, we have shown that loss of transcription factor binding sites significantly decreased both basal and BMP-2-induced Osteoactivin promoter activity. Similarly, site-directed mutagenesis of Runx2 and HD binding sites decreased both basal and BMP-2-induced Osteoactivin promoter activity. Both these studies suggested that Runx2, HD, Smad1 and Smad4 binding sites are important for Osteoactivin transcriptional regulation. These results were further confirmed by mobility shift assay. Specific roles of TFs on Osteoactivin promoter regulation were studied by evaluating the effect of knockdown and over expression of Runx2, HD proteins (Dlx3 and Dlx5), Smad1 and Smad4, respectively on Osteoactivin promoter activity. Lastly, Osteoactivin promoter occupancy by Runx2, HD, Smad1 and Smad4 during osteoblast differentiation was evaluated by ChIP assay. BMP-2 treatment significantly induced differential association of Runx2, Dlx3, Dlx5, Smad1 and Smad4 with Osteoactivin promoter during different stages of osteoblast differentiation. Collectively, our results suggest that Runx2, HD proteins, Smad1 and

Smad4 are involved in both basal and BMP-2-induced regulation of Osteoactivin transcription. The information gained from studies of the transcriptional regulation of Osteoactivin may help in developing potential anabolic factors that can selectively promote bone formation in the treatment of osteoporosis.

Figures:

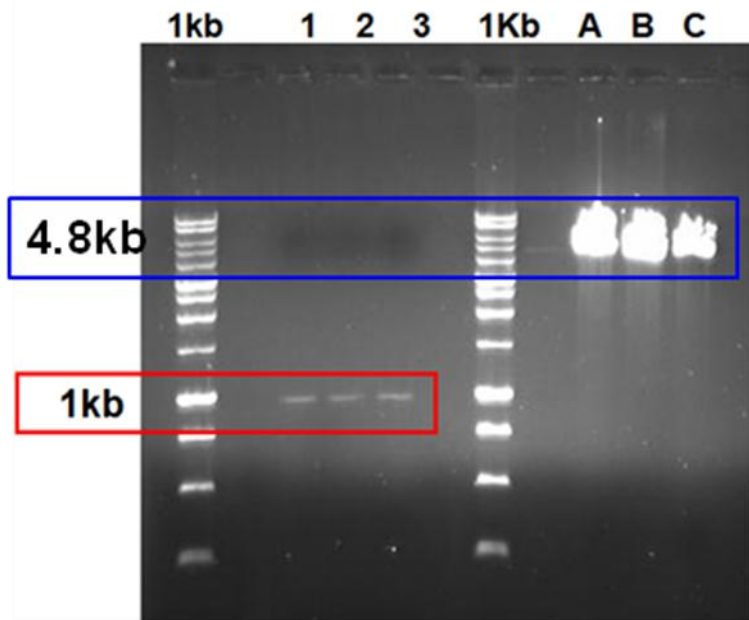


Figure-1. PCR cloning of 1kb upstream of Osteoactivin promoter into a pGL3-Basic luciferase expression vector. Lane1 represents KpnI digested 1kb Osteoactivin promoter, Lane 2 is BglII digested 1kb Osteoactivin promoter and Lane3 is KpnI and BglII digested Osteoactivin promoter. Lane A indicates KpnI digested pGL3-Basic vector (promoter-less vector), Lane B is the BglII digested pGL3-Basic vector and lastly Lane C is the KpnI and BglII double digested linearized vector. After the restriction digestion Osteoactivin promoter was ligated to the pGL3-Basic vector and this OA promoter cloned in luciferase vector was used for further OA promoter experiments.

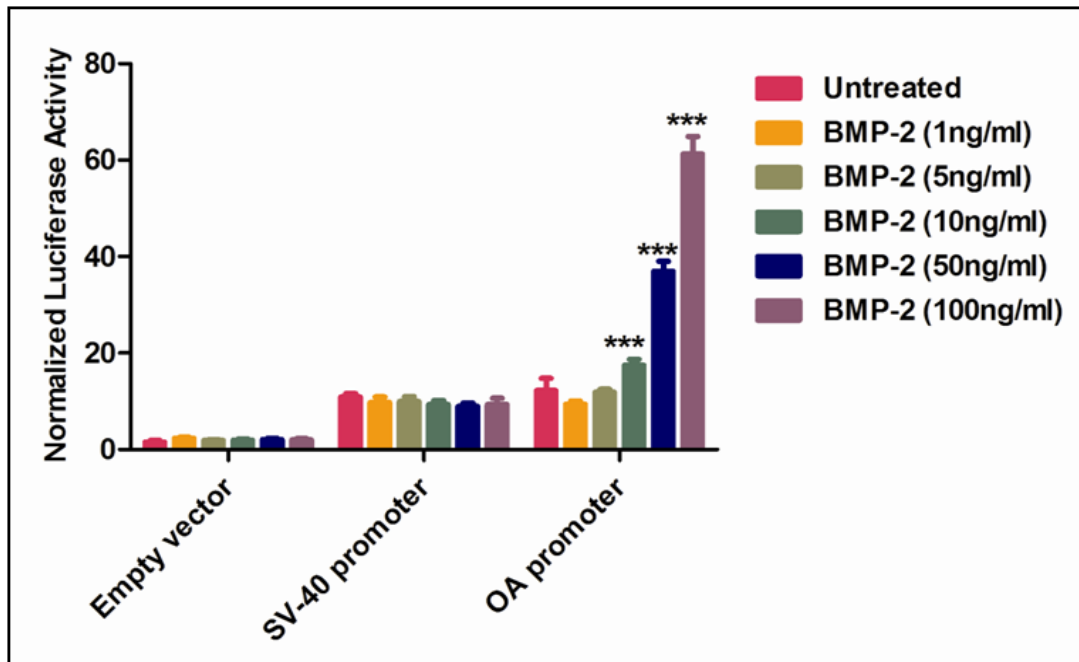


Figure-2. BMP-2 dose dependent Osteoactivin promoter activity. Rat primary osteoblasts were seeded on a 6 well plates. Next day, when the cells were 80% confluent, they were transfected with empty pGL3-Basic vector (negative control), SV-40 promoter vector (constitutively active promoter) and Osteoactivin promoter. Twenty four hours post-transfection, osteoblast cells were treated with 1-100ng/ml of BMP-2 for twenty four hours and then assayed for luciferase activity. Data expressed as mean + SEM(n=3), \*\*p< 0.001 compared to untreated osteoblasts, \*\*\*p<0.0001 compared to untreated osteoblasts.

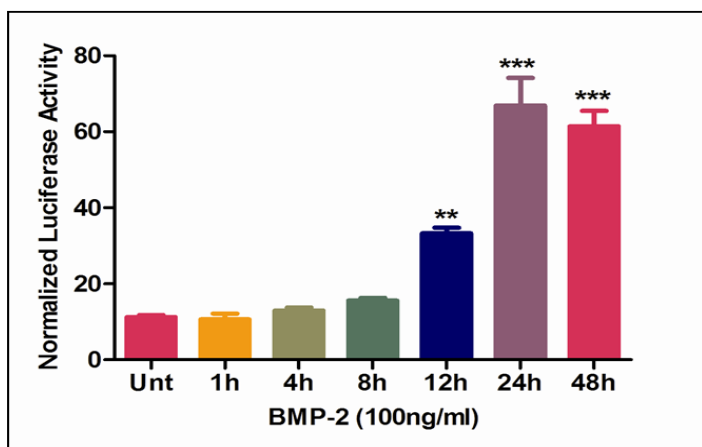


Figure-3. Time dependent effect of BMP-2 treatment on Osteoactivin promoter activity. Rat primary osteoblasts transfected with Osteoactivin promoter (as described above) were treated with BMP-2 for following time periods and assayed for promoter activity. Data expressed as mean + SEM (n=3), \*\*p< 0.001 compared to untreated osteoblasts, \*\*\*p<0.0001 compared to untreated osteoblasts.

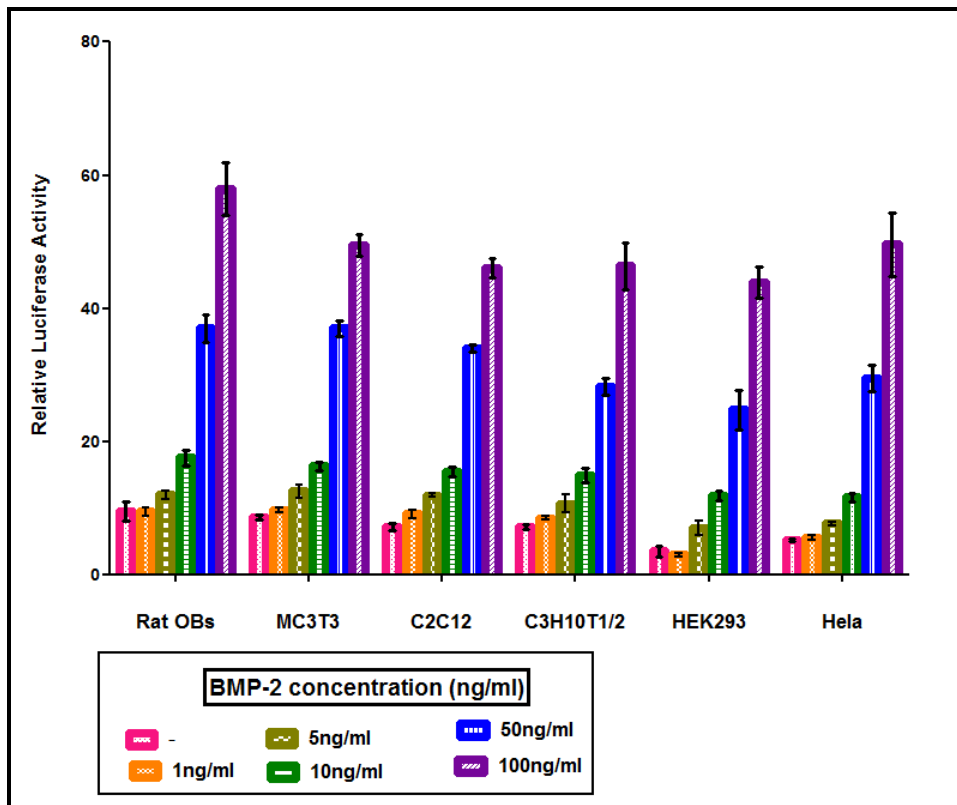


Figure-4. Osteoactivin promoter activity in different cell systems. Rat primary osteoblast, mouse MC3T3 E4, C2C12, C3H10T1/2 and human HEK293 and Hela cells were seeded in a 6 well plate. Cells were treated and assayed for promoter activity as described in figure 2.

Table-1: Consensus transcription factor binding sites present of lost with deletions in Osteoactivin promoter deletion constructs.

No	OA construct	Contains Binding sites	Loss of Binding sites
1.	Full length	Runx2 = 4 HD = 4 Smad1 = 5 Smad4 = 8 SBE = 6	None
2.	#1 (-835)	Runx2 = 4 HD = 2 Smad1 = 5 Smad4 = 8 SBE = 4	HD = 2 SBE = 2
3.	#2)	HD = 2 Smad1 = 5 Smad4 = 8 SBE = 4	Runx2 = 4 HD = 2 SBE = 2
4.	#3	SBE = 1	Runx2 = 4 HD = 4 Smad1 = 5 Smad4 = 8 SBE = 5

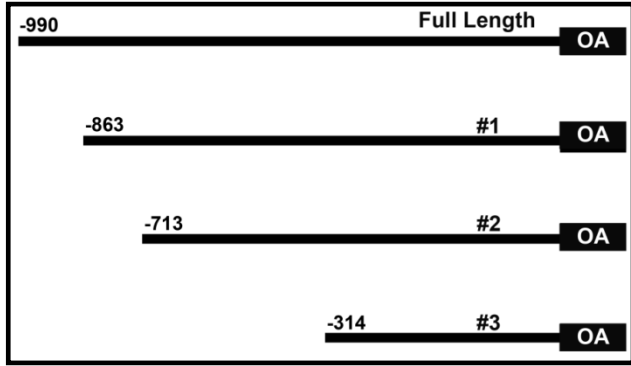
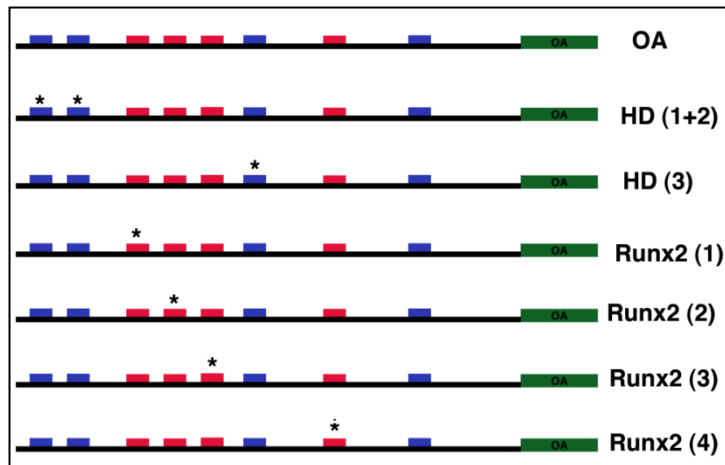
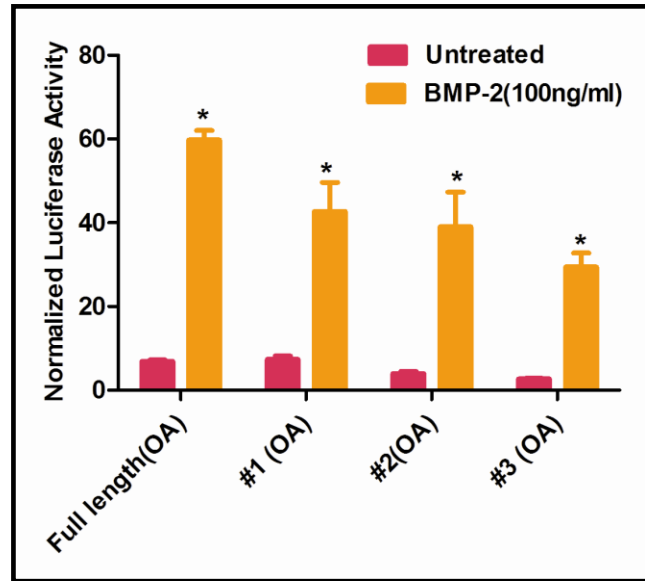


Figure-5a: Osteoactivin promoter deletion mutants. The cloned Osteoactivin promoter sequences indicates as -990, -863, -713 and -314 indicate nucleotide upstream of start codon (ATG) of osteoactivin gene.

Figure-5b: Osteoactivin promoter deletion constructs activity. Each of the deletion constructs were transfected in rat primary osteoblast cells, BMP-2 treated and assayed for promoter activity as described above. Data expressed as mean + SEM (n=3), \*p<0.0001 compared to untreated osteoblasts.



- HD binding sites ( ■ )
- Runx2 binding sites ( ■ )
- Mutations are in ( \* )

Figure-6A. Osteoactivin promoter mutants. Location of mutation is indicated with (\*).

Figure-6B. Effect of site-directed mutagenesis in consensus transcription factor binding sites in Osteoactivin promoter. Osteoactivin mutant constructs were transfected in rat primary osteoblasts and stimulated with BMP-2 and assayed for promoter activity as described above. Data expressed as mean + SEM (n=3), \*\*\*p<0.0001 compared to untreated osteoblasts.

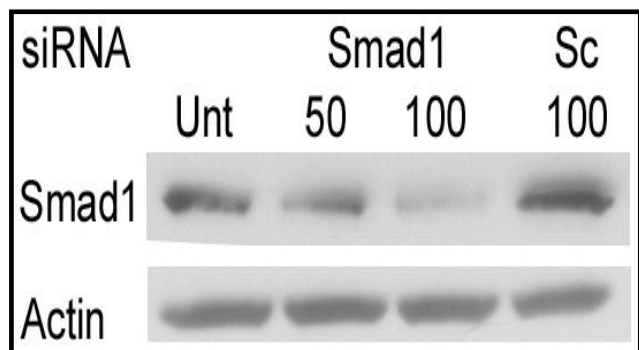
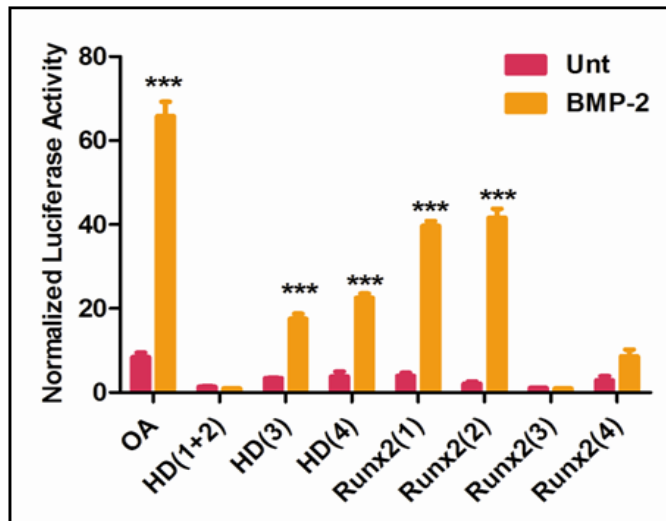
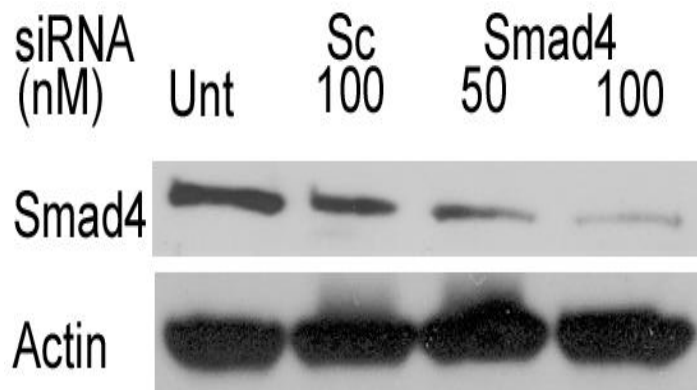


Figure-7A. Immunoblot for Smad1 indicating depletion of Smad1 using Smad1 siRNA (Santacruz). Rat primary osteoblasts seeded in 6 well plates were transfected with Smad1-siRNA at concentrations 50nM and 100nM and control scrambled siRNA (Sc) at 100nM. 48 h post-transfection, cell lysates were collected and run for immunoblot for Smad1 depletion. Smad1siRNA (100nM) decreased the Smad1 expression significantly and this dose of Smad1-siRNA was used for luciferase assay to study the effect of Smad1 depletion on Osteoactivin promoter activity.

Figure7B:Immunoblot for Smad4 indicating depletion of Smad4 using Smad4 siRNA (Santacruz). Procedure similar to described above for Smad1 siRNA were used and assayed for Smad4 antibody (cell signaling). Smad4(100nM) siRNA significantly depleted Smad4 expression levels and this concentration of Smad4 siRNA was used for luciferase experiments to assay effect of Smad4 on Osteoactivin promoter activity.



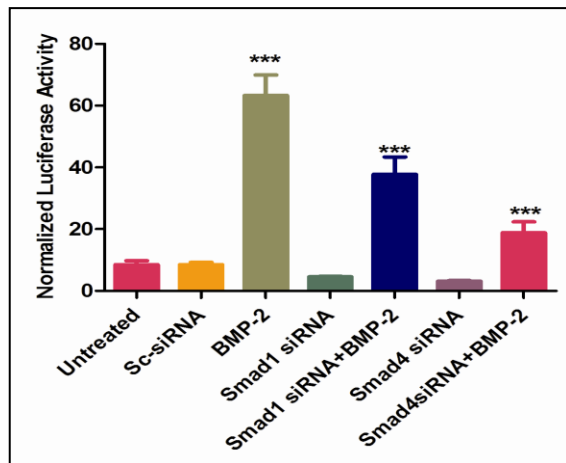


Figure-7C: Effect of Smad1 and Smad4 depletion on Osteoactivin promoter activity. Rat primary osteoblasts were seeded in 6-well plates and co-transfected with Osteoactivin promoter and Smad1-siRNA/Smad4-siRNA. 24h post-transfection, cells were stimulated with BMP-2 (100ng/ml) for 24 h and assayed for promoter activity. Knockdown of Smad1 and Smad4 decreased both basal and BMP-2 induced Osteoactivin promoter activity, suggesting Smad1 and Smad4 to be crucial for Osteoactivin promoter activity.

### **Research Project 24: Project Title and Purpose**

*Defining a Typology of Low-Literacy African Americans for Colorectal Cancer Screening* - To conduct specialized cluster analyses of data collected under a current NCI R21 grant. The cluster analyses will result in a typology of low-literacy African Americans that will provide the foundation for development of communication for minority populations as well as expanded future research and grant applications.

### **Duration of Project**

11/18/2009 – 6/30/2010

### **Project Overview**

The National Cancer Institute has identified screening for colorectal cancer as a high priority area of needed research. Our recent R21 grant to develop more effective colorectal cancer screening decision aids collected data from 102 low-literacy African American patients over the age of 50 who are patients at the Temple University General Internal Medicine clinic. These data include demographics, health life-style factors, attitudes toward health screening, and personality factors. Based on these combined elements, it will be possible to develop a typology of low-literacy African American patients that focuses on their orientation toward their health care, and their willingness to be screened for colorectal cancer. This typology will provide the foundation for developing communication strategies to more effectively encourage the differing types of patients to be screened for colorectal cancer. The resulting typology will be the foundation for an R01 grant application to be prepared during the spring semester, 2010, and will be submitted to the *Health Communication and Informatics Research Branch* of the National Cancer Institute (the branch sponsoring our R21 grant). Our program manager at this branch has encouraged us to build on the R21 results and submit an R01 application to continue to refine and extend the work begun in the R21.

As a data analysis project (using our specialized R21 database), the approach will be to use the combined demographic, psychographic, life-style, and health care orientation factors to create a typology of low-literacy African Americans. It is argued that appeal strategies to encourage colorectal cancer screening will be more effective if targeted to specific types of patients with differing attitudes, health care values, and orientations toward the health care system.

Cluster analysis sub-routines within the Statistical Package for the Social Sciences (SPSS) will be used to conduct the analyses. Our existing database of 102 low-literacy African American patients will provide the data for the analyses. Dr. Gordon, with the aid of our two laboratory research assistants, will plan the project, conduct the analyses, interpret the result, write-up the results, and use the results in the preparation of the R01 grant submission.

### **Principal Investigator**

Thomas F. Gordon, PhD  
Professor of Public Health  
Temple University  
Department of Public Health  
1301 Cecil B. Moore Avenue  
Temple University  
Philadelphia, PA 19122

### **Other Participating Researchers**

Caitlin Wolak, MPH, Michael Rovito, MA, Sarah Bass, MPH, PhD, Stephanie Ward, MD, Anuradha Paranjape, MD – employed by Temple University

### **Expected Research Outcomes and Benefits**

The project will establish the typology of low-literacy African Americans needed to further refine the work begun with the R21 grant, and will provide an important foundation for the development of patient communication to promote willingness of minority populations to get cancer screenings, and development of future expanded research in this area of health communications.

### **Summary of Research Completed**

The goal of this project was to develop a typology of low-literacy African American patients. To achieve this, a survey was conducted of 102 African Americans between the ages of 50 and 74 recruited from the Temple University Hospital General Internal Medicine Clinic. Literacy level was established using the 8-item standardized *Rapid Estimate of Adult Literacy in Medicine – Revised* technique (REALM-R). Questions for the survey were developed based on our prior work involving: (1) Four focus groups conducted with low-literacy African American patients; (2) In-depth interviews with 30 third-year medical residents in internal medicine; and (3) An extensive review of the available research literature on CRC screening. The questions on the final survey fell into 3 categories: 1) Personal attitudes and preferences regarding preventative

screening and health maintenance (11 questions); 2) Perceived barriers to being screened (16 questions), 3) perceptions of colonoscopy, the most recommended method for CRC screening (8 questions).

To establish the typology of patients, a *k-means cluster analysis procedure* was used (SPSS statistical package). The variables specified for clustering were the patient's responses to the 11 questions involving personal attitudes and preferences toward preventative screening and general health maintenance. Three distinct cluster groupings of patients resulted from the analysis. These patient segments were named: 1) *Ready Screeners*; 2) *Fearful Avoiders*; 3) *Cautious Screeners*. Table 1 presents the mean values across these three groups, with resulting significance test p-values (ANOVA). As can be seen, the clustering procedure was highly successful in producing cluster segments that differed significantly across all of the clustering variables. The size of the clusters varied, with the Ready Screeners accounting for 50.0% of the total sample, the Fearful Avoiders were 30.4% and the Cautious Screeners were 19.6%. The following bullet summaries present the core characteristics of each cluster group.

Cluster #1: Ready Screeners (50.0%):

- 65% have had a colonoscopy.
- Don't mind going to the doctor.
- Don't mind preventative testing.
- Would rather know (than not know) if they have cancer.
- Do not let fear of knowing keep them from being tested for cancer.
- Do agree that if they get cancer it is "God's will."
- Feel screening tests are good at finding problems.
- Do not have to be pushed by Family/Friends to get tested.
- Will definitely get tested if their Dr. recommends it.
- Strongly believe that screening tests are "worth the effort."
- Believe in doing screening "to stay healthy."

Cluster #2: Fearful Avoiders (30.4%):

- 24.3% have had a colonoscopy.
- Don't like going to the doctor.
- Trust their body to tell them if there is a problem.
- Don't like doing tests.
- Would rather not know if they have cancer.
- Fear of knowing keeps them from being tested for cancer.
- Do agree that if they get cancer it is "God's will."
- Feel screening tests are moderately good at finding problems.
- Are not likely to get tested if asked to do so by Family/Friends.
- Will get tested if their Dr. recommends it.
- Do agree that screening tests are "worth the effort."
- Agree that they do screenings "to stay healthy."

Cluster #3: Cautious Screeners (19.6%):

- 57.6 % have had a colonoscopy.
- Don't mind going to the doctor.
- Would rather know if they have cancer.
- Do not let fear of knowing keep them from being tested for cancer.
- Do not agree that if they get cancer it is "God's will."
- Feel screening tests are good at finding problems.
- Do not have to be pushed by Family/Friends to get tested.
- Are not overly influenced by a doctor's recommendation to be screened.
- Strongly believe that screening tests are "worth the effort."
- Believe in doing screening "to stay healthy."

Given the establishment of the patient typology based on personal attitudes and preferences regarding preventative screening and health maintenance in general, the groups were profiled on *perceptions of barriers to screening* and *perceptions of colonoscopy* as a specific method for CRC screening. These variables were not involved in establishing the clusters, as such they reveal independent differences across the types of patients.

How Patient Types Perceive Barriers to Colorectal Cancer (CRC) Screening:

Table 2 presents the means and significance tests across the types of patients. From these results we can conclude:

- *Cost of screening* is not seen as a prohibitive factor to being screened across all three types of patients, probably due to insurance or Medicare-Medicaid coverage. Fearful Avoiders do rate cost as a concern significantly higher than do the other types of patients (3.2 v. 1.2 on the 0-10 scale).
- *Transportation, taking time off from work, arranging child care and/or care for older family members*, are rated low as barriers to getting screened (<2.3 on the 0-10 scale).
- *The bother of preparation for testing, unfamiliarity with procedures, or embarrassment* are not perceived as barriers for the Ready Screeners and the Cautious Screeners. However, the Fearful Avoiders rate these factors significantly higher as concerns (4.1 to 4.5 on the 0-10 point scale).
- *Fear of finding they might have cancer* is not a barrier to screening for the Ready Screeners and the Cautious screeners (1.98 & 1.65 on 0-10 scale). However, this concern is significantly higher for the Fearful Avoiders (5.81).
- *Concern that the screening process will be painful* is significantly higher for the Fearful Avoiders (6.35) than for the Ready Screeners (2.69) or the Cautious Screeners (3.60).
- *Worry about serious complications from screening procedures* is significantly higher for the Fearful Avoiders (4.94) than for the Ready Screeners (3.04) or the Cautious Screeners (2.90).

How Patient Types Perceive Colonoscopy as a Method for CRC Screening:

Table 3 presents the means and significance tests across the types of patients. From these results we can conclude:

- There is a high degree of consistency across all patient types on all variables, that colonoscopy is the superior technique for colorectal cancer screening. Across all 8 variables and 3 patient types, mean values ranged from 7.05 to 9.43.
- For 7 of the 8 variables, there were no significant differences across patient types in how they perceive colonoscopy—rating it very high.
- Across all patient types, colonoscopy is seen as the screening technique that is the *most accurate, most effective at finding growths early and removing them, has to be done the least often, is the most recommended by doctors, is covered by insurance, and produces the most peace of mind.*
- All patient types agree that *being sedated during a colonoscopy is a plus.*

Overall, this project successfully defined a typology of low-literacy African Americans relative to their personal attitudes and preferences regarding preventative screening and health maintenance. The three resulting types of patients were profiled on their perceptions of barriers to screening, and perceptions of colonoscopy as a specific method for colorectal cancer screening. These results will be extremely useful in the development of future research projects and grant applications.

Tables follow:

Table 1  
Personal Health Attitudes-Behaviors  
By Type of Patient

Mean Values (variables used for clustering), N, and SD  
(Scale base = 0-10, the larger the values, the more agreement with the statement)

	Cluster 1			Cluster 2			Cluster 3			Sig.*
	<b>Ready Screeners</b>			<b>Fearful Avoiders</b>			<b>Cautious Screeners</b>			
ITEMS:	n	Mean	SD	n	Mean	SD	n	Mean	SD	
<b>1) Don't Go to Docs</b>		<b>2.45</b>			<b>7.65</b>			<b>5.85</b>		<b>.000</b>
I'm the kind of person who doesn't go to the doctor unless I really need to.	51	3.04		31	2.40		20	3.59		
<b>2) I Trust My Body</b>		<b>5.94</b>			<b>8.23</b>			<b>5.65</b>		<b>.002</b>
I trust that my body will let me know when I need to be tested for something.	51	3.36		31	1.82		20	3.69		
<b>3) Don't Like Tests</b>		<b>3.22</b>			<b>7.81</b>			<b>4.30</b>		<b>.000</b>
In general, I don't like to have tests unless I feel something is wrong.	51	3.38		31	2.20		20	3.21		
<b>4) Rather Not Know</b>		<b>0.57</b>			<b>6.32</b>			<b>1.55</b>		<b>.000</b>
I'd rather not know if I have cancer.	51	1.65		31	3.82		20	2.65		
<b>5) Fear Cancer</b>		<b>0.82</b>			<b>6.03</b>			<b>1.45</b>		<b>.000</b>
My fear of cancer keeps me from getting the tests my doctor tells me I should have.	51	1.87		30	3.32		20	2.59		
<b>6) God's Will</b>		<b>8.61</b>			<b>8.39</b>			<b>3.15</b>		<b>.000</b>
If I get cancer, I accept that it is the will of God.	51	3.18		31	3.03		20	3.47		
<b>7) Tests Are Not Good</b>		<b>1.78</b>			<b>3.74</b>			<b>2.25</b>		<b>.001</b>
I feel many of the screening tests are not very good at finding problems.	51	1.98		31	2.73		20	2.25		
<b>8) Only if Family-Friends Rec.</b>		<b>0.45</b>			<b>4.29</b>			<b>1.20</b>		<b>.000</b>
I would only have a colonoscopy if a close family member or friend told me to.	51	1.67		31	3.95		20	1.77		

Table 1 (Cont.)  
**Personal Health Attitudes-Behaviors**  
**By Type of Patient**

Mean Values (variables used for clustering), N, and SD  
(Scale base = 0-10, the larger the values, the closer to self)

	Cluster 1			Cluster 2			Cluster 3			Sig.*
	<b>Ready Screeners</b>			<b>Fearful Avoiders</b>			<b>Cautious Screeners</b>			
ITEMS:	n	Mean	SD	n	Mean	SD	n	Mean	SD	
<b>9) Only if Doc Recommends</b>		<b>9.65</b>			<b>9.10</b>			<b>4.45</b>		<b>.000</b>
I would only have a colonoscopy if a doctor I trusted told me to have it.	51	1.48		31	1.76		20	4.38		
<b>10) Worth the Effort</b>		<b>9.25</b>			<b>8.19</b>			<b>6.70</b>		<b>.000</b>
Although it may be hard to take the time-off and make the arrangements to do a colonoscopy, I think it is well worth the effort.	51	1.32		31	2.72		20	3.64		
<b>11) I Do Screening</b>		<b>9.29</b>			<b>8.06</b>			<b>7.65</b>		<b>.001</b>
I like to avoid getting sick, so I try to do screening tests.	51	1.12		31	1.93		20	3.05		

\*P-value for ANOVA test of mean differences across types of patients.

Table 2  
Perceived Barriers to Colorectal Cancer Screening  
By Types of Patients

Mean Values for Cluster Types, with N, SD  
(Scale base = 0-10, the larger the mean value, the more agreement with the statement)

ITEMS:	Cluster1			Cluster2			Cluster3			Sig*
	<b>Ready Screeners</b>			<b>Fearful Avoiders</b>			<b>Cautious Screeners</b>			
	<u>n</u>	<u>Mean</u>	<u>SD</u>	<u>n</u>	<u>Mean</u>	<u>SD</u>	<u>n</u>	<u>Mean</u>	<u>SD</u>	
<b>1) Cost is Prohibitive</b>		<b>1.24</b>			<b>3.21</b>			<b>1.20</b>		<b>.018</b>
The cost of having a colon screening test keeps me from getting one.	50	2.81		29	4.03		20	1.99		
<b>2) No Transportation</b>		<b>2.08</b>			<b>1.61</b>			<b>1.50</b>		<b>.660</b>
It would be hard getting someone to take me to and from the testing location	51	3.22		31	2.35		20	2.50		
<b>3) No Time Off</b>		<b>0.20</b>			<b>1.90</b>			<b>0.45</b>		<b>.000</b>
It would be hard taking time off from work to get screened.	51	0.69		31	3.15		20	0.83		
<b>4) No Child Care</b>		<b>1.02</b>			<b>2.19</b>			<b>0.55</b>		<b>.045</b>
It would be hard finding someone to care for my children.	51	2.34		31	3.28		20	1.10		
<b>5) No Adult Care</b>		<b>0.76</b>			<b>2.26</b>			<b>0.90</b>		<b>.024</b>
It would be hard finding someone to care for adults I take care of.	51	2.00		31	3.38		20	1.55		
<b>6) Too Much Bother</b>		<b>2.49</b>			<b>4.13</b>			<b>2.50</b>		<b>.032</b>
For me, preparing for the test is too much bother.	51	2.88		31	2.96		20	2.56		
<b>7) Too Unfamiliar</b>		<b>2.24</b>			<b>4.39</b>			<b>1.70</b>		<b>.010</b>
For me, the whole screening process is so unfamiliar, I don't want to do it.	51	3.47		31	3.73		20	3.20		
<b>8) Embarrassing</b>		<b>1.78</b>			<b>4.53</b>			<b>2.15</b>		<b>.001</b>
I would find the screening test to be too embarrassing.	51	3.10		30	3.63		20	3.12		
<b>9) Not Best Method</b>		<b>1.31</b>			<b>3.55</b>			<b>2.10</b>		<b>.001</b>
I don't think colonoscopy is the best method for detecting colon problems.	51	1.58		31	3.48		20	2.38		

Table 2 (Cont.)  
Perceived Barriers to Colorectal Cancer Screening  
By Types of Patients

Mean Values for Cluster Types, with N, SD  
(Scale base = 0-10, the larger the mean value, the more agreement with the statement)

ITEMS:	Cluster1			Cluster2			Cluster3			Sig*
	Ready Screeners			Cautious Screeners			Fearful Avoiders			
	n	Mean	SD	n	Mean	SD	n	Mean	SD	
<b>10) Scared To Know</b>		<b>1.98</b>			<b>5.81</b>			<b>1.65</b>		<b>.000</b>
It scares me to think that I might find out I have cancer and this keeps me from having a colon screening test.	51		2.71	31		3.66	20		3.00	
<b>11) Worry About Sedation</b>		<b>1.41</b>			<b>1.97</b>			<b>2.10</b>		<b>.577</b>
I worry about getting medicine to make me sleepy to have the colonoscopy test.	51		2.72	31		3.14	20		3.21	
<b>12) Worry About Pain</b>		<b>2.69</b>			<b>6.35</b>			<b>3.60</b>		<b>.000</b>
I'm concerned that the screening test might be painful.	51		3.64	31		3.56	20		3.65	
<b>13) Worry About Complications</b>		<b>3.04</b>			<b>4.94</b>			<b>2.90</b>		<b>.018</b>
Although I know it is very rare, I am worried that I could have a serious complication.	51		3.27	31		2.86	20		3.08	
<b>14) Women More Willing</b>		<b>7.37</b>			<b>7.60</b>			<b>7.70</b>		<b>.927</b>
In general, I think women are more willing than men to have a colonoscopy.	51		3.62	30		3.49	20		3.51	
<b>15) Don't Want Rectum Probe</b>		<b>2.12</b>			<b>5.48</b>			<b>2.50</b>		<b>.000</b>
I wouldn't want to have a colonoscopy because they would be putting something in my rectum.	51		3.51	31		4.13	20		3.55	
<b>16) Seems Sexual</b>		<b>0.34</b>			<b>2.70</b>			<b>0.50</b>		<b>.000</b>
Having a colonoscopy seems sexual.	50		1.64	30		3.70	20		1.10	

\*P-value for ANOVA test of mean differences across types of patients.

**Table 3**  
**Perceptions of Colonoscopy**  
**By Types of Patients**

Mean Values for Cluster Types, with N, SD  
(Scale base = 0-10 the larger the mean, the more agreement with the statement)

ITEMS:	Cluster1			Cluster2			Cluster3			Sig*
	<b>Ready Screeners</b>			<b>Fearful Avoiders</b>			<b>Cautious Screeners</b>			
	<u>n</u>	<u>Mean</u>	<u>SD</u>	<u>n</u>	<u>Mean</u>	<u>SD</u>	<u>n</u>	<u>Mean</u>	<u>SD</u>	
<b>1) Most Accurate</b> Colonoscopy is the most accurate way to check for colon or rectal cancer		<b>9.41</b>			<b>8.29</b>			<b>9.05</b>		<b>.021</b>
	49		1.58	28		1.84	20		1.64	
<b>2) Finds Problems Early</b> Having the test is a good way to find colon or rectal cancer very early		<b>9.14</b>			<b>8.50</b>			<b>8.80</b>		.301
	49		1.68	28		1.97	20		1.64	
<b>3) Can Remove Growths</b> During the test the doctor can remove growths before they become cancer.		<b>8.80</b>			<b>8.04</b>			<b>8.15</b>		.164
	49		1.73	28		1.86	20		2.06	
<b>4) Not Done Often</b> A colonoscopy doesn't have to be done as often as other screenings.		<b>7.43</b>			<b>6.57</b>			<b>7.05</b>		.311
	49		2.26	28		2.28	20		2.69	
<b>5) Provides Peace Mind</b> For me, the peace of mind that comes with knowing about my health is a good reason for having the test.		<b>9.51</b>			<b>9.23</b>			<b>9.00</b>		.462
	49		1.39	28		1.52	20		2.18	
<b>6) Recommended By Docs</b> I like the fact that the test is recommended by most doctors.		<b>9.43</b>			<b>8.93</b>			<b>8.80</b>		.220
	49		1.47	28		1.55	20		1.85	
<b>7) If Insurance Covers, I'll Do It</b> If my health insurance covers the cost of the test, I feel I should have one.		<b>8.86</b>			<b>8.83</b>			<b>9.30</b>		.597
	49		1.86	28		1.93	20		1.22	
<b>8) Being Sedated Good</b> I think getting medicine to make me sleepy and not feel uncomfortable during the colonoscopy test is a plus.		<b>9.33</b>			<b>9.27</b>			<b>8.55</b>		.237
	49		1.93	28		1.31	20		1.93	

\*P-value for ANOVA test of mean differences across types of patients.

## **Research Project 25: Project Title and Purpose**

*Understanding Drug Binding to the M2 Channel of the Influenza A Virus* - Funds will be used to support research at the new Institute for Computational Molecular Science (ICMS) in the Temple University College of Science & Technology (CST). The research in question will use computational methods to understand how the so-called M2 proton channel on the surface of the influenza A virus is able to acidify the virus interior as a prelude to replication. The research will also help understand how traditional drugs such as rimantadine act to inhibit the replication cycle of the virus. Importantly, the research will also address the question of how mutations of the flu virus that are involved in the bird flu (so called H5N1) and swine flu (H1N1) enable the flu virus M2 to function in the presence of drugs such as rimantadine. The aim of the computational studies is to inform the rational design of new drugs.

### **Anticipated Duration of Project**

12/1/2009 – 12/31/2011

### **Project Overview**

Novel computer simulation studies will be used to investigate aspects of the way the flu virus functions. The target of the research is the so-called M2 channel, a membrane-bound tetrameric protein bundle that resides in the membrane of the flu virus. This protein bundle serves as a channel for protons that in turn acidify the virion, a process needed to trigger viral replication. The M2 channel has been a target for prophylactic drugs such as amantadine and rimantadine. Unfortunately, mutations in the flu virus have caused these drug molecules to be ineffective against the threat of pandemic flu associated with the H5N1 (Bird Flu) and H1N1 (Swine Flu) mutations of the virus. The recent H1N1 outbreak in the USA makes this work particularly timely.

The computational studies will compare and contrast the structure and dynamical behavior of the membrane-bound M2 protein bundle under different conditions of pH (i.e., different protonation states of channel lining residues). The effect of different mutations will also be studied, especially with respect to the interaction with drug molecules. The outcome will be a deeper understanding of the function of this key membrane protein associated with the flu.

### **Principal Investigator**

Michael L. Klein, PhD  
Carnell Professor in the College of Science & Technology and  
Professor of Chemistry  
Temple University  
Carnell Hall 400  
1803 N. Broad Street  
Philadelphia, PA 19122

## Other Participating Researchers

Giacomo Fiorin, PhD, Vincenzo Carnevale, PhD – employed by Temple University

## Expected Research Outcomes and Benefits

Research in the Institute for Computational Molecular Science (ICMS) in the College of Science and Technology (CST) at Temple University will aim to yield insights into the way the flu virus employs mutations to allow it to render traditional prophylactic drugs ineffective against this target.

The outcomes of this research will be a molecular level understanding of a process that could be key to dealing with the pandemic threat from the flu.

## Summary of Research Completed

### Computer Simulation Studies of the M2 Proton Channel from the Influenza A Virus: Effects of Mutations on Channel Function and Drug Binding.

The progress outlined below has been made through contributions of the PI (one month per year effort) and two postdoctoral research associates: Enzo Carnevale (50% effort) and Giacomo Fiorin (50% effort). The research began soon after the ICMS was established at Temple in August 2009. Progress has been made in three areas, which are reported on separately below.

#### *Modulation of the proton conductance by pH*

The M2 channel's proton conductance is controlled by the pH level in the extra-viral space. Two years ago, a nuclear magnetic resonance (NMR) structure of the trans-membrane segment (M2TM) was determined for the high-pH non-conducting state (Schell and Chou, 2008). At the same time, an X-ray structure of the low-pH conducting state (Stouffer *et al*, 2008) was reported by the DeGrado group at Penn, who are our long-time collaborators. Our group has previously investigated the relationship between these two structures by molecular dynamics (MD) simulations, observing conformational rearrangements consistent with a transporter-like mechanism (Khurana *et al*, 2009). More recently, the DeGrado group has resolved an intermediate-pH structure (unpublished), which possesses features from both the high-pH and the low-pH structure. This important structure exhibits several water clusters in the channel pore. We are in the process of carrying out MD simulations on all of these structures. The aim is to resolve the water distributions across all pH conditions, namely the high pH: neutral; intermediate pH: 2<sup>+</sup> charge; and low pH: 4<sup>+</sup> charge states. In addition, the intermediate-pH structure has been explored at other charge states, to explore possible conformational changes to and from the other two structures.

The orientation of water molecules in the pore and the intensity of the associated water wires is modulated primarily by the charge of the H37 tetrad, and only to a minor extent by the bundle structure. The average orientation of water molecules in the pore does not change across different structures at the same charge state (*Figure 1 - left*), with the exception of the low-pH structure, which represents the *discharge* step of the M2 cycle. Furthermore, with increasing

charge the water density decreases at the outward end of the channel and increases at the inward end. Therefore, at the highest charge state water molecules are oriented to favor forward proton flow of and disfavor backward proton flow (*Figure 1 – right*). These results, together with the conformational transitions, contribute to explain the pH triggering of the M2 conductance, and the unidirectional flow of the protons.

### *M2 mutations*

The effect on the channel activity of mutations of pore-lining residues in the N-terminal portion of the channel has been explored in collaboration with the Pinto group at Northwestern. Experimental data exist for a wide spectrum of different mutants, both naturally occurring and those produced in the laboratory. Tetramer-forming mutants can be classified as: (a) proton-selective mutants with similar conductance to the wild type (WT); (b) conducting mutants with no selectivity towards protons; (c) non-conducting mutants. This behavior could be rationalized mostly in terms of steric hindrance (Balannik *et al*, 2010). We focused our computational efforts on the remaining mutations, by using MD simulations of the membrane-embedded M2TM 4-helix bundle. The A30K mutant is conducting but not proton-selective, even though the similar V27K mutant is fully functional (Balannik *et al*, 2010). Based on our MD simulations, this may be due to the conformational change induced by the K30 side chains in A30K, which destroys the narrow selective pore between the V27 position and the H37 tetrad. Instead, in V27K only the side chains themselves rearrange, while the backbone structure is preserved (*Figure 2 - left*). Furthermore, insertion of hydrophobic side chains (A30F, S31F and G34V) produces a non-conducting channel even if the pore structure is not permanently distorted; pores with a diameter of at least 3 Å are left open. This is due to a drop in water density near the hydrophobic side chains (*Figure 2 - right*), rather than steric hindrance. Mutations with polar side chains of comparable or equal size, such as S31N and G34T, exhibit a continuous water density throughout the entire pore (Balannik *et al*, Biochemistry 2010). As for the pH-dependence, we unambiguously correlated channel activity of M2 mutants to the connectivity of the water wires.

### *MD simulations of M2 in complex with novel inhibitors*

The natural occurrence of point mutations of specific pore-lining residues, such as L26F, V27A, and S31N, results in amantadine-resistant viral strains. Recently discovered compounds based on spiro[5,5]undecane have been shown to be more potent than amantadine on the wild type and to significantly retain the activity on the L26F and V27A mutants (Wang *et al*. 2009; Balannik *et al*.2009). Generating chemical diversity on the spirene scaffold is currently one of the most promising approaches to target the M2-S31N channel, the most common mutation found in drug-resistant strains. The experimental evidence coming from solid-state NMR indicates that the spirane group establishes more interactions than amantadine with the pore-lining residues on the N-terminal of the TM region; however, the details of the binding mode and, more important, a rationale for the complete loss of binding affinity upon mutation of Ser31 into an asparagine are still lacking. Therefore we performed MD simulations on the complex between M2 and spiropiperidine (the most active spiran-based compound) for both the wild type and the S31N mutant. The complex between spiropiperidine and WT-M2 is stable during the time-span of our simulation (~20 ns), in particular, after a relaxation phase occurring during the first few nanoseconds of trajectory, the drug molecule is locked into the bound conformation and does not experience significant fluctuations. An interesting feature revealed by the simulations concerns the role of the water molecules within the channel pore in determining the affinity: the drug

molecule displaces all the waters lying in the hydrophobic region of the channel by filling the pocket with its alkyl moiety and interacts, via the secondary amine of the piperidine group, with two layers of structured waters lying right above the histidine residues (*Figure 3 - left*). A significantly different behavior is observed in the case of S31N, which is insensitive to the drug molecule. Indeed, the replacement of the hydroxyl group of the serine sidechain with the carboxamide moiety of asparagine dramatically alters the hydrophobic character of the N-terminal region of the pore and draws more waters into the channel. As a result the hydrophobic moiety of the drug molecule does not stick anymore to the sidechains of the pore-lining residues. Furthermore, the conformation found to be stable in the WT simulation, in which the amine groups points toward the histidine residues, turns out to be unstable in S31N; after ~5 ns of simulation the drug molecule suddenly changes its orientation with respect to the channel axis, retaining this configuration for the rest of the trajectory (*Figure 3 middle and right*).

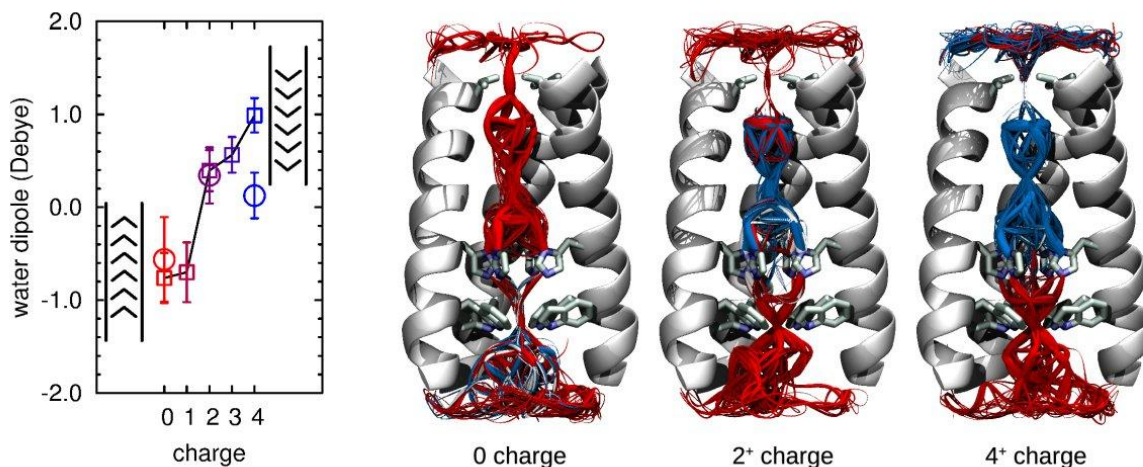


*Figure 1. Left panel:* average projection of the pore water dipoles along the membrane normal: circles represent simulation of the three experimental structures at the 0, 2<sup>+</sup> and 4<sup>+</sup> charge states, respectively; squares represent position-restrained simulations of the intermediate-pH structure at different states (0 to 4<sup>+</sup>). *Right panels:* ribbon representation of the water wires through the intermediate pH structure in three different charge states. Red indicates inward wires (favoring forward proton flow), while blue indicates outward wires (favoring backward proton flow). The protein backbone is seen from across the membrane, with the extra-viral space at the top of the figure.

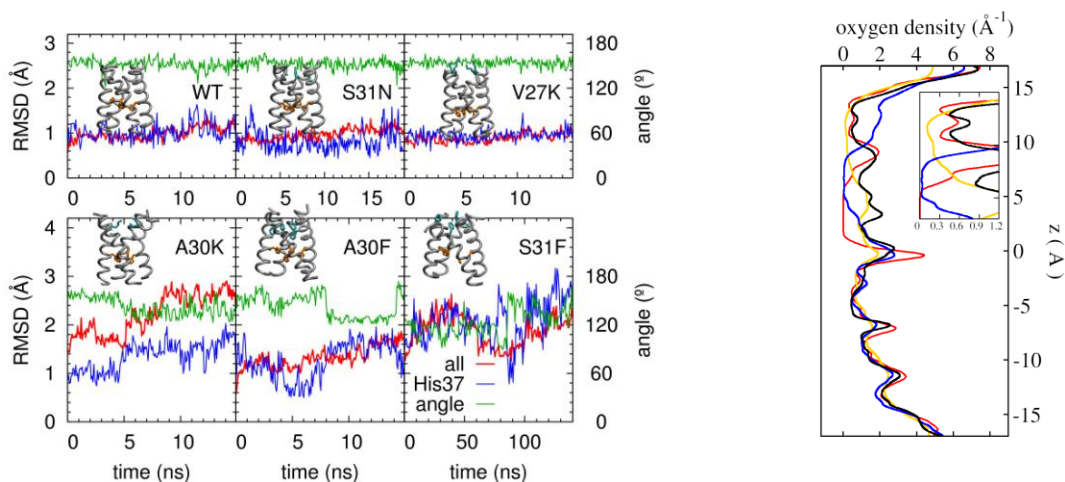


*Figure 2. Left panel:* root mean square deviation (RMSD) from the X-ray structure of the heavy atoms of the entire M2TM tetramer (red) and of the H37 tetrad (blue) as a function of simulated time for WT-M2TM and five mutants. Also shown is the average angle between the N<sub>δ</sub>-N<sub>ε</sub> vectors of the H37 side chains and the membrane normal (green). The final simulated structures in ribbon representation are overlaid. *Right panel:* average number of water molecules throughout the channel pore (H37 side chains are comprised between 0 Å and -5 Å); shown are the density profiles for the WT (black), the A30F (yellow), S31F (blue) and G34V (red).

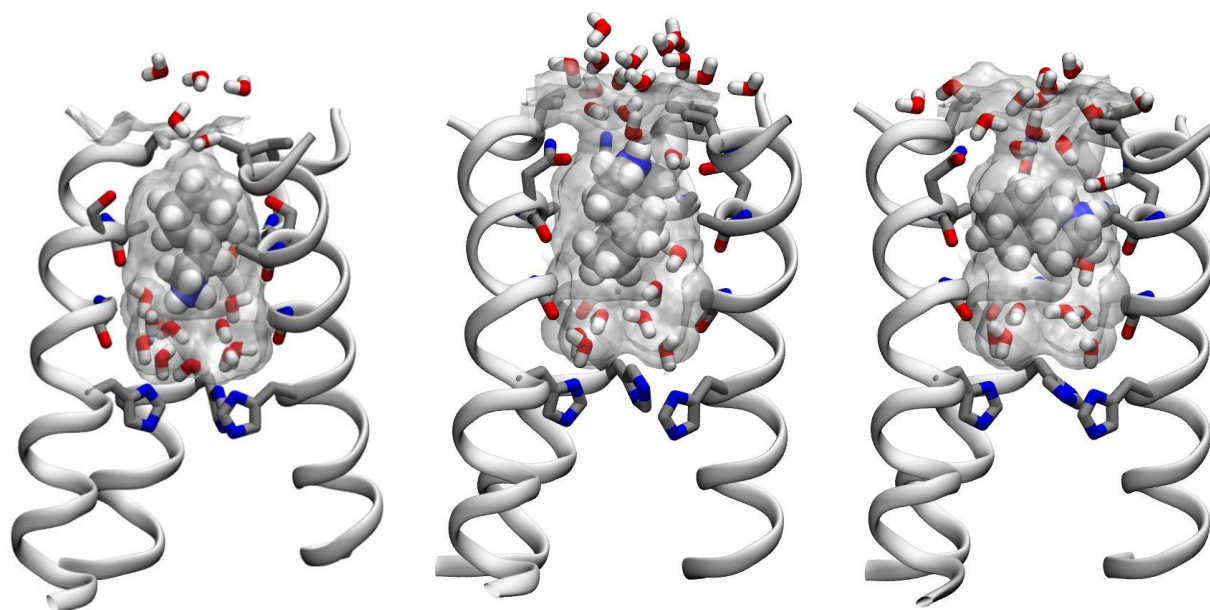


*Figure 3.* Structure of the M2-spiropiperidine complex. Three of the four helices of the M2 bundle are shown together with the sidechains and carbonyls groups of the residues interacting with the drug molecule (Val27, Ala30, Ser/Asn31, Gly34, and His37). Grey shading highlights the binding pocket. *Left panel:* Final snapshot from the trajectory of the WT; *Middle panel:* Structure of M2/S31N-spiropiperidine complex after ~5 ns of MD simulation; *Right panel:* Final configuration of M2/S31N-spiropiperidine complex after ~20 ns of MD simulation.

### **Research Project 26: Project Title and Purpose**

*Improving Cell Therapy for the Damaged Heart* - Loss of cardiomyocytes associated with either longstanding heart failure or acute myocardial infarction could be therapeutically addressed by a treatment that specifically replaces lost myocytes. Currently, a number of clinical trials to test the efficacy of injecting different types of stem cells into the damaged heart are ongoing. Our research is basic in nature and explores the idea that there are already cells within the heart that have the capacity to repair it if it is damaged. The purpose of our research is to modify adult stem cells so that they will repair the damage of the heart after a myocardial infarction.

### **Anticipated Duration of Project**

07/01/10 – 6/30/2011

### **Project Overview**

We will test the idea that cardiac repair will be enhanced if we use cardiogenic stem cells with a greater potential to survive in the hostile environment of the injured heart and a greater ability to make electrical contact with myocytes in this heart. The first step in the research is to generate genetically modified cardiac stem cells. We have already shown that the cardiac stem cells have the potential to differentiate into a cardiac myocyte when cultured on a feeder layer of neonatal

ventricular myocytes. We will use this system to test the idea that we have made new stem cells with an enhanced ability to differentiate into cardiac myocytes and survive hostile environments.

Stem cells will be infected with viruses containing normal and modified gap junctional proteins. We have these reagents in hand. Stem cells will be expanded in vitro, infected with gap junctional viruses and then plated on neonatal myocytes. We will then measure the percent of these cells that differentiate into cardiac myocytes and over what time course. We have 5 different gap junctional modifications to test. We will determine which of these modifications makes the stem cells best suited for cardiac regeneration. Once these studies are completed we will move on to studies in animal models of cardiac injury.

Cardiac stem cells with documented ability to improve cardiac function will be injected into damaged hearts. These cells will be labeled with molecules that allow us to track these cells. We will determine the ability of these cells to improve cardiac pump function. Noninvasive imaging techniques will be used to quantify cardiac function changes 3, 7 and 28 days after cell injection. At sacrifice we will fix hearts and determine the fate of the injected cells.

These studies have the potential to determine if cardiac stem cells with enhanced engraftment capabilities can increase cardiac regeneration and improve cardiac function.

### **Principal Investigator**

Steven R. Houser, PhD  
Professor and Chair of Physiology Department  
3420 N. Broad Street  
Medical Research Building 204A  
Philadelphia, PA 19140

### **Other Participating Researchers**

Fang Wang, BA – employed by Temple University

### **Expected Research Outcomes and Benefits**

In this study we expect to develop methods to modify adult cardiac stem cell survival and engraftment. Recent studies have shown that when stem cells are injected into the damaged heart, most if not all of these cells die and there is little improvement in cardiac function. Our research will explore novel methods to improve the survival of stem cells and to enhance their coupling to cardiac myocytes in the parent myocardium. Our basic research has shown that in order for a stem cell to differentiate into a cardiac myocyte it must make physical contact with the myocyte. Unfortunately, in the environment of the damaged heart, myocytes uncouple from their neighbors. Our approach will improve stem cell - myocyte interactions that we believe will increase cardiac regeneration. If we are successful we will rapidly translate these techniques to a small scale clinical trial. Our long term plan is to develop more effective therapies for individuals with poor cardiac function secondary to myocardial infarction.

## Summary of Research Completed

Project start date has been postponed to 07/01/10. There is no research or expenses to report.

## Research Project 27: Project Title and Purpose

### *Determining the Role of c-Abl in Nongenomic Hormone Signaling of Estrogen Receptor Alpha -*

The purpose of this work will be to determine if the nongenomic signaling of the nuclear hormone receptors contributes to tumorigenesis via activation of both cytoplasmic tyrosine kinases c-Src and c-Abl. The project will deal with the activation of c-Src via nongenomic signaling of nuclear hormone receptors which in turn could cause the activation of c-Abl. This would perhaps define a role for c-Abl in solid tumorigenesis.

## Anticipated Duration of Project

09/01/10– 6/30/2011

## Project Overview

Our goal is to mechanistically derive a singular signaling pathway from cytoplasmic nuclear receptors to Src and Abl as found in solid tumors. To accomplish this we will 1) use mutant constructs of AR, ER, MNAR, Src, and Abl to demonstrate linear signaling; 2) test the role of MNAR, a known scaffold protein as a direct link between c-Abl and the nuclear receptors; and 3) determine the efficacy of both Src and Abl tyrosine kinase inhibitors on hormone-dependent mammary and prostate tumorigenesis. To complete these tasks, MNAR will first have to be cloned to determine its relationship with both Src and Abl. The use of multiple nuclear hormone receptors will also have to be implemented in the study of this signaling cascade. Currently we are focusing on the interaction between ER- $\alpha$  and c-Abl and we plan to biochemically characterize this interaction. This will be executed through a series of experiments including a GST pulldown assay demonstrating the ability of Abl-SH3 to interact with full length human ER- $\alpha$ . In addition to this, we will perform *in vitro* transcription translation binding reactions for both ER- $\alpha$  and c-Abl to determine if the interaction is direct or facilitated by another protein. Using c-Abl P131L in this experiment, we will be capable of verifying the SH3 domain is essential for the interaction of c-Abl and ER- $\alpha$ . To prove the interaction's existence *in vivo* we will transfect various cell lines to transiently express these proteins. At this point, it can be determined whether the interaction is ligand-dependent or independent by treatment with E2. Furthermore, it would be necessary to establish whether this interaction activates the Abl kinase by performing immunoprecipitation experiments with an anti-phospho-Abl antibody and a kinase assay using the GST-Crk substrate. After characterizing the role of Abl, we intend to map the interaction domain of ER- $\alpha$  which we hypothesize is the AF-1 domain. If possible, we would also like to examine the specificity of this ER-Abl reaction and broaden our experiments to include hER- $\beta$ .

## **Principal Investigator**

Scott K Shore, PhD  
Fels Institute for Cancer Research and Molecular Biology  
Temple University School of Medicine  
3400 North Broad St  
Philadelphia, PA 19140

## **Other Participating Researchers**

Meghan E Jordan – employed by Temple University

## **Expected Research Outcomes and Benefits**

It is expected that we should determine Abl and hER- $\alpha$  interact to initiate the nongenomic hormone receptor signaling cascade, activating both c-Src and PI3K. This interaction may or may not be E2-dependent. Provided the interaction is E2-dependent, we will elucidate a new role for Abl and a new aspect to a known signaling pathway in cancer. We expect to provide data characterizing a previously unidentified relationship between c-Abl and hER- $\alpha$ , which would progress our knowledge about the pathway, the interaction, and the rationale to inhibit this pathway as a novel approach for treating cancer. By characterizing the interaction of c-Abl and hER- $\alpha$ , we believe we can provide a role for c-Abl in solid tumorigenesis which as of yet has proved to be rather difficult. In doing this, we will provide a singular pathway that can be addressed by a novel therapeutic approach to treat the solid tumors in breast and prostate cancer. Much like Imatinib is used as an Abl inhibitor for Bcr-Abl in patients with chronic myelogenous leukemia, we hope to provide proof-of-principle for a novel therapeutic approach to treat mammary and other steroid hormone-induced solid tumors.

## **Summary of Research Completed**

No Research or expense to Report: The project was rescheduled due to the delayed approval of this project.

## **Research Project 28: Project Title and Purpose**

*Protection from Atherosclerosis in IL-19 Transgenic Mice* - Cardiovascular disease is the number one killer of Americans. Vascular diseases such as atherosclerosis, hypertension, restenosis, and transplant vasculopathy are inflammatory in nature. Very little has been reported on the potential protective effects of anti-inflammatory cytokines on development of vascular disease. We have novel preliminary data which shows that the naturally occurring anti-inflammatory compound, Interleukin-19 (IL-19) can have protective effects on vascular cells grown in culture. The purpose of this project is to determine if IL-19 can reduce atherosclerosis in an important animal model of this disease.

## **Anticipated Duration of Project**

7/01/2010 – 6/30/2011

## **Project Overview**

Vascular diseases such as atherosclerosis, hypertension, restenosis, and transplant vasculopathy are inflammatory in nature. Although a great deal of attention has been given to the role and effects of pro-inflammatory cytokines, very little has been reported on the potential protective effects of anti-inflammatory cytokines on the vascular response to injury, particularly with respect to direct effects on VSMC pathophysiology. IL-19 is a newly described member of the IL-10 family of anti-inflammatory cytokines. There are three papers which suggest that IL-19 has similar anti-inflammatory effects on immune cells, but we are the only laboratory to publish concerning the expression or presumed function of IL-19 in VSMC pathophysiology or a role in modulation of vascular diseases.

We have preliminary data which indicate that IL-19 is not present in normal vascular smooth muscle cells (VSMC), but can be expressed in response to inflammation and injury. Addition of IL-19 to cultured VSMC reduces their growth, signal transduction in response to inflammatory stimuli, and expression of several inflammatory genes. We have preliminary data in cultured cells indicating that IL-19 modifies post-transcriptional processing of inflammatory gene mRNA. This information has led to the hypothesis that IL-19 can have protective effects on the development of atherosclerosis.

Despite this information NO studies on in vivo effects of IL-19 expression have been reported. We have recently generated an IL-19 VSMC – specific IL-19 transgenic mouse. In this strategy, IL-19 transcription is driven by the SM22 alpha VSMC-specific promoter, and is only over expressed in VSMC. In preliminary experiments, we have shown that the IL-19 knock out mouse has an exacerbated response to a high-fat diet with increased atherosclerosis. These data drive the hypothesis to be tested that the IL-19 VSMC transgenic mouse will have a decreased response to a high fat/high cholesterol diet compared with the control mice, likely as a result of decreased VSMC proliferation.

In Aim 1 we will determine if there will be decreased development of atherosclerosis in VSMC restricted IL-19 transgenic mice fed a high-fat diet. In Aim 2, we will characterize the cellular component of atherosclerotic lesions in the wild-type and transgenic mice by immunohistochemistry.

## **Principal Investigator**

Michael Autieri, PhD  
Associate Professor of Medicine  
Temple University School of Medicine  
1050 MERB  
3500 N. Broad Street  
Philadelphia, PA 19140

## **Other Participating Researchers**

Stephen Ellison, BS – employed by Temple University

## **Expected Research Outcomes and Benefits**

Vascular restenosis, atherosclerosis, and other vascular diseases are inflammatory in nature, but ultimately depend on vascular smooth muscle cells (VSMC), which make up most of the cellular content of the artery. Accordingly, any compound which may decrease VSMC activation could represent a therapeutic intervention to attenuate most vascular diseases. IL-19 is a compound which occurs naturally in humans and functions to modify inflammatory cells and dampen the immune response. We have previously shown that IL-19 is also turned on in VSMC under inflammatory conditions. We have previously shown that IL-19 has suppressive functions on VSMC which are grown in culture. In this application, we will determine if mice which are genetically modified to always have high levels of IL-19 are protected against atherosclerosis. One outcome we expect is that mice which constitutively express IL-19 will have much less atherosclerosis when fed a high-fat diet. If these experiments are successful, then a major benefit is that IL-19 could represent a new class of naturally occurring therapy to combat multiple vascular diseases.

## **Summary of Research Completed**

No Research to Report: We rescheduled for a July 1 start date due to the late submission and subsequent approval of this project.